



LUND UNIVERSITY

The Connection Between a Real Fire Exposure and the Heating Conditions According to Standard Fire Resistance Tests - With Special Application to Steel Structures

Pettersson, Ove

1975

[Link to publication](#)

Citation for published version (APA):

Pettersson, O. (1975). *The Connection Between a Real Fire Exposure and the Heating Conditions According to Standard Fire Resistance Tests - With Special Application to Steel Structures*. (Bulletin of Division of Structural Mechanics and Concrete Construction, Bulletin 39; Vol. Bulletin 39). Lund Institute of Technology.

Total number of authors:

1

General rights

Unless other specific re-use rights are stated the following general rights apply:

Copyright and moral rights for the publications made accessible in the public portal are retained by the authors and/or other copyright owners and it is a condition of accessing publications that users recognise and abide by the legal requirements associated with these rights.

- Users may download and print one copy of any publication from the public portal for the purpose of private study or research.
- You may not further distribute the material or use it for any profit-making activity or commercial gain
- You may freely distribute the URL identifying the publication in the public portal

Read more about Creative commons licenses: <https://creativecommons.org/licenses/>

Take down policy

If you believe that this document breaches copyright please contact us providing details, and we will remove access to the work immediately and investigate your claim.

LUND UNIVERSITY

PO Box 117
221 00 Lund
+46 46-222 00 00

LUND INSTITUTE OF TECHNOLOGY · LUND · SWEDEN · 1975

DIVISION OF STRUCTURAL MECHANICS AND CONCRETE CONSTRUCTION · BULLETIN 39

OVE PETTERSSON

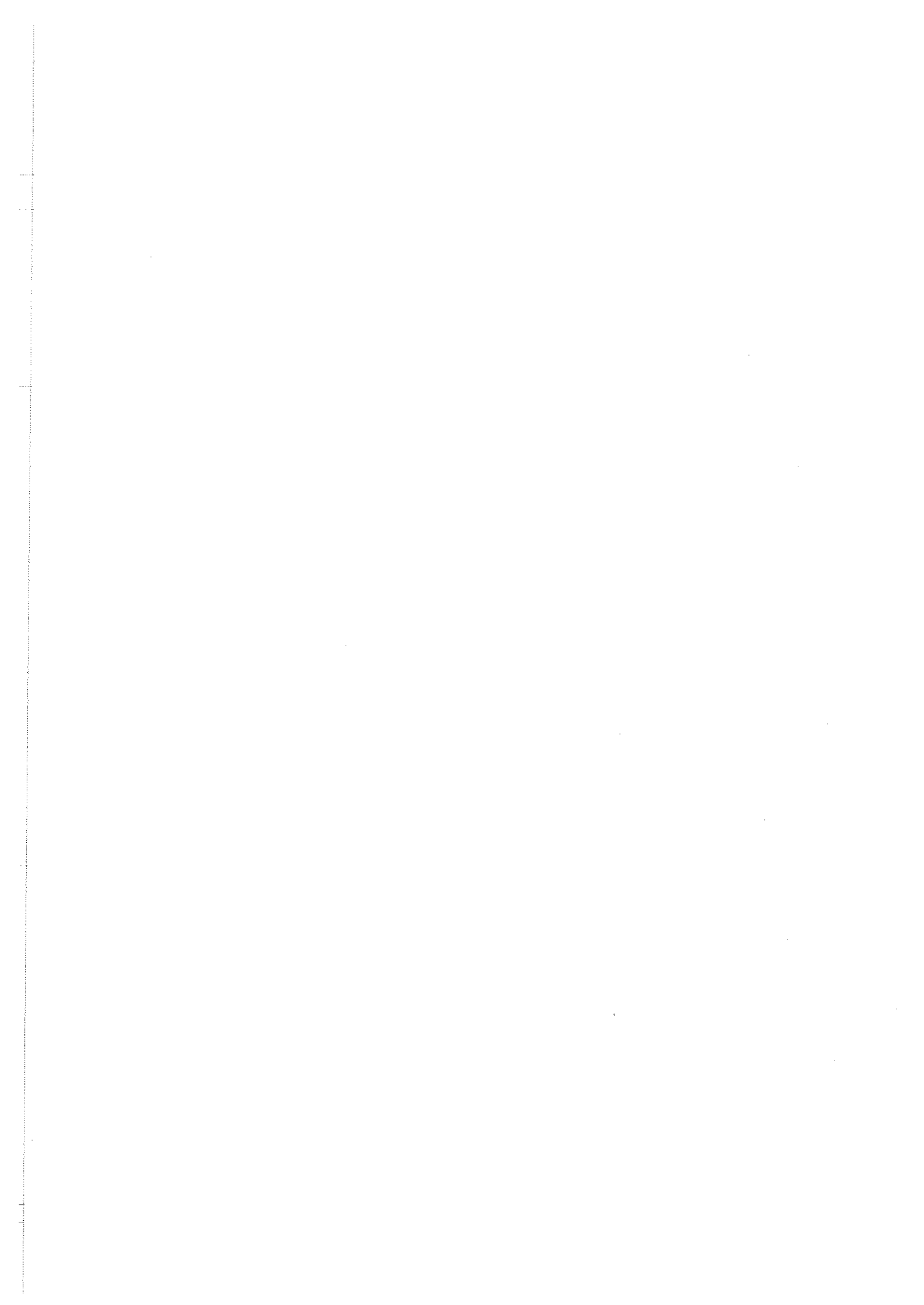
THE CONNECTION BETWEEN A REAL FIRE EXPOSURE AND THE HEATING CONDITIONS ACCORDING TO STANDARD FIRE RESISTANCE TESTS – WITH SPECIAL APPLICATION TO STEEL STRUCTURES

LUND INSTITUTE OF TECHNOLOGY · LUND · SWEDEN · 1974
DIVISION OF STRUCTURAL MECHANICS AND CONCRETE CONSTRUCTION · BULLETIN 39

OVE PETTERSSON

THE CONNECTION BETWEEN A REAL FIRE EXPOSURE AND THE HEATING CONDITIONS
ACCORDING TO STANDARD FIRE RESISTANCE TESTS - WITH SPECIAL APPLICATION
TO STEEL STRUCTURES

Reprint of European Convention for Constructional Steelwork, Fire Safety
in Constructional Steelwork, CECM-III-74-2E. Also distributed as CIB
Document - CIB/W14/44/74



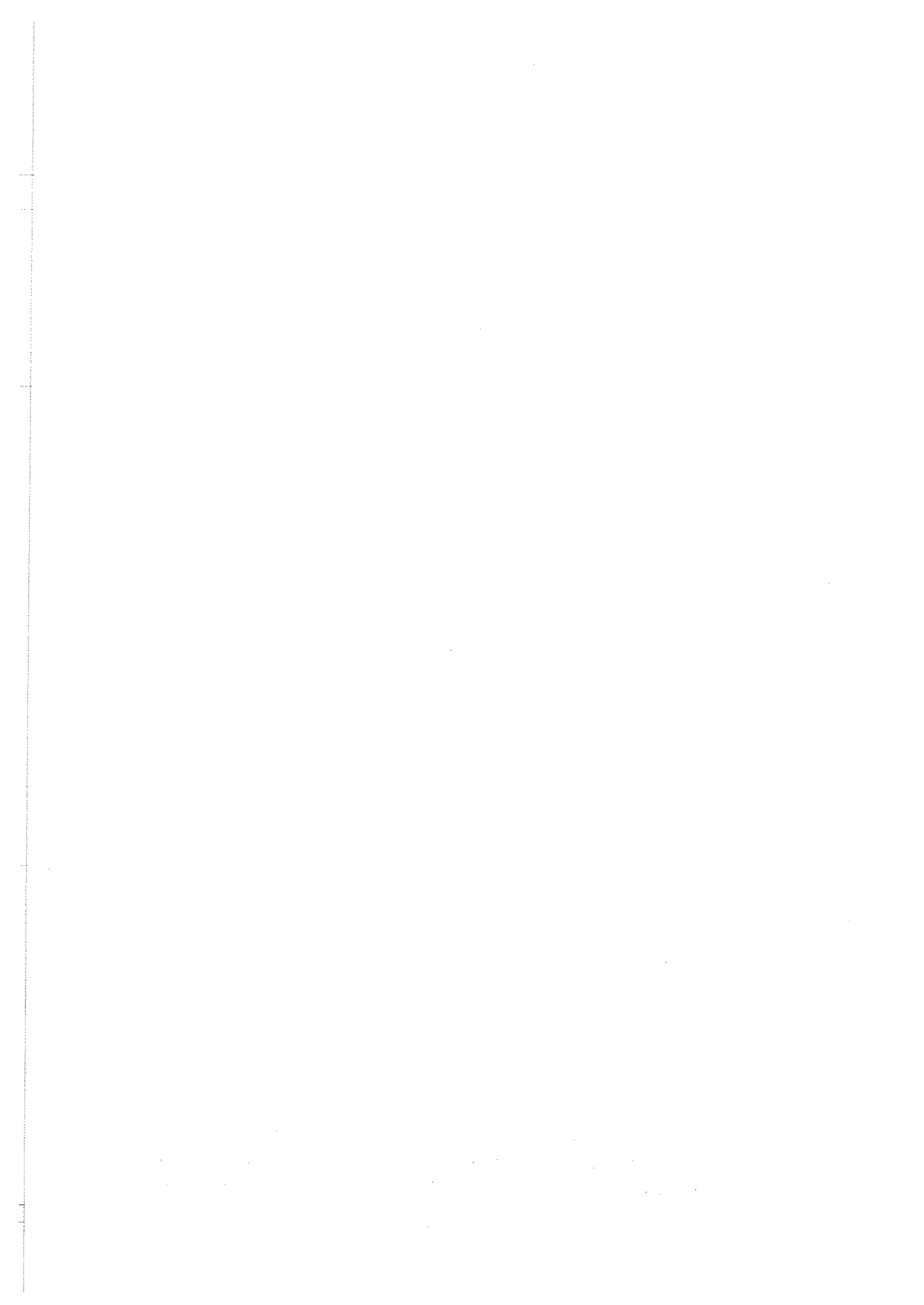
FIRE SAFETY
IN
CONSTRUCTIONAL
STEELWORK

CHAPTER II

Results and conclusions of a
European research study

Research work carried out with financial aid
from the European Coal and Steel Community

Europäische Konvention für Stahlbau
European Convention for Constructional Steelwork
Convention Européenne de la Construction Métallique



II - 1

THE CONNECTION BETWEEN A REAL FIRE EXPOSURE AND
THE HEATING CONDITIONS
ACCORDING TO STANDARD FIRE RESISTANCE TESTS, WITH
SPECIAL APPLICATION TO STEEL STRUCTURES

THE CONNECTION BETWEEN A REAL FIRE EXPOSURE AND THE HEATING CONDITIONS
ACCORDING TO STANDARD FIRE RESISTANCE TESTS, WITH SPECIAL APPLICATION
TO STEEL STRUCTURES

The present development of building codes and regulations towards functionally more well-defined requirements continually increases the need of methods for a differentiated structural fire engineering design. During the last years several such design methods have been presented in the literature. Mainly, these methods can be referred to one of two different groups with respect to the use of the basic data of the process of fire development. Characteristic for the methods of the first group is a design procedure with the varying properties of the fire development taken into account over an equivalent time of fire duration, connected to the heating according to the standard time-temperature curve. The methods of the second group are characterised by a design procedure, directly based on gastemperature-time curves of the complete process of fire development, specified in detail with regard to the influence of the fire load and the geometrical, thermal and ventilation properties of the fire compartment. The methods of the two groups, which in their basic principles are equivalent and in their more specific details complete each other, are generally taking into account the complete process of real fire development - the heating period as well as the subsequent cooling down period.

1. Basic characteristics of the process of real fire development

The basic characteristics of a compartment fire depend on a large number of influences of which the most important are:

- (a) the amount and type of combustible materials in the compartment - the fire load,
- (b) the porosity and particle shape of the fire load,
- (c) the distribution of the fire load in the compartment,
- (d) the ventilation properties of the fire compartment,
- (e) the geometry of the compartment, and
- (f) the thermal properties of the structures, enclosing the compartment.

In spite of a large number of important investigations, our present state of knowledge on the detail characteristics of compartment fires is far from satisfactory.

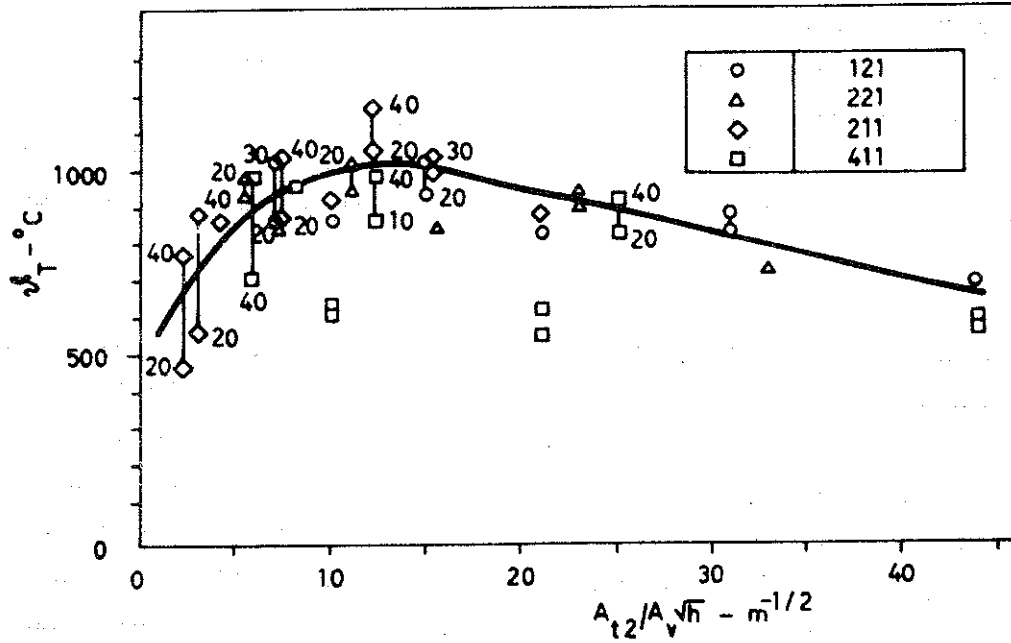


Fig. II,1

Relation between average gastemperature for the active part of a fire \bar{T}_g and an inverse, modified opening factor $A_{t2}/A_v \sqrt{h}$. Summary of results of a comprehensive CIB co-operative programme on model scale studies of compartment fires with fuel of piles of wooden sticks. The three figure code for the shape of the compartment characterizes the three principal dimensions of width, depth and height, relative to height, e.g. a 221 compartment measures 2 units wide, 2 units deep and 1 unit high [2]

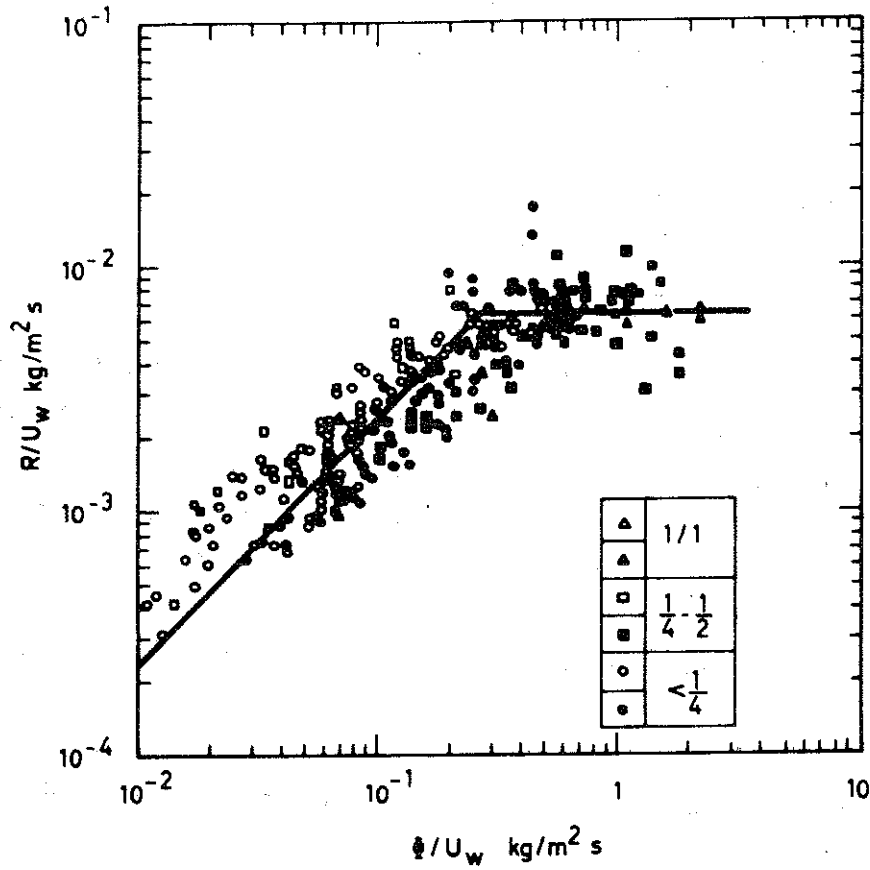


Fig. II,2

Ratio R/U_w between average burning rate R and initial free surface area of the fire load U_w versus ratio ϕ/U_w between ventilation parameter ϕ and initial free surface area of the fire load U_w . Summary of results of full and model scale compartment fires, available from the literature. Fire loads of wooden crib type {5}

imation of whether a wooden crib fire will be ventilation controlled or not. In Eq. (II-7) $A_v \sqrt{h}/A_t$ = the opening factor of the fire compartment in $m^{1/2}$, A_v = the area of the window opening in m^2 , h = the height of the window opening in m , A_t = the total surrounding area of the compartment, opening areas included, in m^2 , q_t = the fire load, defined as the corresponding heat value per unit area of the surrounding compartment area A_t in $Mcal/m^2$, and d_w = the width of each individual stick of the wooden crib in m . Graphically, the relation is shown in Fig. II, 3. For smaller values of the opening factor $A_v \sqrt{h}/A_t$ than those determined by Eq. (II-7) or Fig. II,3, a wooden crib compartment fire roughly can be anticipated to be ventilation controlled.

Going over from fuel of wooden crib type to more realistic fire loads of furniture, it can be stated summarily, that the average burning rate of the active part of the ventilation controlled fires still can be determined from Eq. (II-1) or (II-2) with an accuracy which is sufficient in most practical cases of a structural fire engineering design. For fuel bed controlled fires considerable difficulties are added, primarily in defining a representative free surface area U_w or hydraulic radius r of a furniture fire load from a combustion point of view. Furthermore, some full scale tests of compartment fire with fire loads of furniture, representative for dwellings seem to indicate a not inconsiderable displacement of the transition point or regime between ventilation controlled and fuel bed controlled fires in the direction of a larger value of ϕ/U_w or a smaller value of $B/r \cdot A_v \sqrt{h}$ {6}, {7}. At present, the only way to take into account in a practical fire engineering design the specific, favourable characteristics of a fuel bed controlled fire will be initially to calibrate the real furniture fire load in a full-scale test. With regard to the large scatter of the fire load properties for each single type of compartment in practice ' accentuated in an international comparison - such a calibration procedure ordinarily will require very extensive series of full-scale fire tests with authentic fire loads chosen with the probabilistic characteristics taken into consideration.

2. Theoretical analysis of the process of fire development over the heat and mass balance equations

At known input data, a theoretical determination of the gastemperature-time curve ϕ_T -T of the complete process of fire development in a compartment can be carried out in the single case over the heat and mass balance equations of

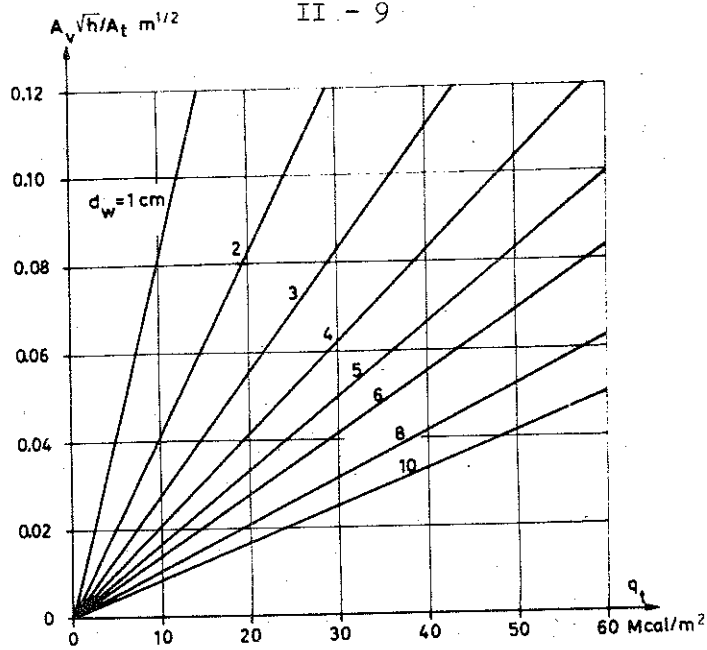


Fig. II,3 Diagram for a rough determination of whether a wooden crib fire will be ventilation or fuel bed controlled. The condition is given as a relation between the opening factor of the compartment $A_v \sqrt{h}/A_t$ and the fire load q_t for different values of the width d_w each individual stick of the wooden crib. For smaller values of the opening factor than those obtained from the curves, the fire can be estimated to be ventilation controlled.

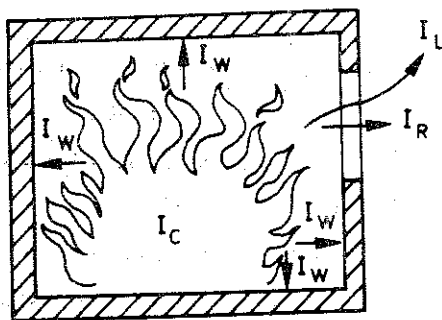


Fig. II,4 The heat and mass balance of a fire compartment

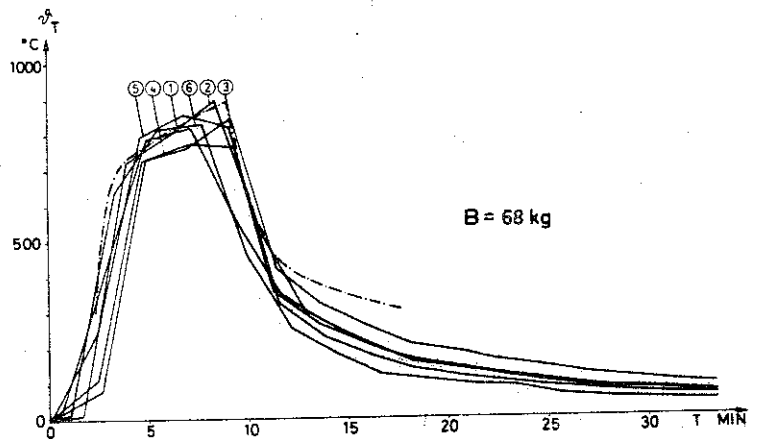


Fig. II,5 Experimentally determined gas temperature time curves at different points of a compartment for a fire load of kerosene (full-line curves) compared with a calculated gas temperature time variation (dash and dotted-line curve) [10]

changes in size and shape of window and door openings during the process of fire development. The procedure is applicable to compartments, which contain up to three different types of surrounding structures with one of these structures composed of up to three different materials.*

A practical application of the design procedure presupposes that the time variation of the combustion rate, specified as the quantity of released heat per unit of time, is known. Such a variation can easily be given for well-defined fuels without any smoulder phase. The procedure has also been applied successfully in analysing the results of compartment fire tests with fuels of this type [10]. An example is given in Fig. II,5, showing experimentally determined gastemperature-time curves at different points of a compartment for a fire load of kerosene fuel (full-line curves), compared with the corresponding, calculated temperature-time variation (dash and dotted-line curve). For not well-defined fuels - for instance fire loads of wooden type - a determination of the time-variation of the amount of the released heat per unit of time during a complete fire process is connected to great experimental difficulties. Further development of recently published laboratory test methods for a small-scale determination of the rate of heat release of materials and linings at accurately specified heating conditions could be a future way of solving this problem cf. e.g. [11], [12]. At present essential, necessary informations are lacking concerning such fundamental problems as a transformation of the time curve of the burning rate expressed as weight loss per unit of time R to a corresponding time curve of the burning rate given as the quantity of released heat per unit of time I_C or a division of the total amount of the released heat during a fire to the flame and cooling periods.

With the goal of deriving gastemperature-time curves for the complete process of compartment fires, which can be used as a provisional basis for a differentiated structural fire engineering design, giving values which are not unsafe of the fire resistance of structures, the problems summarised above have been tackled in [6], [9] in the following way.

.....

* The computer programme is available for unlimited use. For further particulars apply to the Division of Structural Mechanics and Concrete Construction, Lund Institute of Technology, Fack 725, 220 07 Lund, Sweden.

From the discussion carried through in Chapter II-1, some general conclusions can be drawn of basic interest in this connection. For ventilation controlled fires, the burning rate of the active part of the fire can be determined from Eq. (II-1) or (II-2) for different types of fire loads, furniture included, with an accuracy which is sufficient in most practical cases of a structural fire engineering design. For fuel bed controlled fires, the present state of knowledge is too incomplete to enable a satisfactory corresponding calculation of the burning rate in practice with the fire load consisting of furniture very difficult to define with regard to a representative free surface area U_w or hydraulic radius r . In such a position it seems reasonable to base a differentiated structural fire engineering design on characteristics for the process of fire development which constantly have been determined on the assumption of the fire to be ventilation controlled, and then to exclude the influence of varying porosity of the fire load, which influence is of minor importance for ventilation controlled fires. For fuel bed controlled fires, such a simplifying assumption leads to a fire engineering design which will be on the safe side in practically every case.

With this philosophy, full-scale experiments with wood fuel fires in compartments which have been reported in the literature in a sufficiently accurate manner are analysed {6}, {9}. For each individual experiment a theoretical determination has been carried through of that time curve for the released quantity of heat per unit of time which gives the best agreement for the complete process of fire development between the theoretically calculated and experimentally determined gas temperature-time curves for the compartment. Examples from this analysis are given in Fig. II,6 and II,7 {6}, showing comparisons between measured and computed gas temperature-time curves for two full-scale tests. The test according to Fig. II,6 {13} belongs to a test series, carried out at the Fire Research Station, Borehamwood, and is characterised by a fire load $q_o = 60 \text{ kg/m}^2$ floor area and an opening factor $A_v \sqrt{h}/A_t = 0.06 \text{ m}^{1/2}$ where A_t = total surrounding area of the compartment, floor and opening areas included. The test, exemplified in Fig. II,7 {14}, is characterised by a fire load $q_o = 30 \text{ kg/m}^2$ floor area and an opening factor $A_v \sqrt{h}/A_t = 0.091 \text{ m}^{1/2}$. The test is one of a test series, accomplished at the fire laboratory at Metz within the activities of Committee 3 of European Convention of Constructional Steelwork Associations. The two full-line curves of the calculated

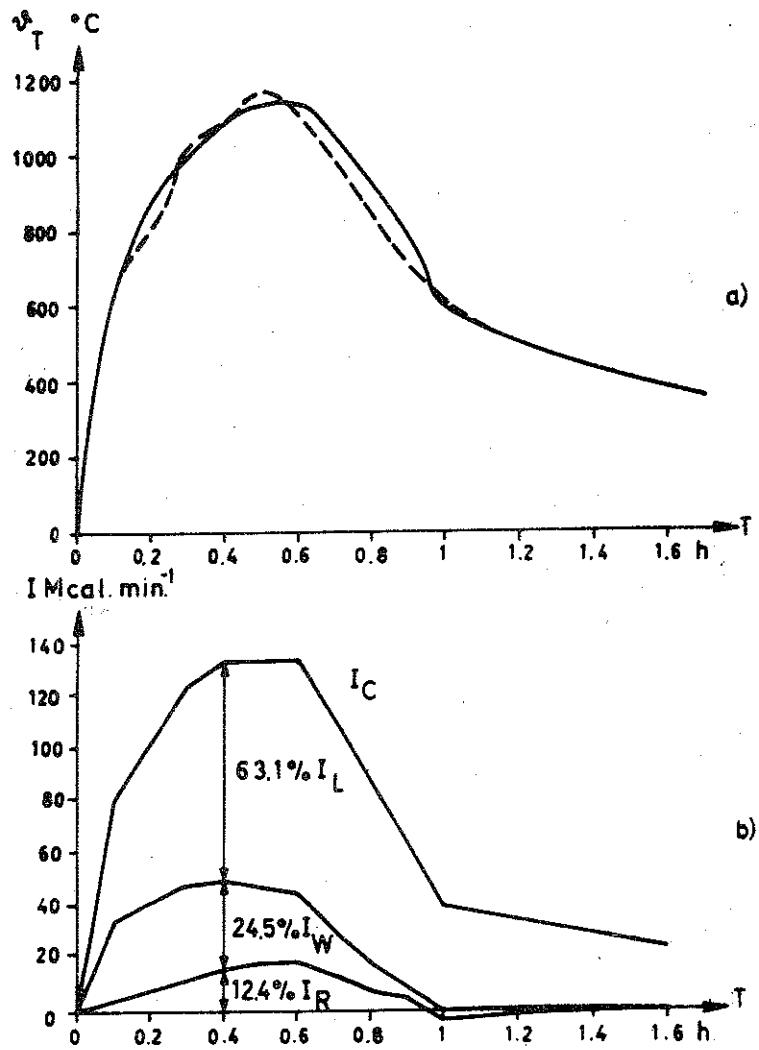


Fig. II,6 a) Measured (dash-line curve) and computed (full-line curve) gastemperature θ_T for a full-scale test, carried out at Fire Research Station, Borehamwood. Fire load $q_o = 60 \text{ kg/m}^2$ floor area. Opening factor $A_V \sqrt{h}/A_t = 0.06 \text{ m}^{1/2}$ {13} {6}

b) Computed, corresponding time curves for I_C , I_L , I_W and I_R in Eq. (11-8) {6}

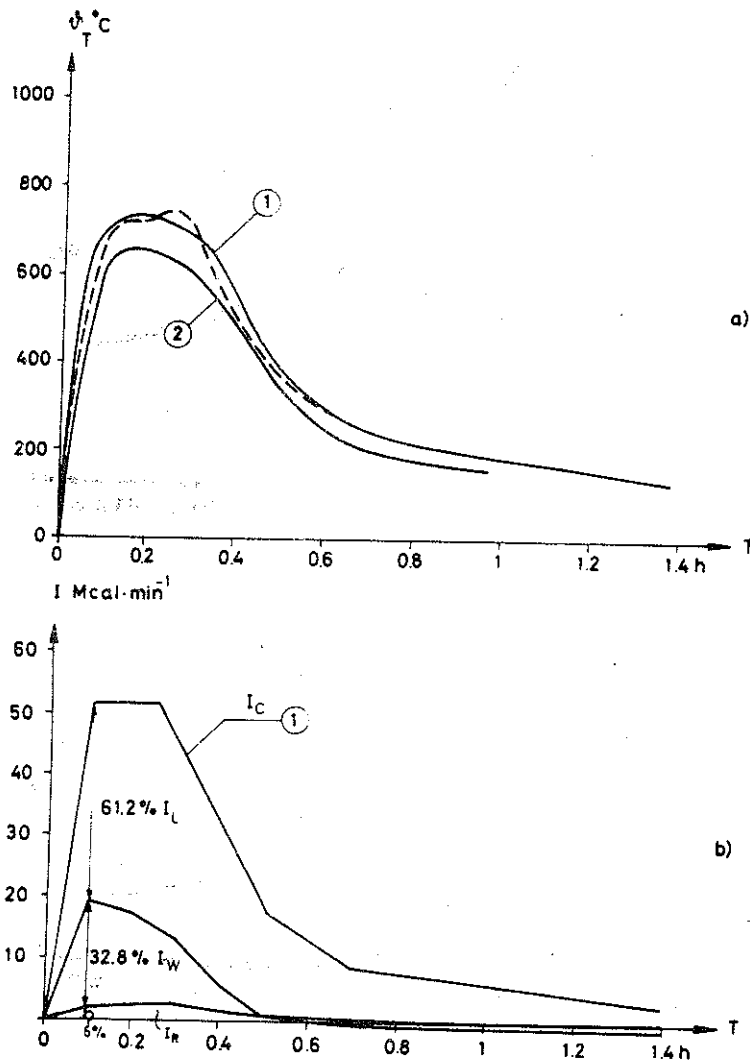


Fig. II,7 a) Measured (dash-line curve) and computed (full-line curves) gastemperature ϑ_T for a full-scale test, carried out at Metz. Fire load $q_0 = 30 \text{ kg/m}^2$ floor area. Opening factor $A_v \sqrt{h}/A_t = 0.091 \text{ m}^{1/2}$ {14} {6}

b) Computed, corresponding time curves I_C , I_L , I_W and I_R in Eq. (11-8) {6}

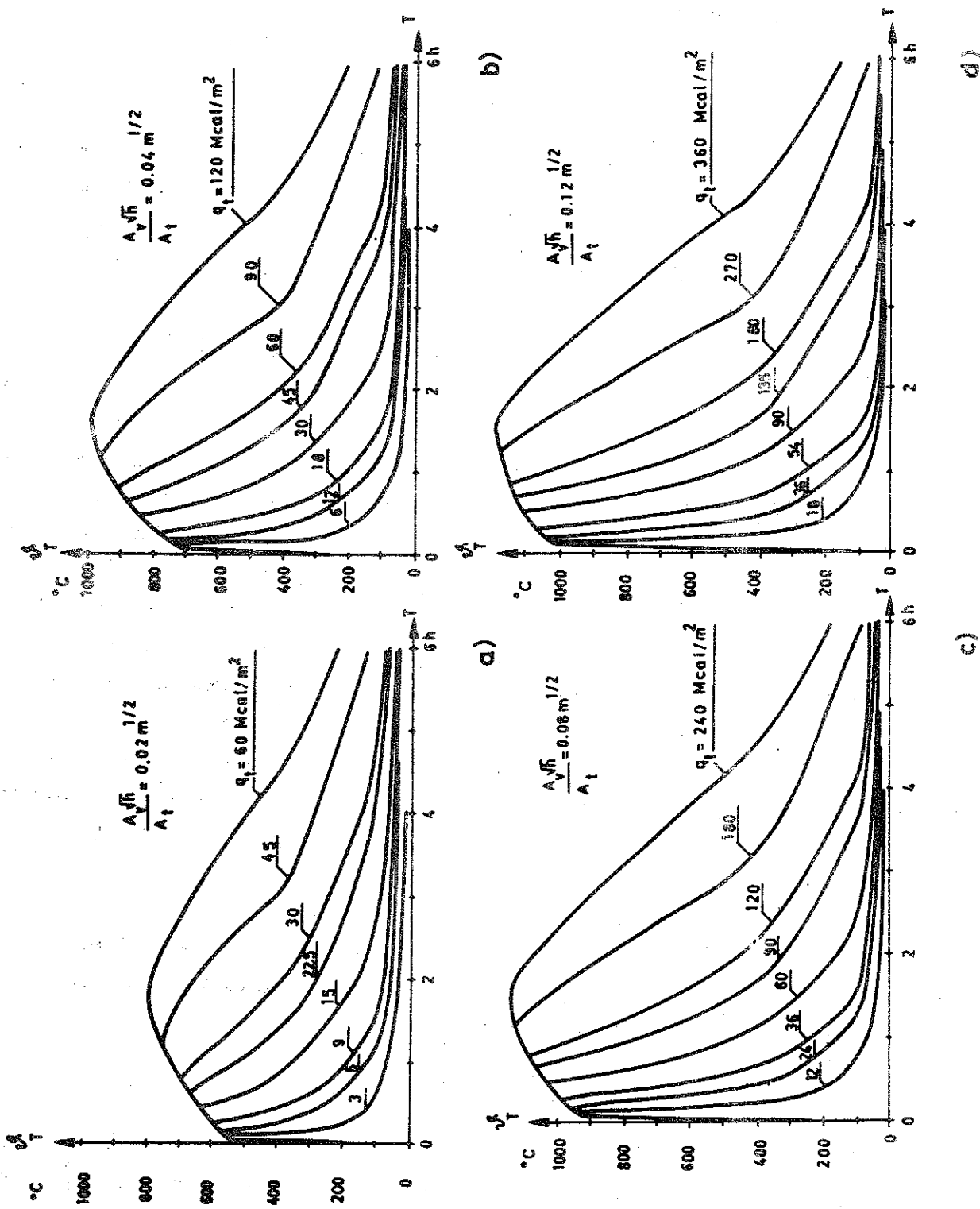


Fig. II,8

Gastemperature-time curves (ϑ_T -T) of the complete process of fire development for different values of the opening factor $A_v \sqrt{h}/A_t$ and the fire load q_t . Fire compartment, type A [9]

It is important to stress that the gastemperature-time curve, published in {9} and exemplified in Fig.II,8, generally have been determined on the assumption of ventilation controlled fires. As a consequence, the curves are not intended to be used directly for theoretical comparisons with experimentally obtained results from wooden crib compartment fires of strongly marked fuel bed controlled type. In such a connection, the method of calculation according to {6}{9} of course is to be based on Eq. (II-4) for the rate of combustion. The agreement between the theoretical and experimental results then will be satisfactory too. One principle reason for choosing ventilation controlled fire characteristics as a general assumption for the determination of the gastemperature-time curves according to {9} is dictated by the great difficulty in finding a representative value of the free surface area or the hydraulic radius of a real fire load of furniture for a combustion description of a fuel bed controlled fire. Another principal reason is connected to the fact that the gastemperature-time curves themselves do not constitute the primary interest of the problem in this connection but an intermediate part of a determination of the decisive quantity, viz. the minimum value of the load-bearing capacity of a fire exposed structure during a complete process of fire development. For fuel bed controlled fires, the assumption of ventilation control in combination with the fulfilment of the condition, given by Eq. (II-9), leads to a structural fire engineering design which will be on the safe side in practically every case, giving an overestimation of the maximum gas-temperature level and a simultaneous, partly balancing underestimation of the time of fire duration. For the minimum load-bearing capacity or the fire resistance time, the gastemperature-time curves according to {9} give reasonably correct results, which has been verified partially in {15} and also will be confirmed further in chapter II-4.

The gastemperature-time curves $\vartheta_T - T$, reproduced in Fig.II,8, belong to a fire compartment with surrounding structures 20 cm in thickness and made of a material with a thermal conductivity $\lambda_w = 0.7 \text{ kcal/m/h/}^\circ\text{C}$ and a heat capacity $\rho C_p = 400 \text{ kcal/m}^3/\text{C}$ as representative average values within the temperature range associated with fires. This compartment will be named fire compartment, type A in the following treatment and all design diagrams will be directly referred to this type of compartment. For enabling

a more general fire engineering design, in Table II-1 * are specified rules for a transformation - via fictitious values of the fire load q_t and the opening factor $A_v\sqrt{h}/A_t$ - of the gastemperature-time characteristics for compartments with other thermal properties of the surrounding structures to the gastemperature-time curves for fire compartment, type A. The following types of compartments then are included.

Fire compartment, type B: Boundary structures of concrete.

Fire compartment, type C: Boundary structures of lightweight concrete (density $\rho = 500 \text{ kg/m}^3$).

Fire compartment, type D: 50% of the boundary structures of concrete, and 50% of lightweight concrete (density $\rho = 500 \text{ kg/m}^3$).

Fire compartment, type E: Boundary structures with the following percentage of boundary surface area.
50% lightweight concrete (density $\rho = 500 \text{ kg/m}^3$)
33% concrete and the remaining
17% made up from the interior to the exterior of plasterboard panel (density $\rho = 790 \text{ kg/m}^3$), 13 mm in thickness - diabase wool (density $\rho = 50 \text{ kg/m}^3$)
10 cm in thickness - brickwork (density $\rho = 1800 \text{ kg/m}^3$), 20 cm in thickness.

Fire compartment, type F: 80% of the boundary structures of sheet steel, and 20% of concrete. The compartment corresponds to a storage space with a sheet steel roof, sheet steel walls and a concrete floor.

Fire compartment, type G: Boundary structures with the following percentage of boundary surface area.
20% concrete
80% made up from the interior to the exterior of double plasterboard panel (density $\rho = 790 \text{ kg/m}^3$), 2 x 13 mm in thickness - air space, 10 cm in thickness - double plasterboard panel (density $\rho = 790 \text{ kg/m}^3$), 2 x 13 mm in thickness.

.....

* Tables II-1 and II-2 are printed at end of text

The basic gastemperature-time curves $\vartheta_T - T$, reproduced in Fig.II,8, have been determined without taking into consideration the influence on the heat and mass balance of structures or structural elements inside the compartment. As a consequence a direct application of the curves can lead to a not inconsiderable overestimation of the fire exposure for compartments with heavy interior structures or structural elements. In solving the heat and mass balance equations, this influence can be included in the term I_W and in the computer programme, referred to on p. II-8, the influence also has been regarded. A partial illustration of the influence is given in {8} and {26}.

The gastemperature-time curves according to Fig.II,8, are intended primarily to be used in a differentiated fire engineering design of structures or structural elements located within the fire compartment or forming a part of the surrounding structures of the compartment. For the thermal conditions outside a fire compartment, which are decisive in a fire engineering design of external steel columns, several of the influences, enumerated (a) to (f) in chapter II-1, are characterised by a considerably stronger importance than for the properties of the fire development within a compartment, e.g. the amount and distribution of the fire load, flammable linings, and carpets. The diagrams in Fig.II,8 therefore have to be applied with a certain caution in a fire engineering design of load-bearing structures outside a facade.

3. Heating conditions according to standard fire resistance tests

The different national regulations and the corresponding ISO Recommendation {16} concerning fire resistance tests of elements of building construction have been developed on the basis of the classification requirements, stipulated in the building codes and regulations {17}

The scope of the test method consists of a determination of the fire resistance of an element of building construction, defined as that period of time which extends from the beginning of a fixed heating process to an instant when the element no longer complies with the functional requirements to be fulfilled. The function required then can be

- (a) a load-bearing function (e.g. a column or a beam),
- (b) a separating function (e.g. a partition or a non-load-bearing wall),

furnace temperature in °C. The relationship gives the values shown in Table II-2. *

A specification of a time curve of the furnace temperature is not sufficient as an external characteristic for a determination of the time-temperature fields in an element of building construction exposed to a fire. In addition, another decisive factor in this connection is the coefficient of heat transmission for the exterior surfaces of the fire exposed element. This coefficient is primarily influenced by the convection and radiation conditions. For a prescribed furnace time-temperature curve the convection and radiation characteristics can vary considerably from one furnace to another, depending on the detail design of the furnace and the type of fuel. For that reason comparative estimations of test results, obtained in different fire engineering laboratories, can be very difficult - and sometimes impossible - to carry through. In order to facilitate such comparisons of test results, it is recommended in the commentary on ISO/R 834 [17] that the thermal properties of the furnace shall be calibrated with reference to a well-defined standard test specimen and be given in terms of that variation in the coefficient of heat transmission with the time which is associated with the standard time-temperature curve. It is also recommended that this calibration curve of the furnace generally shall be included in the test report.

As concerns the restraint conditions of a test specimen, it is well-known that variations of restraint characteristics considerably can influence the structural behaviour and the time of fire resistance for an element of building construction. Usually the effect of increased degree of restraint is beneficial for the fire resistance of a structural element but sometimes a detrimental effect can be introduced. For instance, a thrust restraint can accelerate an instability failure in fire. For a concrete structural element, a thrust restraint also can give rise to an increased risk of spalling.

From these facts it is obvious that results from fire resistance tests carried out under undefined restraint conditions - which is not infrequent today - are very difficult to use in a differentiated structural fire engineering design as well as for a qualified classification. Additions

* After text.

to the present ISO Recommendation on this point - successively leading to, for instance, a series of precisely defined restraint conditions relevant to real structures - consequently have high degree of priority.

In the revised draft proposal for ISO/R 834 this problem is noticed by the general prescription: "If restraint is applied in the test, then the restraint conditions have to be specified with regard to free movements of the element and, so far as possible, those external forces and moments, which are transmitted to the element by restraint during the test" {16}. In the commentary on ISO/R 834, further guidance is given for the planning, performance and reporting of a fire resistance test with respect to restraint conditions, as concerns columns, walls, beams and girders {17}.

In addition to the heating and restraint characteristics, the ISO Recommendation on fire resistance tests comprises insufficiently accurate specifications in other respects too, for instance concerning the environment of the furnace, and the thermocouples for measuring the furnace temperature {17}, {18}. In {18} also the reproducibility of fire resistance tests is discussed with reference to tests carried out in the same equipment as well as to tests made in corresponding test furnaces of different fire engineering laboratories. Important suggestions are put forward for making the procedure of fire resistance tests more precise. At present, the possibilities of realising such an urgent development are thoroughly studied within the Working Groups 10 and 11 of ISO/TC 92 in co-operation with the CIB Commission W 14.

4. The concept equivalent time of fire duration as a means of translating from a real fire exposure to standard heating conditions

One way of taking into account the influence of varying fire development characteristics in a differentiated structural fire engineering design, is based on the concept equivalent time of fire duration for making possible a direct translation from a real fire exposure to the standard heating conditions for fire resistance tests, Eq. (II-10).

In principle, the concept equivalent time of fire duration T_e can be defined according to Fig. II,9 which gives an illustration for a fire exposed

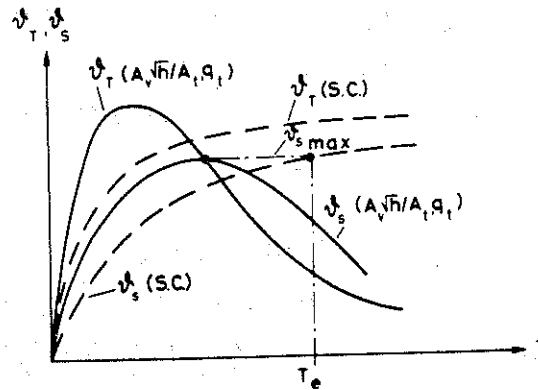


Fig. II,9

The principle of defining the equivalent time of fire duration T_e , exemplified for a fire exposed, uninsulated steel structure. The full-line curves refer the gastemperature ϑ_T and the steel temperature ϑ_S for a real fire action. The dash-line curves give the corresponding temperatures at a fire exposure according to the standard time-temperature curve (S.C.)

non-insulated steel structure {18} - {20}. The figure shows by the full-line curves the time-variation of the gastemperature ϑ_T and the steel temperature ϑ_s corresponding to a real fire action, determined by the fire load q_t , the opening factor $A_v\sqrt{h}/A_t$, and the thermal properties of the structures bounding the compartment. The dash-line curves give the standard time-temperature variation ϑ_T (S.C.), Eq. (II-10), and the appurtenant time-curve of the temperature ϑ_s (S.C.) of the steel structure. A transfer of the maximum steel temperature $\vartheta_{s_{max}}$ for the real fire action to the curve ϑ_s (S.C.), belonging to the standard time-temperature curve, determines the equivalent time of fire duration T_e .

Defined according to Fig. II,9, the equivalent time of fire duration T_e will be a function of the basic influences on the process of fire development as well as structural parameters. For fire exposed steel structures, Fig. II, 10 to II, 25 illustrate this in more detail.

Fig. II,10 to II,21 then apply to non-insulated steel structures, exposed to a fire with characteristics according to Fig. II,8 - fire compartment, type A. The figures give the equivalent time of fire duration T_e as a function of the opening factor $A_v\sqrt{h}/A_t$, the fire load q_t , the resultant emissivity ϵ_r , and the structural parameter U/F . U is the fire exposed surface and F the volume of the steel structure per unit of length. As concerns the resultant emissivity ϵ_r , it can be estimated very roughly that $\epsilon_r = 0.7$ approximately represents the conditions for a steel column within a fire compartment, $\epsilon_r = 0.5$ the conditions for a steel beam of a ceiling structure, and $\epsilon_r = 0.3$ the conditions for an external steel column, cf. however the comments on p.II-13 as concerns external structures. For a more precise determination of the resultant emissivity ϵ_r of fire exposed, non-insulated steel structures, reference is made to {21}. With respect to the resultant emissivity ϵ_r , the curves in Fig. II,10 to II,21 are based on the assumption that $\epsilon_r = 0.5$ for the standard heating conditions of the test furnace while ϵ_r has the value according to the respective diagram for the real fire exposure.

Fundamental for the diagrams in Fig. II,10 to II,21 is that the temperature of the fire exposed steel structure will reach the same maximum value $\vartheta_{s_{max}}$ for the real, complete process of fire development and for the heating according to the standard time-temperature curve. As a consequence, the

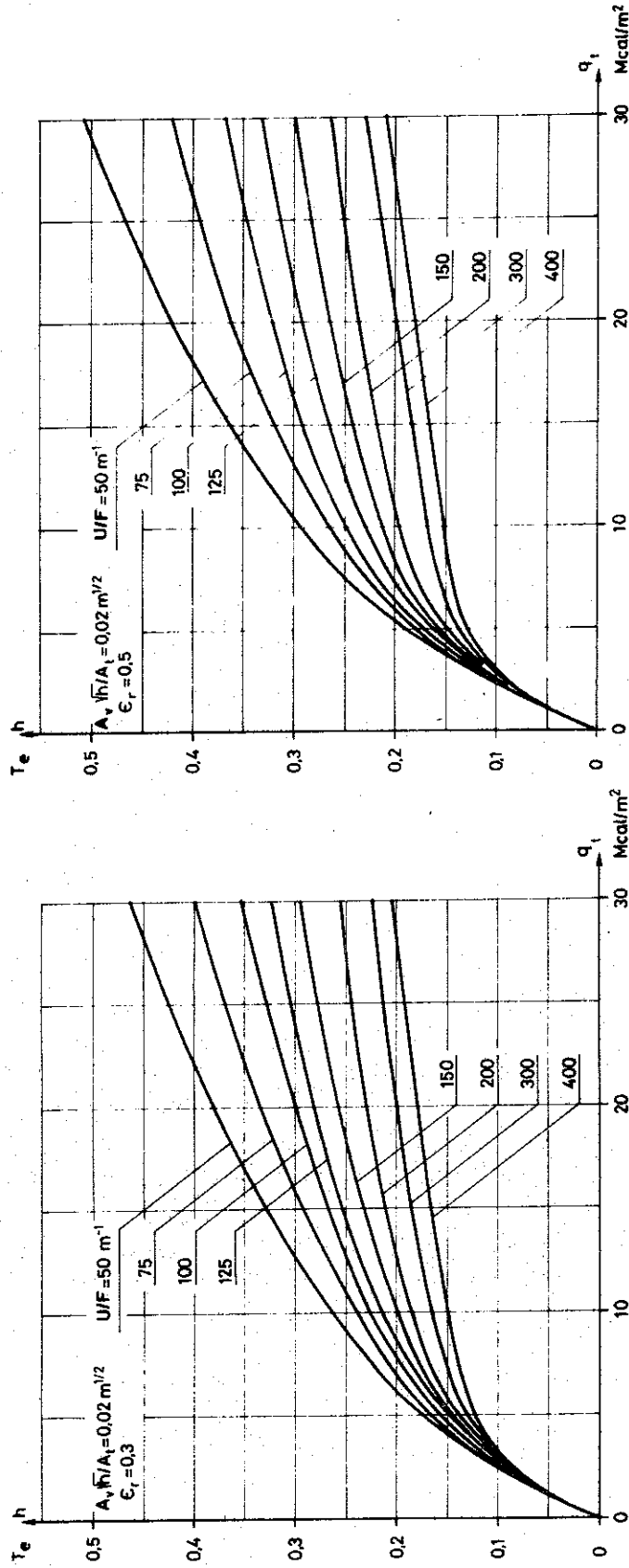


Fig. II,11

Fig. II,10

Equivalent time of fire duration T_e , defined according to Fig. II,9, for a fire exposed, non-insulated steel structure at varying opening factor $A_v \sqrt{h}/A_t$, fire load q_t , structural parameter U/F , and resultant emissivity ϵ_r . The curves are based on characteristics of the complete process of fire development according to Fig. II,8 - fire compartment, type A.

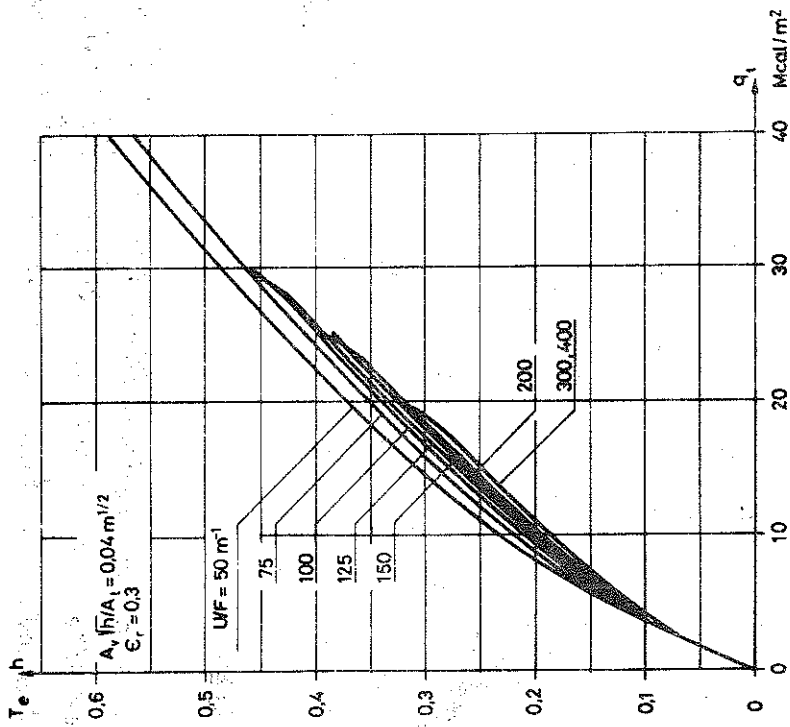


Fig. II,13

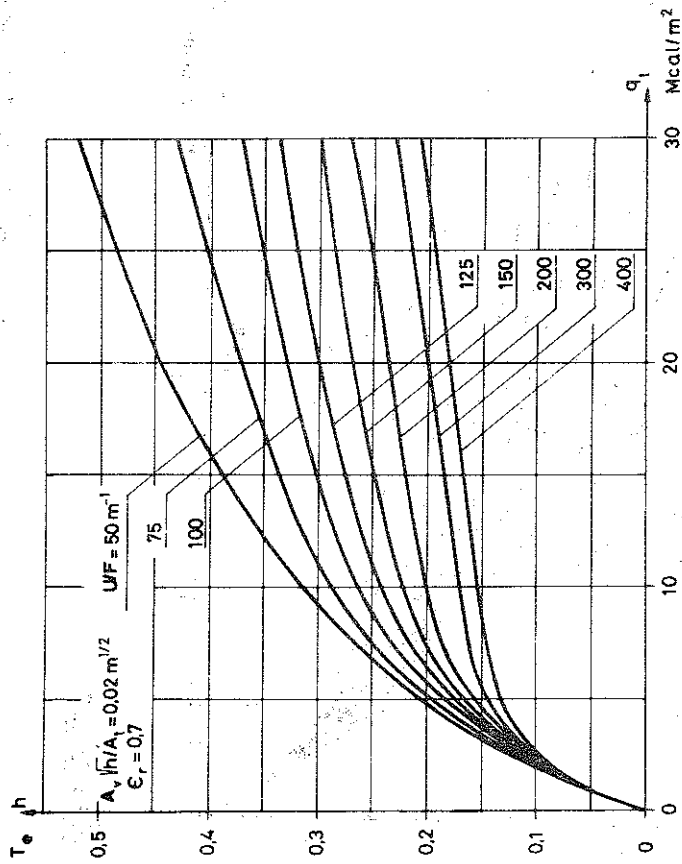


Fig. II,12

Equivalent time of fire duration T_e , defined according to Fig. II,9, for a fire exposed, non-insulated steel structure at varying opening factor $A_v \sqrt{h}/A_t$, fire load q_t , structural parameter U/F, and resultant emissivity ϵ_r . The curves are based on characteristics of the complete process of fire development according to Fig. II,8 - fire compartment, type A.

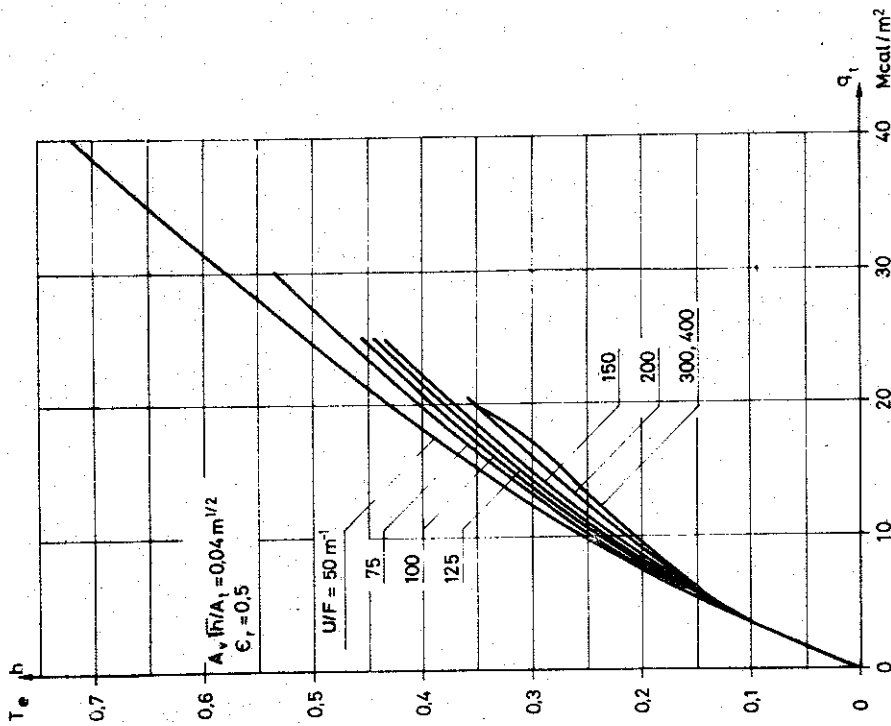


Fig. II, 14

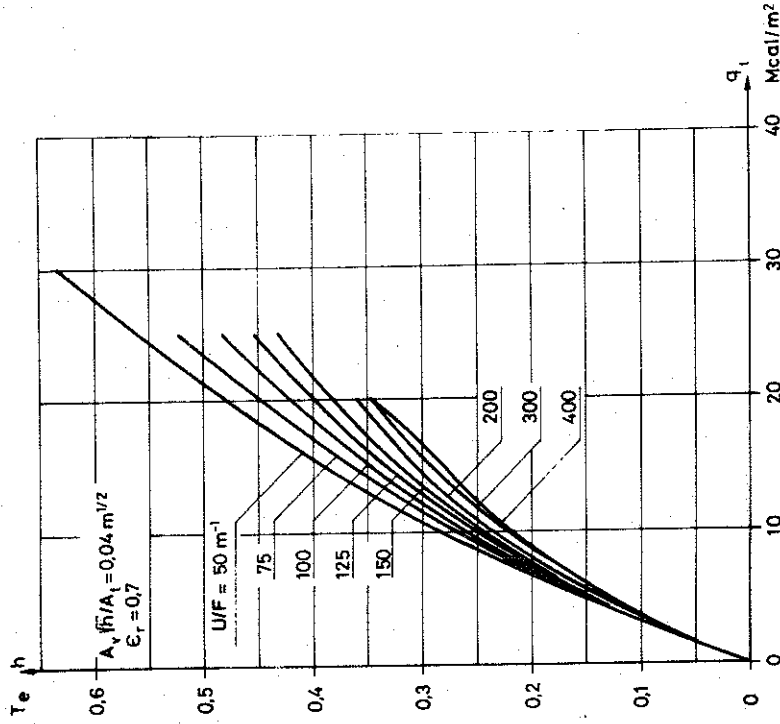


Fig. II, 15

Equivalent time of fire duration T_e , defined according to Fig. II, 9, for a fire exposed, non-insulated steel structure at varying opening factor $A_v h/A_t$, fire load q_t , structural parameter U/F , and resultant emissivity ϵ_r . The curves are based on characteristics of the complete process of fire development according to Fig. II, 8 - fire compartment, type A.

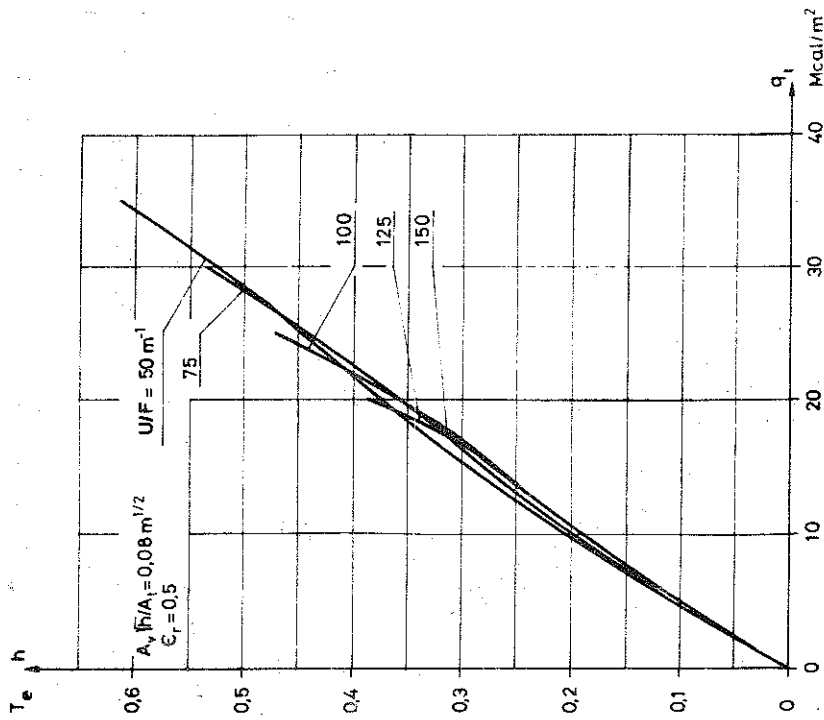


Fig. II,17

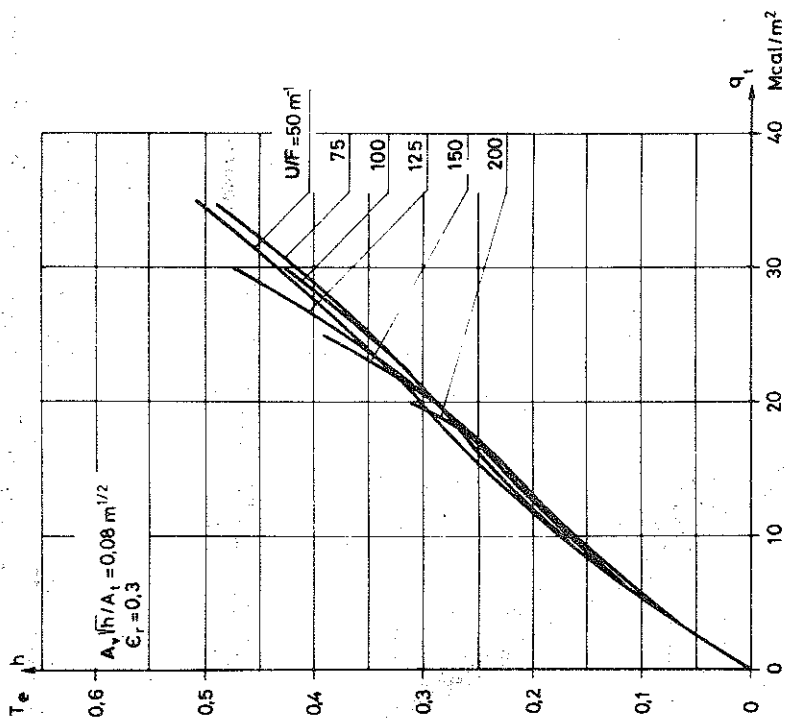


Fig. II,16

Equivalent time of fire duration T_e , defined according to Fig. II,9, for a fire exposed, non-insulated steel structure at varying opening factor $A_v \sqrt{h}/A_t$, fire load q_t , structural parameter U/F , and resultant emissivity ϵ_r . The curves are based on characteristics of the complete process of fire development according to Fig. II,8 - fire compartment, type A.

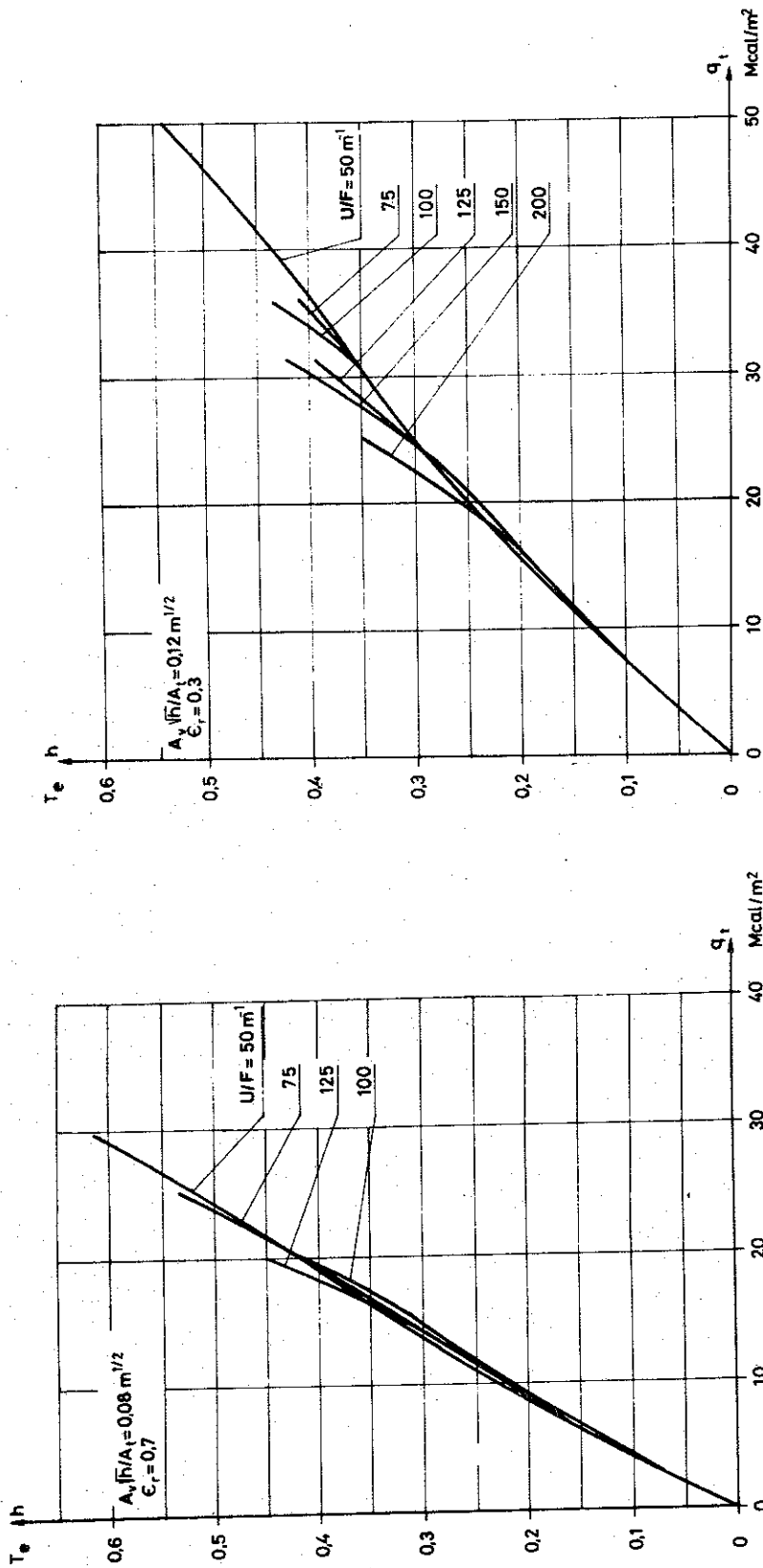


Fig. II,18

Fig. II,19

Equivalent time of fire duration T_e , defined according to Fig. II,9, for a fire exposed, non-insulated steel structure at varying opening factor $A_v \sqrt{h}/A_t$, fire load q_t , structural parameter U/F , and resultant emissivity ϵ_r . The curves are based on characteristics of the complete process of fire development according to Fig. II,8 - fire compartment, type A.

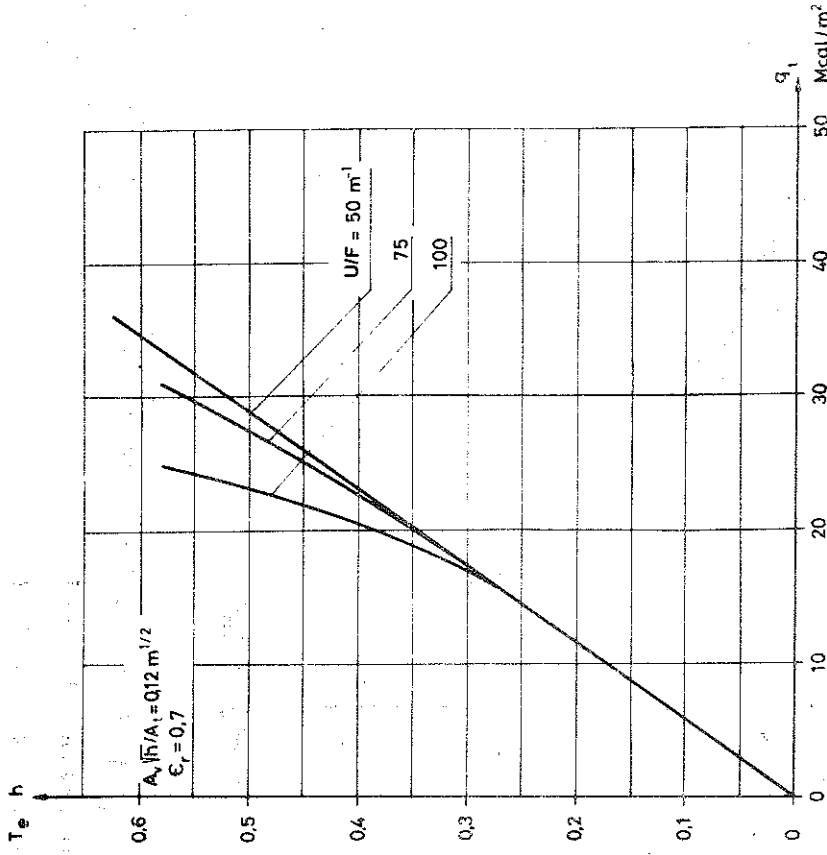


Fig. II,21

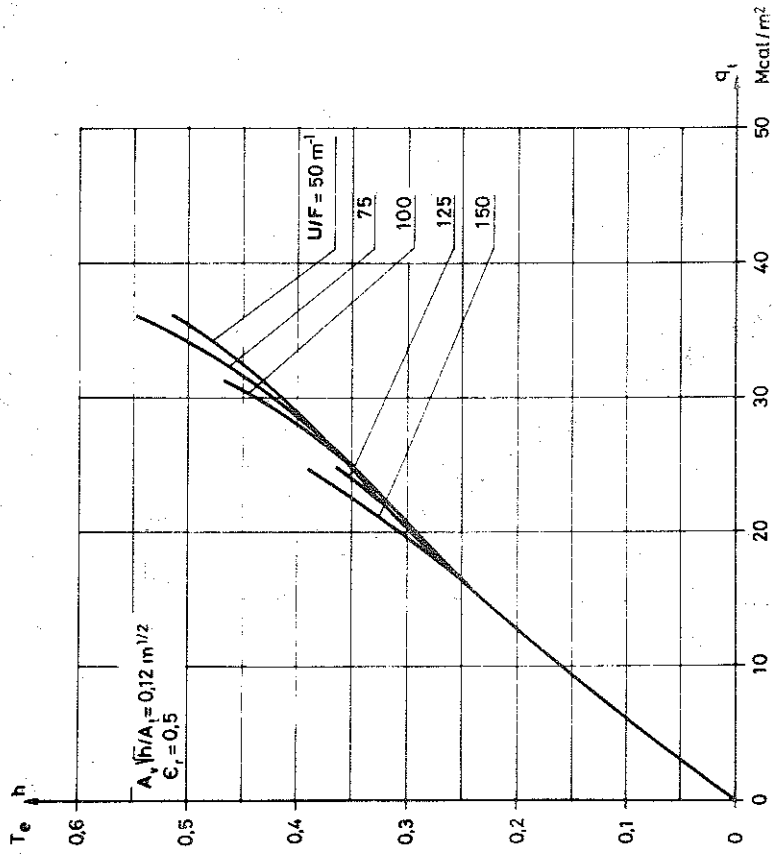


Fig. II,20

Equivalent time of fire duration T_e , defined according to Fig. II,9, for a fire exposed, non-insulated steel structure at varying opening factor $A_v \sqrt{h}/A_t$, fire load q_t , structural parameter U/F , and resultant emissivity ϵ_r . The curves are based on characteristics of the complete process of fire development according to Fig. II,8 - fire compartment, type A.

level of $\vartheta_{s_{\max}}$ will vary with the fire load q_t , the opening factor $A_v \sqrt{h}/A_t$, the structural parameter U/F , and the resultant emissivity ϵ_r . For a given practical application, the actual value of the maximum steel temperature $\vartheta_{s_{\max}}$ can be determined directly from the diagram in Fig II,32 to II,43.

In Fig. II,22 to II,25, design curves are presented, giving the equivalent time of fire duration T_e for insulated, fire exposed steel structures as a function of the opening factor $A_v \sqrt{h}/A_t$, the fire load q_t , and the structural parameter $U\lambda_i/Fd$. U is the inside jacket surface of the insulation per unit length of the structure, λ_i the thermal conductivity of the insulation material, and d the thickness of the insulation. For insulated steel structures the influence on the equivalent time of fire duration of variations in the resultant emissivity is of little importance. The dash-line curves of the figure are giving directly the level of the maximum steel temperature $\vartheta_{s_{\max}}$ for the different combinations of q_t , $A_v \sqrt{h}/A_t$ and $U\lambda_i/Fd$.

A modified way of defining the equivalent time of fire duration T_e has been presented by Law {22}- {24} with limited application to fire exposed insulated steel structures. Among elements of construction with varying thermal characteristics with respect to fire exposure that element is chosen, which for a given gastemperature-time curve of a real fire development gets a maximum steel temperature of a fixed value. T_e is then determined over the standard time-temperature curve for the same element and the same steel temperature. By repeating this procedure for different characteristics of real fires, a diagram can be constructed, applicable to a rough determination of the equivalent time of fire duration T_e for an insulated steel structure, irrespective of the detail properties of the structure.

Diagrams constructed in this way are exemplified in Fig. II,26 and II,27. The first figure {24} then is based on gastemperature-time curves of the process of fire development, experimentally determined in full scale tests in brick and concrete compartments. Most tests are characterized by a fire load of wooden crib type, but also some tests with a fire load of furniture have been included. The figure gives the equivalent time of fire duration T_e as a function of the parameter $B/\sqrt{A_v A_{t1}}$, where B is the total fire load in kg, A_v the window area of the compartment in m^2 , and A_{t1} the

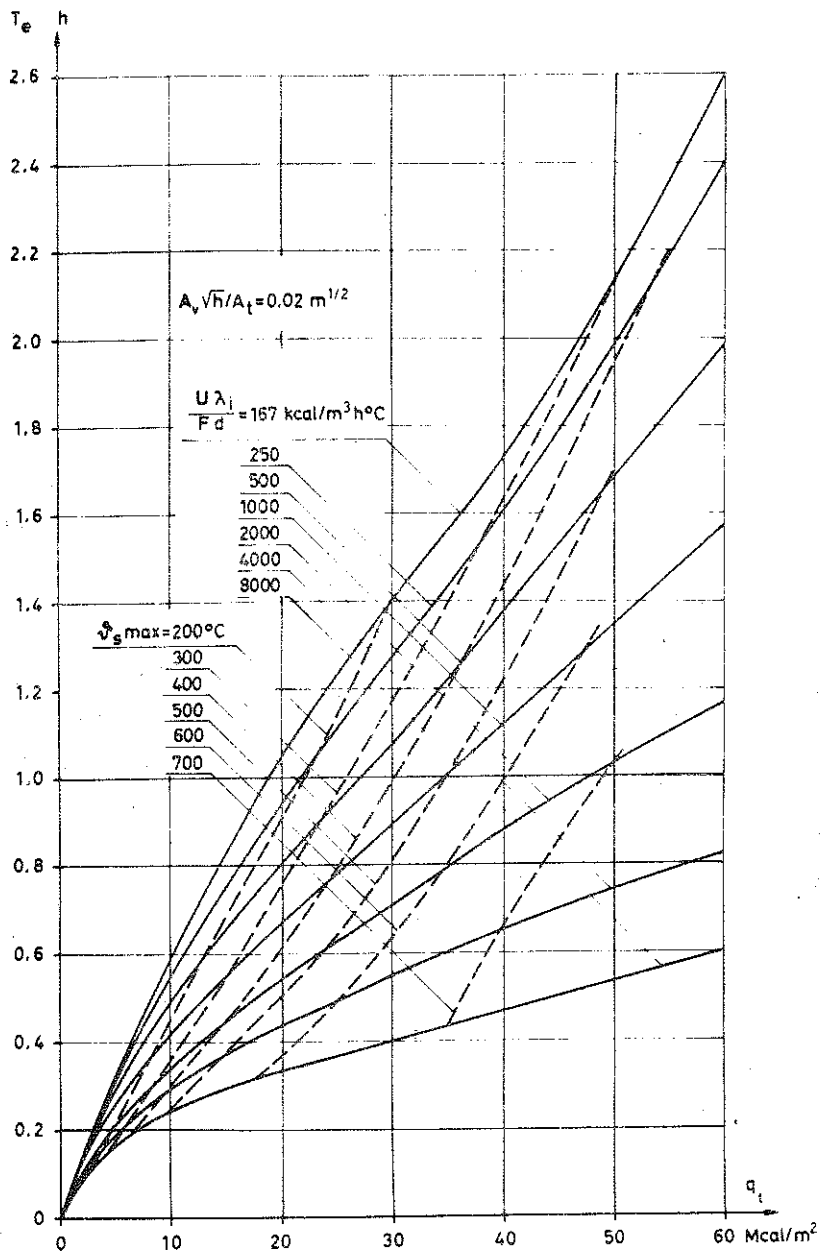


Fig. II,22

Equivalent time of fire duration T_e , defined according to Fig. II,9, for a fire exposed, insulated steel structure at varying opening factor $A_v \sqrt{h} / A_t$, fire load q_t , and structural parameter $U \lambda_i / F d$. The dash-line curves are giving the corresponding maximum steel temperature $\theta_{s \max}$. The diagrams are based on characteristics of the complete process of fire development according to Fig. II,8 - fire compartment, type A.

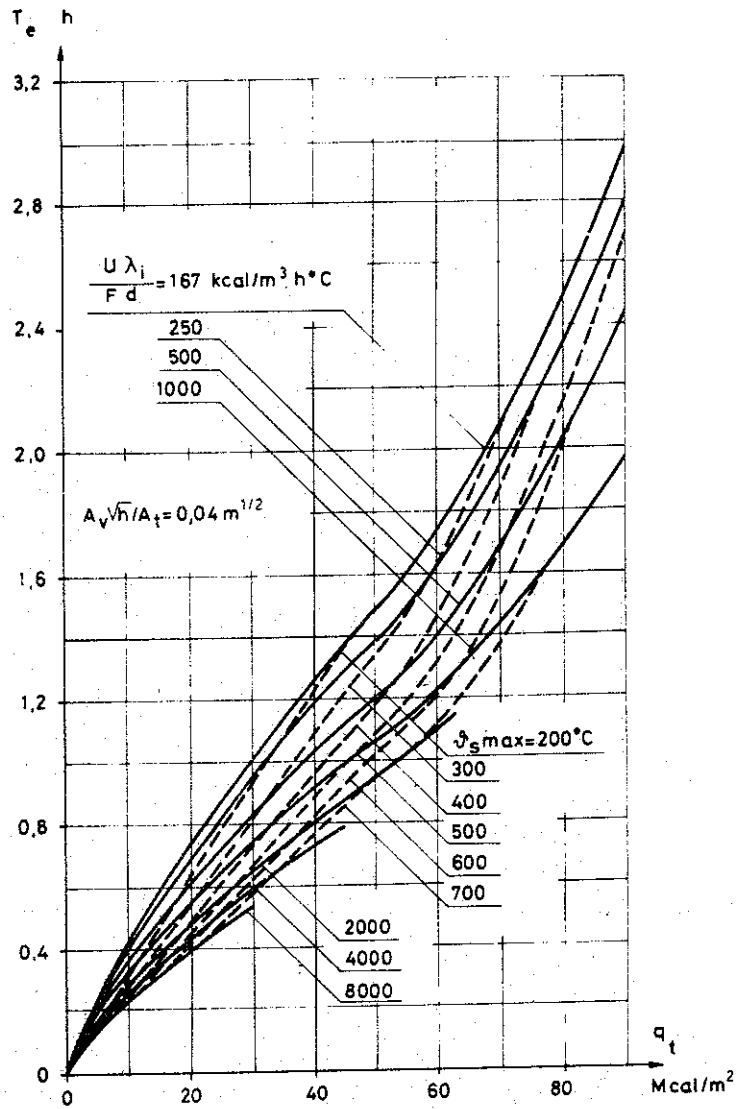


Fig. II,23

Equivalent time of fire duration T_e , defined according to Fig. II,9, for a fire exposed, insulated steel structure at varying opening factor $A_v\sqrt{h}/A_t$, fire load q_t , and structural parameter $U\lambda_i/Fd$. The dash-line curves are giving the corresponding maximum steel temperature $\phi_{s,max}$. The diagrams are based on characteristics of the complete process of fire development according to Fig. II,8 - fire compartment, type A.

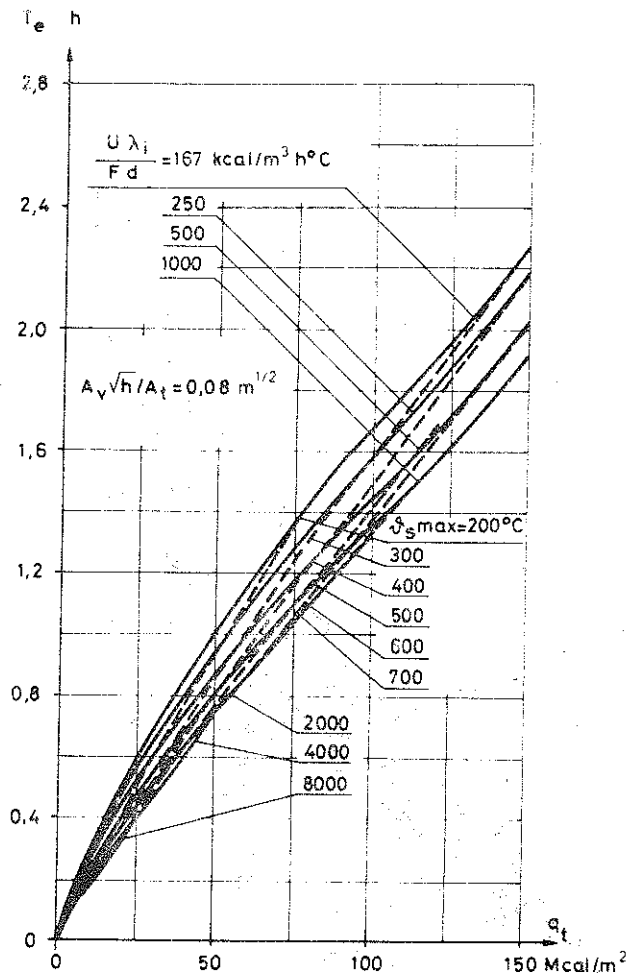


Fig. II,24

Equivalent time of fire duration T_e , defined according to Fig. II,9, for a fire exposed, insulated steel structure at varying opening factor $\frac{A_v \sqrt{h}}{A_t}$, fire load q_t , and structural parameter $\frac{U \lambda_1}{F d}$. The dash-line curves are giving the corresponding maximum steel temperature $\theta_{s,max}$. The diagrams are based on characteristics of the complete process of fire development according to Fig. II,8 - fire compartment, type A.

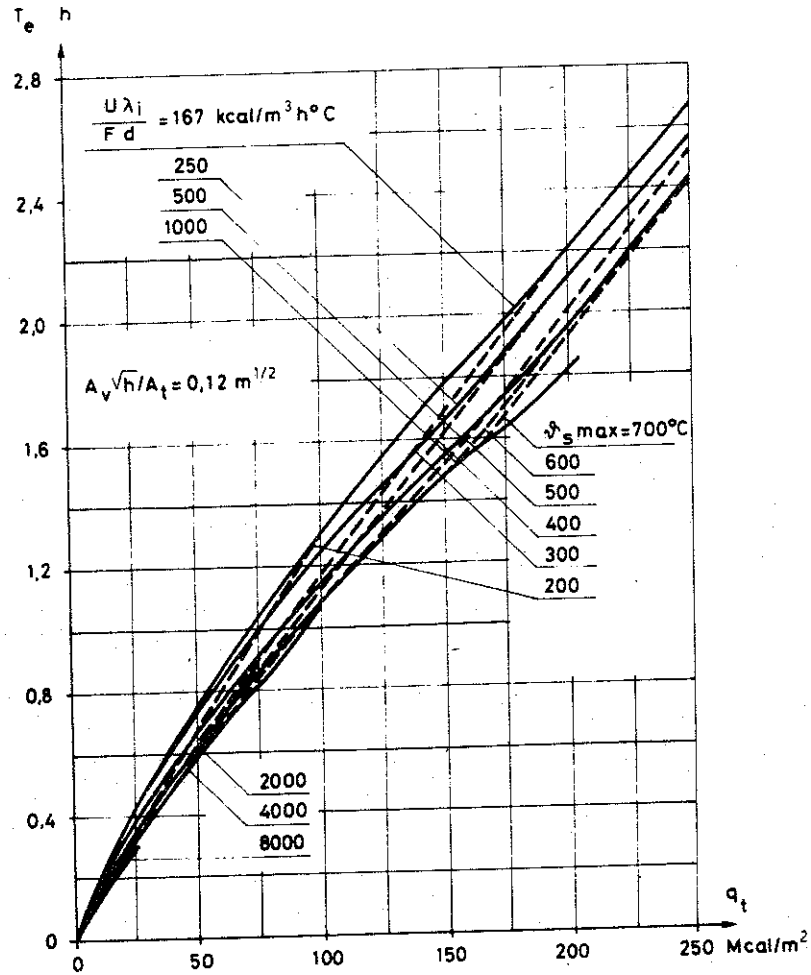


Fig. II,25

Equivalent time of fire duration T_e , defined according to Fig. II,9, for a fire exposed, insulated steel structure at varying opening factor $A_v\sqrt{h}/A_t$, fire load q_t , and structural parameter $U\lambda_i/Fd$. The dash-line curves are giving the corresponding maximum steel temperature $\vartheta_{s \text{ max}}$. The diagrams are based on characteristics of the complete process of fire development according to Fig. II,8 - fire compartment, type A.

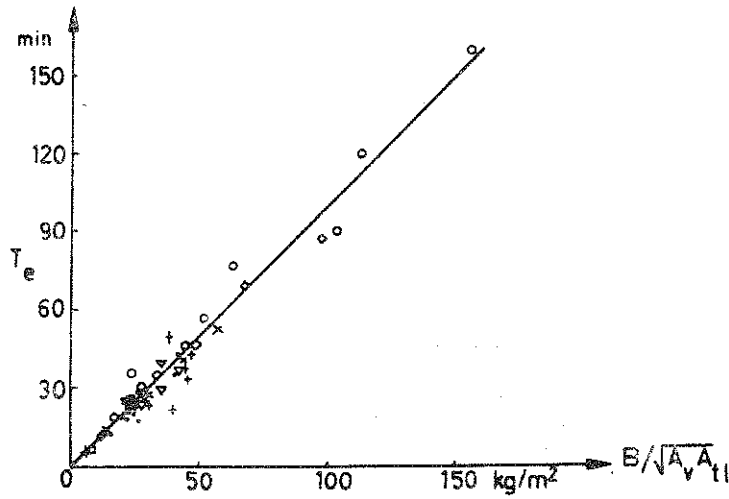


Fig. II,26

Equivalent time of fire duration for insulated steel structures T_e , determined in a more approximate way, as a function of the parameter $B/\sqrt{A_v A_t1}$. The straight line corresponds to the formula

$$T_e = 0.95 \frac{B}{\sqrt{A_v A_t1}} \quad (\text{min})$$

The diagram is based on gastemperature-time curves of full-scale tests in brick and concrete compartments. {24}

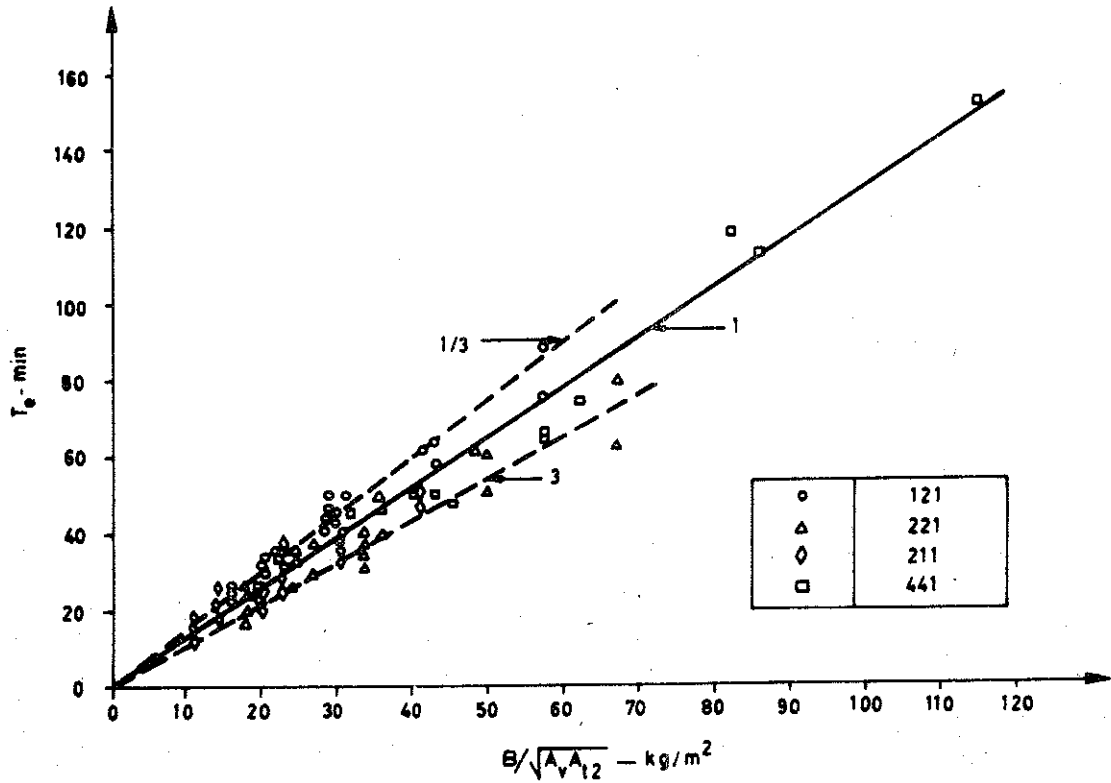


Fig. II,27

Equivalent time of fire duration for insulated steel structures T_e , determined in a more approximate way, as a function of the parameter $B/\sqrt{A_v A_{t2}}$. The straight full-line corresponds to the formula

$$T_e = 1.3 \frac{B}{\sqrt{A_v A_{t2}}} \quad (\text{min})$$

The figure is based on gastemperature-time curves from a comprehensive CIB model test investigation. For the three figure code for the shape of the compartment, cf. Fig. II, 1 {2}

surrounding area of the compartment, excluding the opening area. The analogous Fig. II,27 {2} is based on the results of a very comprehensive CIB model test investigation concerning the process of fire development with wooden crib fires. The equivalent time of fire duration T_e is presented as a function of the parameter $B/\sqrt{A_t} A_{t2}$, where A_{t2} is the area of the internal surfaces of the compartment in m^2 , excluding floor and opening areas. The figure gives a range of variation of T_e connected to varying porosity properties or spacing of the fire load.

The experimental-theoretical values shown in Fig. II,26 and II,27 are connected to a critical steel temperature of $550^\circ C$. In calculating the equivalent time of fire duration, the influence of the height of the window opening h is omitted, although the theory behind suggests that it should be included. The influence was omitted because the values of T_e for these experiments showed no significant variation with h .

Curves, analogous to those presented in Fig. II,26 and II,27, also can be deduced in a pure theoretical way, starting from the gastemperature-time curves according to Fig. II,8, valid for a fire compartment of type A. For a given level of a critical steel temperature ϑ_s , such an analysis primarily results in a diagram, applicable to un-insulated or insulated steel structures, presenting the equivalent time of fire duration T_e as a function of the opening factor $A_v \sqrt{h}/A_t$ and the fire load q_t . Fig. II,28, exemplifies such a diagram for insulated steel structures and Fig. II,29, a corresponding diagram for un-insulated steel structures. Both diagrams are calculated for a critical steel temperature ϑ_s of $500^\circ C$.

In Fig. II,28, the curve for the fire load $q_t = 60 \text{ Mcal}/m^2$ is compared with the related curves according to Fig. II,26 - dash-line curve - Fig. II,27 - dash-and-dot-line curve. Since the latter two curves are directly based on experimental fire development characteristics for ventilation controlled as well as fuel bed controlled compartment fires, the relatively good agreement between the three curves can be seen as an exemplifying confirmation on the statement in Chapter II, 2, that the gastemperature-time curves according to Fig. II,8 can be used in practice as an intermediate part of a determination of the decisive quantity of a fire exposed, load-bearing structure, viz. the minimum value of the load-bearing capacity during a complete process of fire

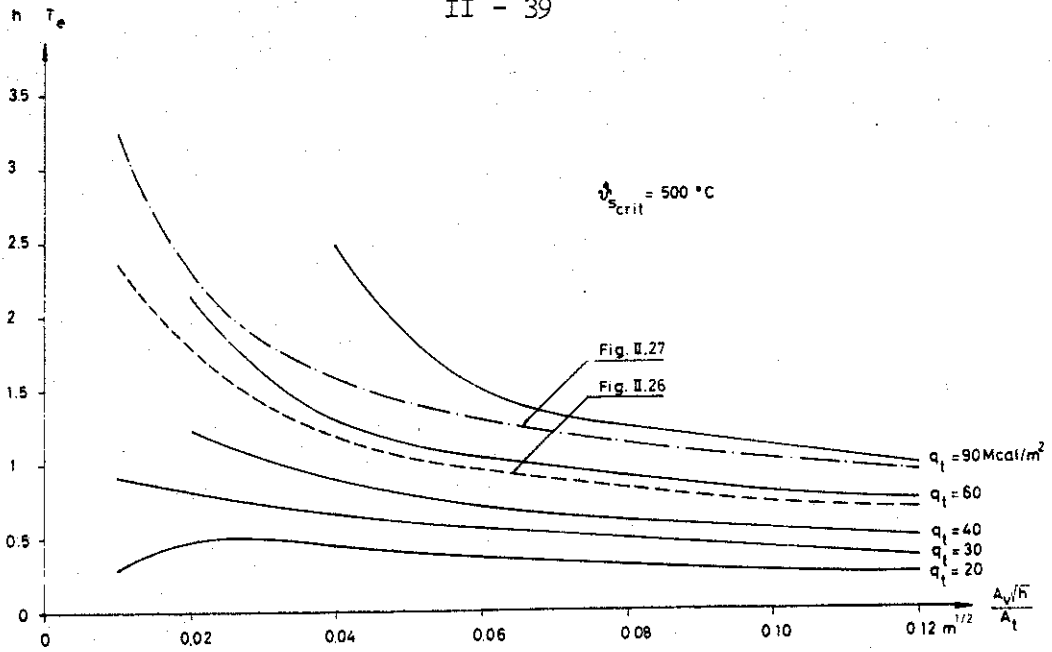


Fig. II,28

Approximate equivalent time of fire duration for insulated steel structures T_e as a function of the opening factor $\frac{A_v \sqrt{h}}{A_t}$ and the fire load q_t . The curves are based on a critical steel temperature $\theta_{s_crit} = 500^\circ C$. Fire compartment, type A.

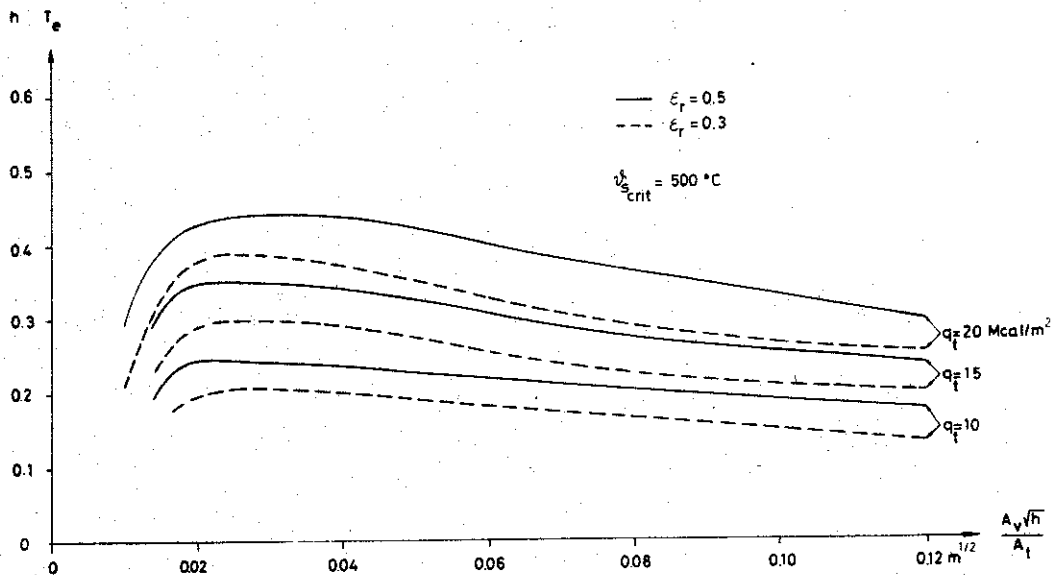


Fig. II,29

Approximate equivalent time of fire duration for uninsulated steel structures T_e as a function of the opening factor $\frac{A_v \sqrt{h}}{A_t}$, the fire load q_t , and the resultant emissivity ϵ_r . The curves are based on a critical steel temperature $\theta_{s_crit} = 500^\circ C$. Fire compartment, type A.

development. The curves generally demonstrate a reduction of the equivalent time of fire duration with increasing opening factor or ventilation of the fire compartment.

Fig. II,29, which is deduced for un-insulated, fire exposed steel structures, demonstrates fragmentarily the influence on the equivalent time of fire duration T_e of variations in the resultant emissivity ϵ_r . The curves in this figure have been calculated on the assumption, that the value of ϵ_r is 0.5 in the standard fire resistance test. For such furnace characteristics, the curves give T_e as a function of the opening factor $A_v \sqrt{h}/A_t$ and the fire load q_t for the resultant emissivity at a real fire exposure $\epsilon_r = 0.5$ and 0.3, respectively. The curves accentuate the desirability of having a fire test furnace calibrated with respect to the heat transmission characteristics, with reference to well-defined standard test specimens. This problem is of great importance for un-insulated steel structures. For a fire exposed, insulated steel structure, the influence of variations of the resultant emissivity usually is practically negligible.

The curves, shown in Fig. II,28, and II,29, are determined on the assumption of a critical steel temperature of 500°C. The influence on the equivalent time of fire duration T_e of varying level of the critical steel temperature ϑ_s is illustrated in Fig. II,30 for an insulated steel structure, fire exposed according to Fig. II,8, at a fire load $q_t = 30 \text{ Mcal/m}^2$. The curves comprise the steel temperature range 200 to 600°C. At a hasty glance the results seem to be surprising in giving an increased equivalent time of fire duration with a decreasing level of the critical steel temperature ϑ_s . This fact is due to the character of the applied concept of the equivalent time of fire duration. At a given, real fire exposure - given values of the opening factor $A_v \sqrt{h}/A_t$ and the fire load q_t - a maximum steel temperature of 300°C corresponds to a steel structure with much better insulation properties than for a steel structure, for which the same fire exposure causes a maximum steel temperature of 600°C. It follows from the figure, that the influence on T_e of variations in the critical steel temperature is considerable for lower values of the opening factor $A_v \sqrt{h}/A_t$. Within the regime $A_v \sqrt{h}/A_t > 0.05 \text{ m}^{1/2}$ the same influence is comparatively small. This can also be seen directly from the more accurate curves of Fig. II,22 to II,25. Fig. II,30 convincingly demonstrates the great difficulties in surveying the detail consequences and in estimating the inaccuracies at different applications for a concept of the equivalent time of fire duration, which

is independent of the structural design.

On the basis of the curves, presented in Fig. II,28, a rough design diagram can be constructed similar to the diagrams according to Fig. II,26 and II,27. In studying the possibilities for doing so, it was then found appropriate from a physical point of view to use the parameter $B/\sqrt{A_v A_t} \sqrt{h}$ for a characterization of the compartment and fire load properties instead of the parameter $B/\sqrt{A_v A_{t1}}$ or $B/\sqrt{A_v A_{t2}}$ which offers the advantage that the influence of varying the shape of the window openings can be taken into account. Fig. II,31, shows, in the form of a family of dash-line curves, the transformation of the curves of Fig. II,28 to a relation between the equivalent time of fire duration T_e and the parameter $B/\sqrt{A_v A_t} \sqrt{h}$. Approximately, the point values can be summarised by the formula

$$T_e = 0.28 \frac{B}{\sqrt{A_v A_t} \sqrt{h}} \quad (\text{min}) \quad \dots \quad \dots \quad \dots \quad \dots \quad \dots \quad (II-11)$$

The formula requires that the total fire load B is given in Mcal, the opening area A_v and the total area, surrounding the compartment, A_t in m^2 , and the opening height h in m.

The fact that a direct transformation of a number of theoretical curves results in another group of curves according to Fig. II,31, shows that a unique relationship does not exist between the equivalent time of fire duration T_e and the fire load-compartment parameter $B/\sqrt{A_v A_t} \sqrt{h}$. For frequent values of the opening height h and the quotient A_{t1}/A_t , the formulae according to Fig. II,26, and eq. (II-11) are giving about the same equivalent time of fire duration T_e .

Summing up, it can be established, that the equivalent time of fire duration T_e can be determined roughly from Fig. II,28 or still more roughly from Fig. II,31, or Eq. (II-11) for insulated steel structures and roughly from Fig. II,29, for un-insulated steel structures. Generally, the curves in these figures are deduced on the assumption of a critical steel temperature of 500°C . For insulated steel structures, Fig. II,28, or II,31, can be used for other levels of critical steel temperature, too, within the regime $A_v \sqrt{h}/A_t > 0.05m^{1/2}$. For lower values of the opening factor $A_v \sqrt{h}/A_t$, the curves of Fig. II,28 and II,31, are to be applied with the greatest caution,

when the critical steel temperature obviously deviates from the value 500°C , cf. Fig. II,30. The concept of equivalent time of fire duration T_e , valid for Fig. II,28 to II,31, and for Eq. (II-11), makes T_e dependent only on the compartment and fire load properties, but independent of the design of the structure. As a consequence different combinations of the opening factor $A_v\sqrt{h}/A_t$ and the fire load q_t are associated with steel structures having different characteristics with respect to the structural design. In that way, estimations of the inaccuracies of the concept at different applications are rendered difficult.

A more accurate, differentiated determination of the equivalent time of fire duration T_e can be quickly carried out from Fig. II,10 to II,21 for un-insulated steel structures and from Fig. II,22 to II,25 for insulated steel structures. These figures are directly based on the concept of T_e according to Fig. II,9 and give T_e as a function of the fire process parameters as well as the structural parameters. To different combinations of the fire process and structural parameters then belong different levels of the maximum steel temperature θ_s . In each individual case, this level can be determined in a direct way from Fig. II,32 to II,43 for un-insulated steel structures and from Fig. II,22 to II,25 for insulated steel structures.

5. Main characteristics of a structural fire engineering design, directly based on differentiated gastemperature-time curves

In chapter II.4, methods have been described for a differentiated fire engineering design of load-bearing steel structures over an equivalent time of fire duration, connected to the heating according to the standard time-temperature curve. Alternatively, a differentiated, structural fire engineering design directly can be based on the gastemperature-time curves of the complete process of fire development. Such a design comprises the following main components {20}, {25} to {29}:

- (a) The choice, in each particular case, of representative combustion characteristics of the fire load.
- (b) The determination for these combustion characteristics of the gastemperature-time curve and the convection and radiation properties of the complete process of fire development, taking into account the geometry of

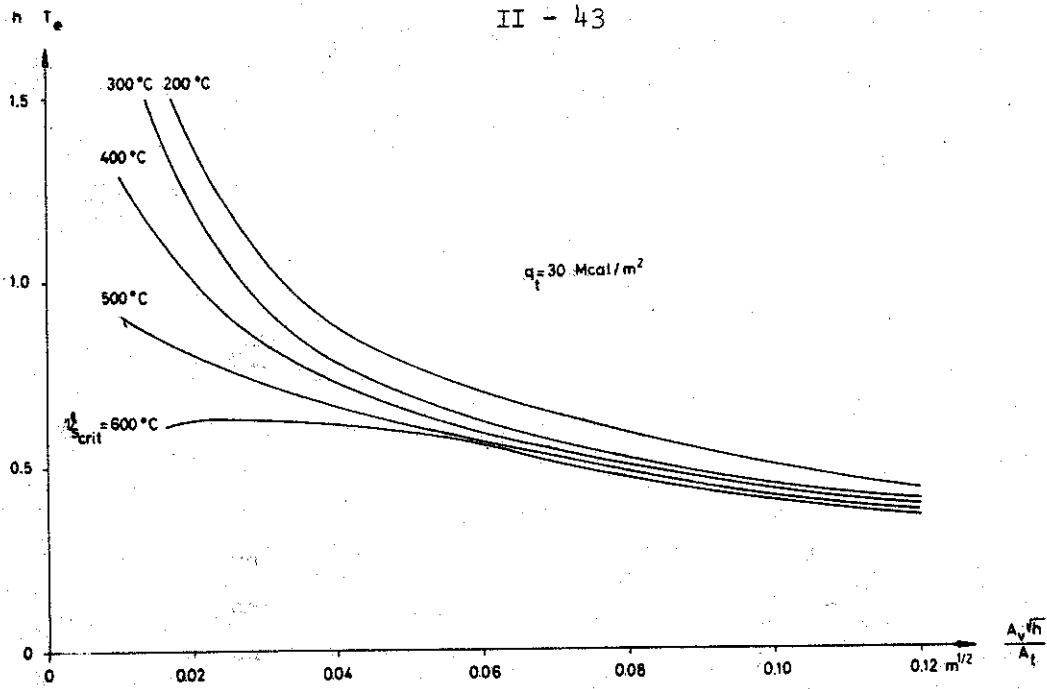


Fig. II,30 The influence on the approximate equivalent time of fire duration T_e of varying level of the critical steel temperature $\vartheta_{s_{crit}}$ for an insulated steel structure. Fire compartment, type A.

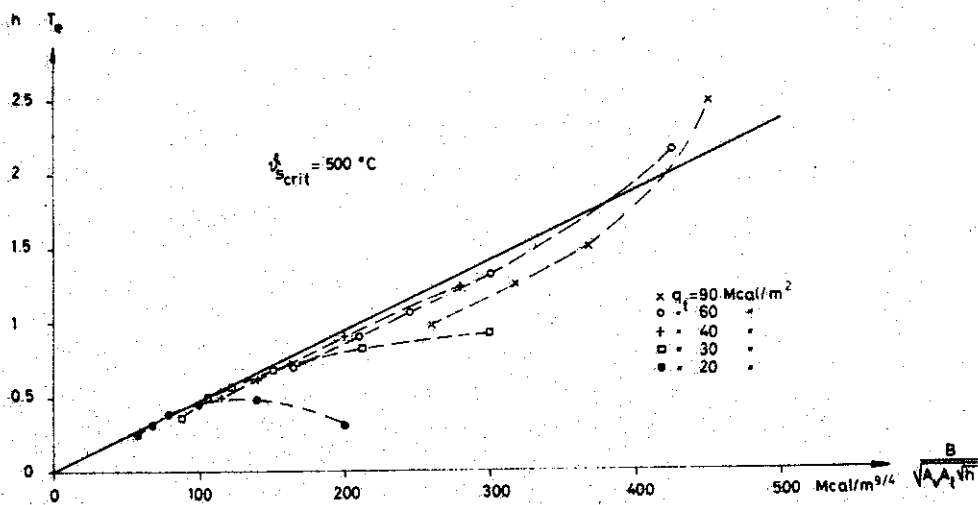


Fig. II,31 Equivalent time of fire duration for insulated steel structures T_e , determined in a more approximate way, as a function of the parameter $B/\sqrt{A_v A_t} \sqrt{h}$. The figure is based on gastemperature-time curves according to Fig. II,8 and on a critical steel temperature $\vartheta_{s_{crit}} = 500^\circ C$. Fire compartment, type A.

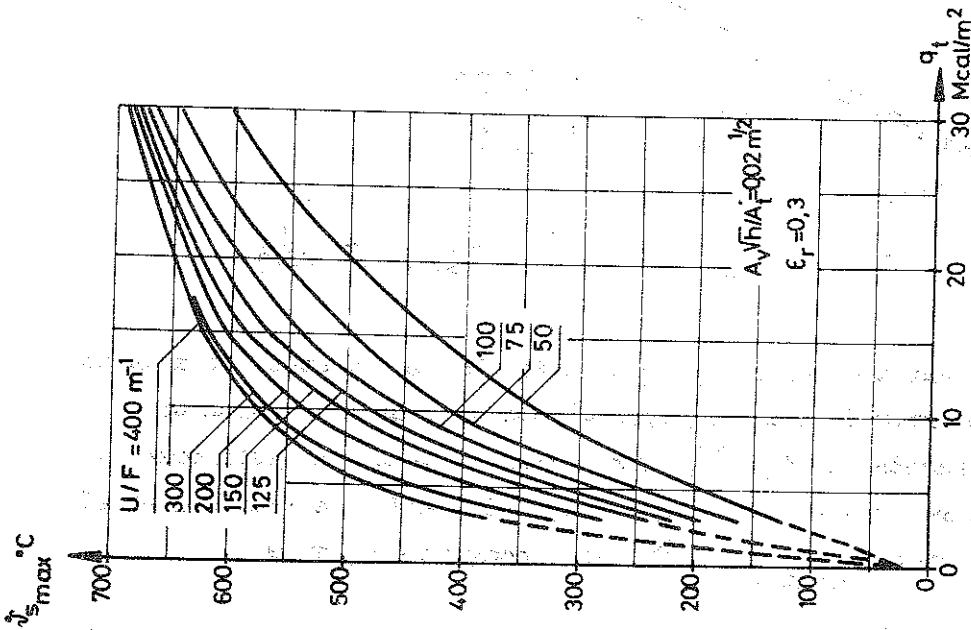


Fig. II, 32

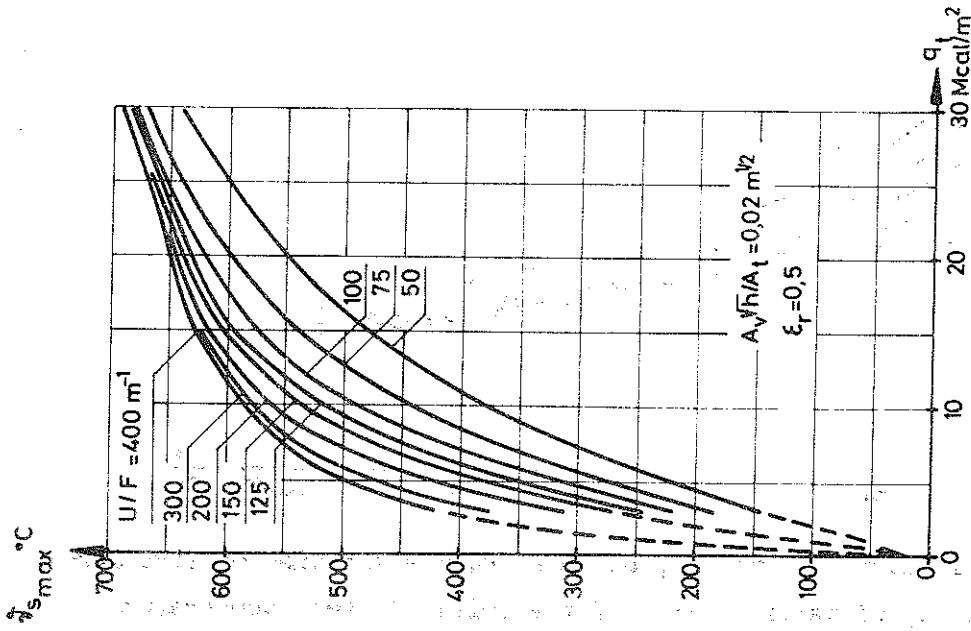


Fig. II, 33

Maximum steel temperature $\vartheta_{s,max}$ for a fire exposed, non-insulated steel structure at varying opening factor $A_v \sqrt{h}/A_t$, fire load q_t , structural parameter U/F , and resultant emissivity ϵ_r . The curves are based on characteristics of the complete process of fire development according to Fig. II, 8 - fire compartment, type A (28)

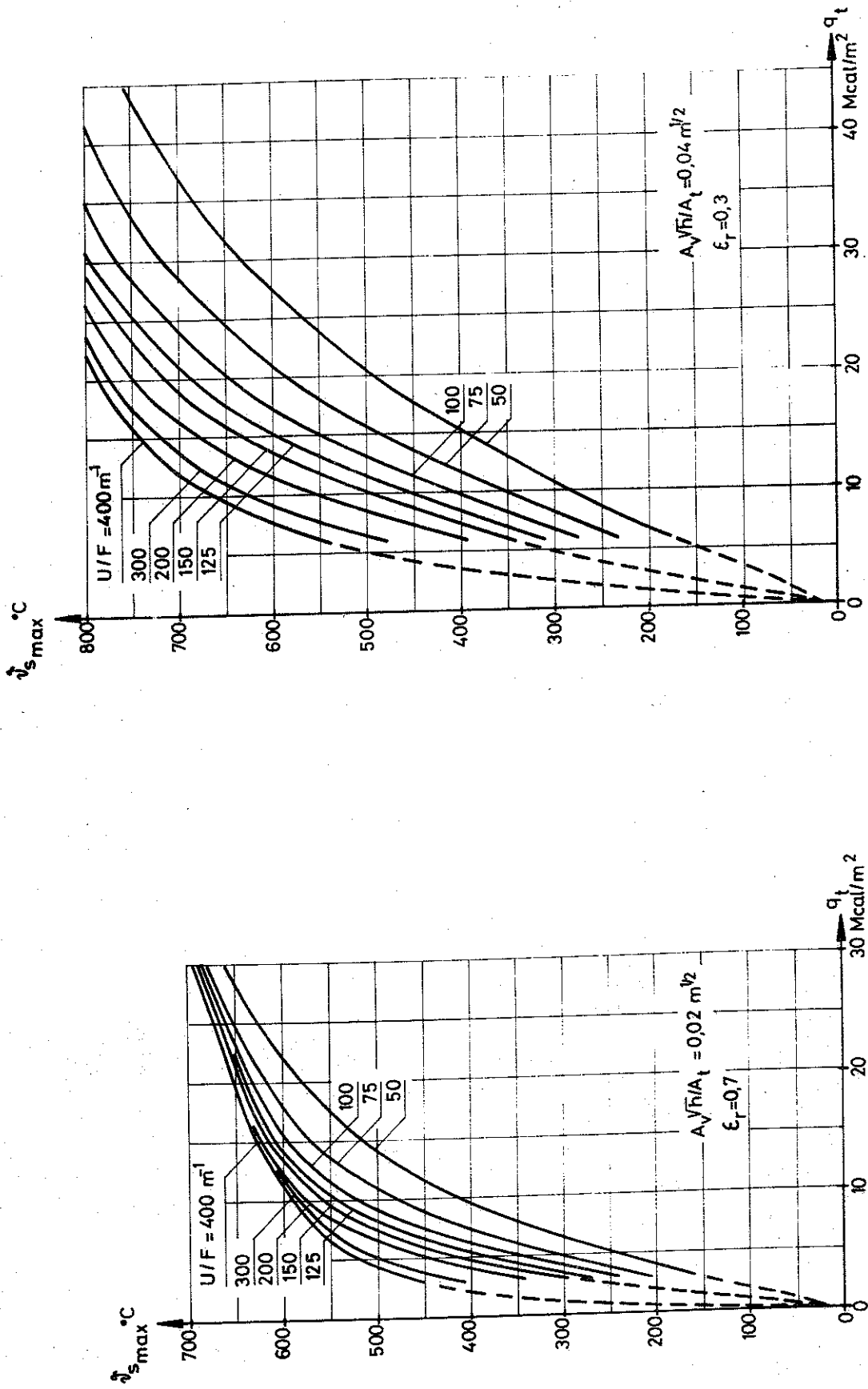


Fig. II, 35

Fig. II, 34

Maximum steel temperature $\vartheta_{s,max}$ for a fire exposed, non-insulated steel structure at varying opening factor $A_v\sqrt{h}/A_t$, fire load q_t , structural parameter U/F , and resultant emissivity ϵ_r . The curves are based on characteristics of the complete process of fire development according to Fig. II, 8 - fire compartment, type A (28)

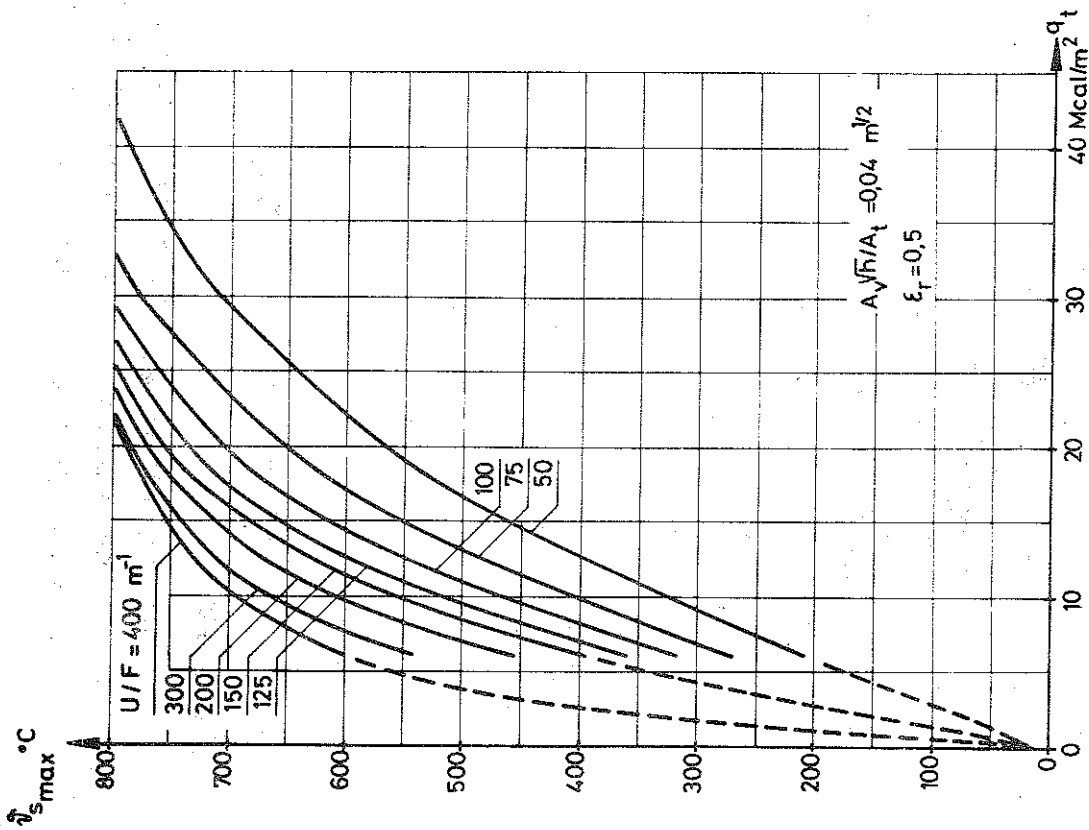


Fig. II, 36

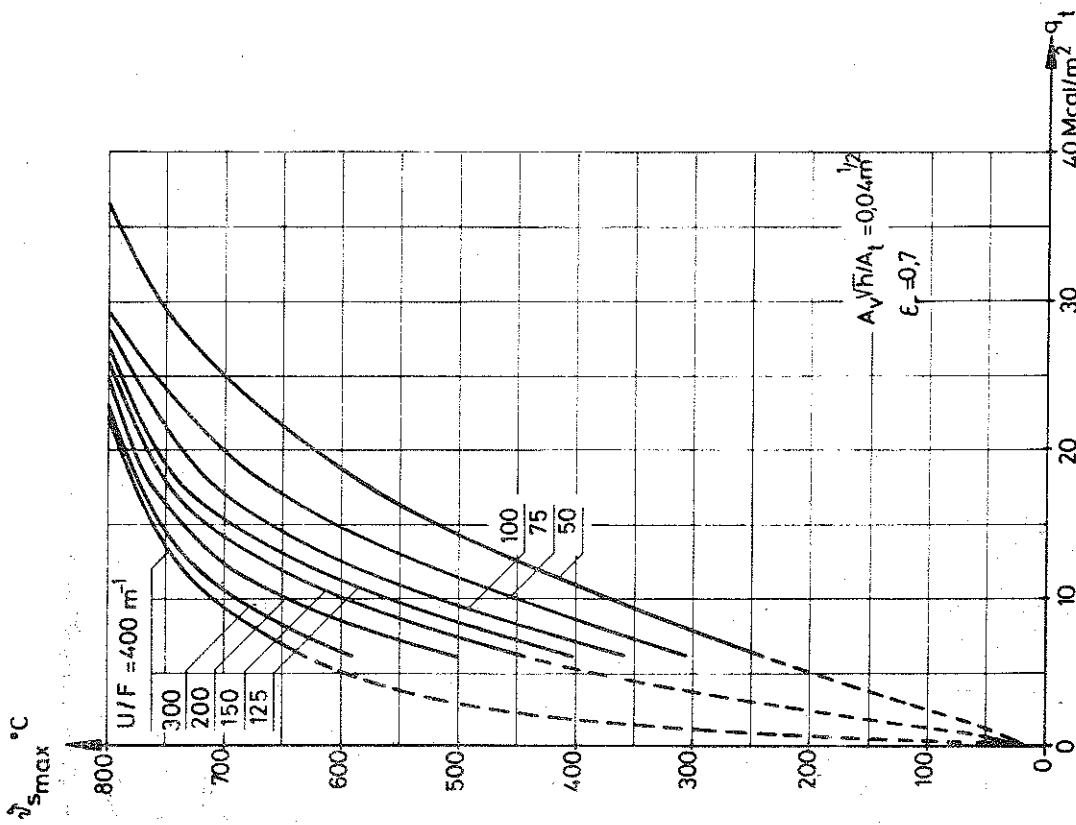


Fig. II, 37

Maximum steel temperature $\theta_{s,max}$ for a fire exposed, non-insulated steel structure at varying opening factor $A_v \sqrt{h}/A_t$, fire load q_t , structural parameter U/F , and resultant emissivity ϵ_r . The curves are based on characteristics of the complete process of fire development according to Fig. II, 8 - fire compartment, type A (28)

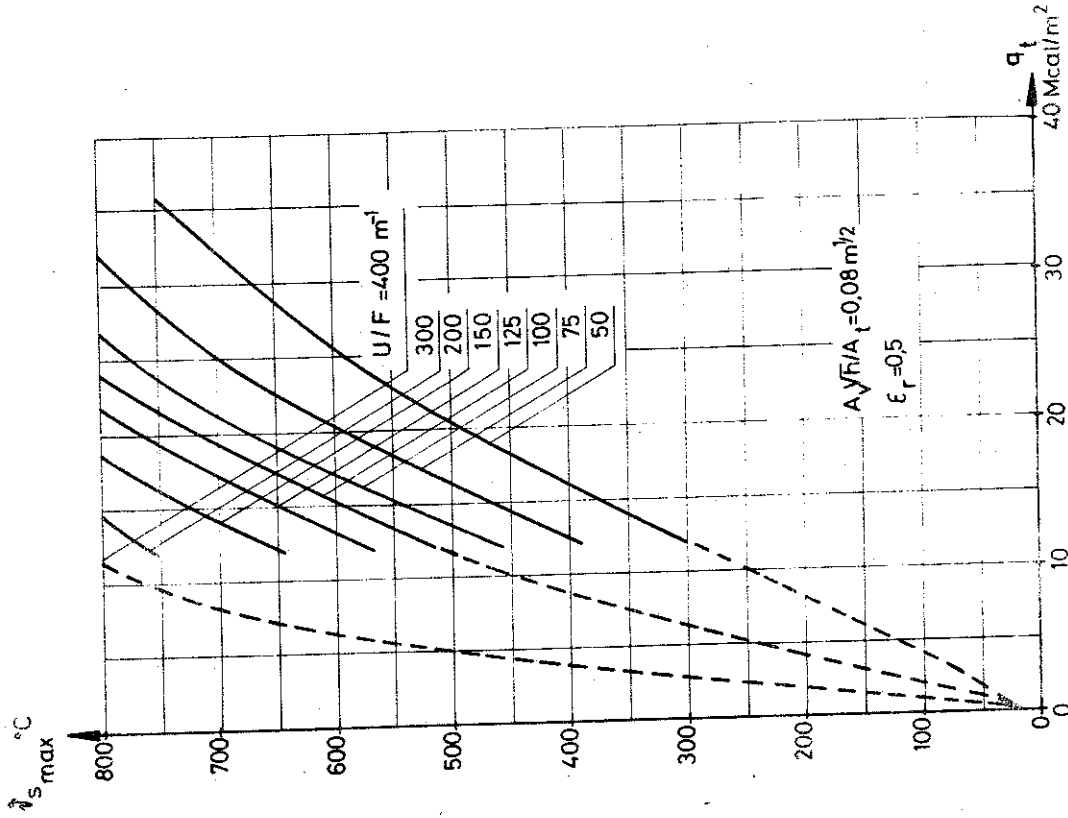


Fig. II, 39

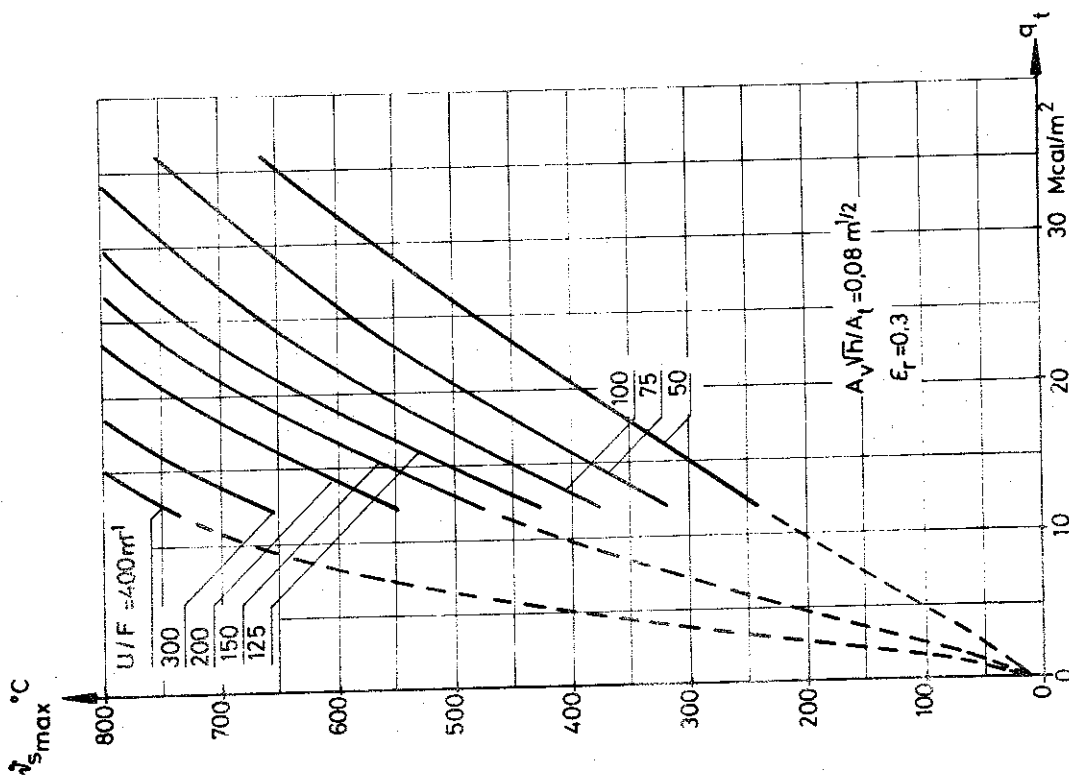


Fig. II, 38

Maximum steel temperature Δs_{max} for a fire exposed, non-insulated steel structure at varying opening factor $A_v\sqrt{h}/A_t$, fire load q_t , structural parameter U/F , and resultant emissivity ϵ_r . The curves are based on characteristics of the complete process of fire development according to Fig. II, 8 - fire compartment, type A {28}

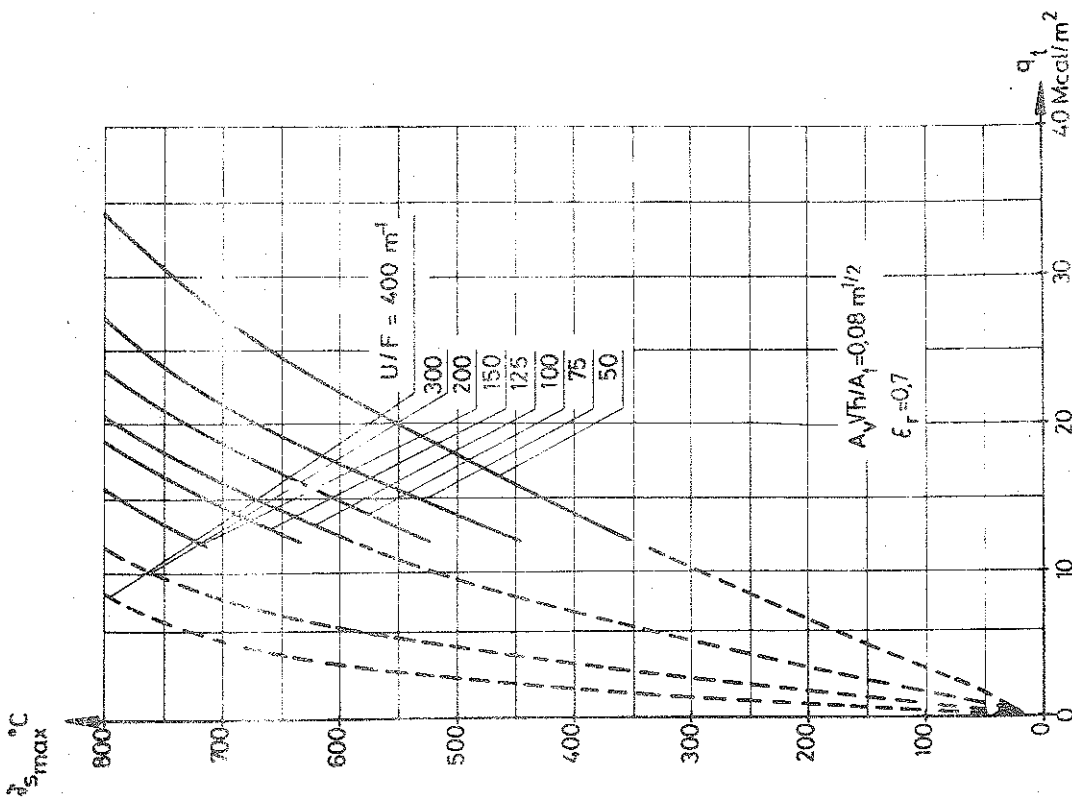


Fig. II, 40

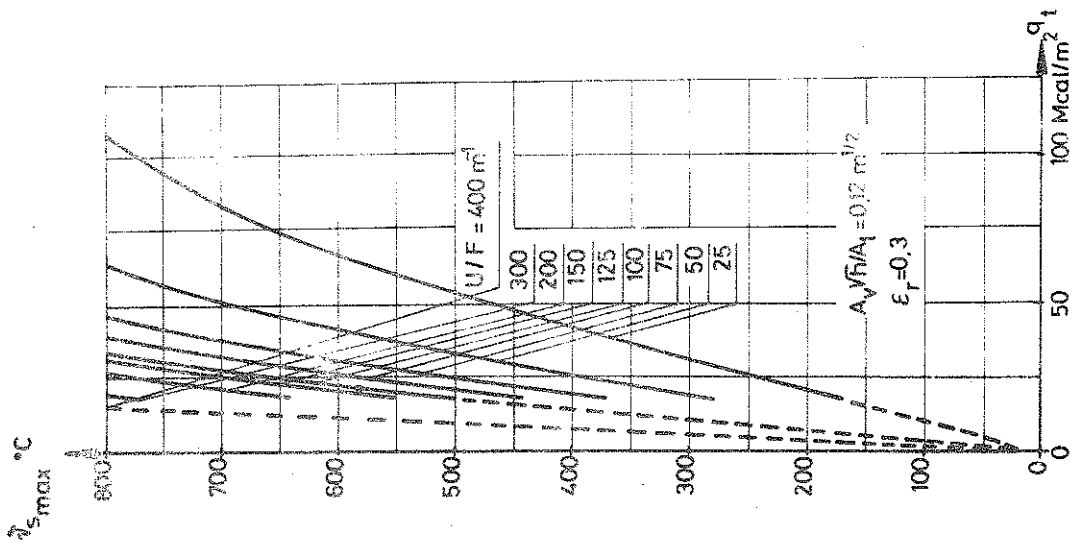


Fig. II, 41

Maximum steel temperature $t_{s,max}$ for a fire exposed, non-insulated steel structure at varying opening factor $A_v F/A_1$, fire load q_1 , structural parameter U/F , and resultant emissivity ϵ_r . The curves are based on characteristics of the complete process of fire development according to Fig. II,8 - fire compartment, type A (28)

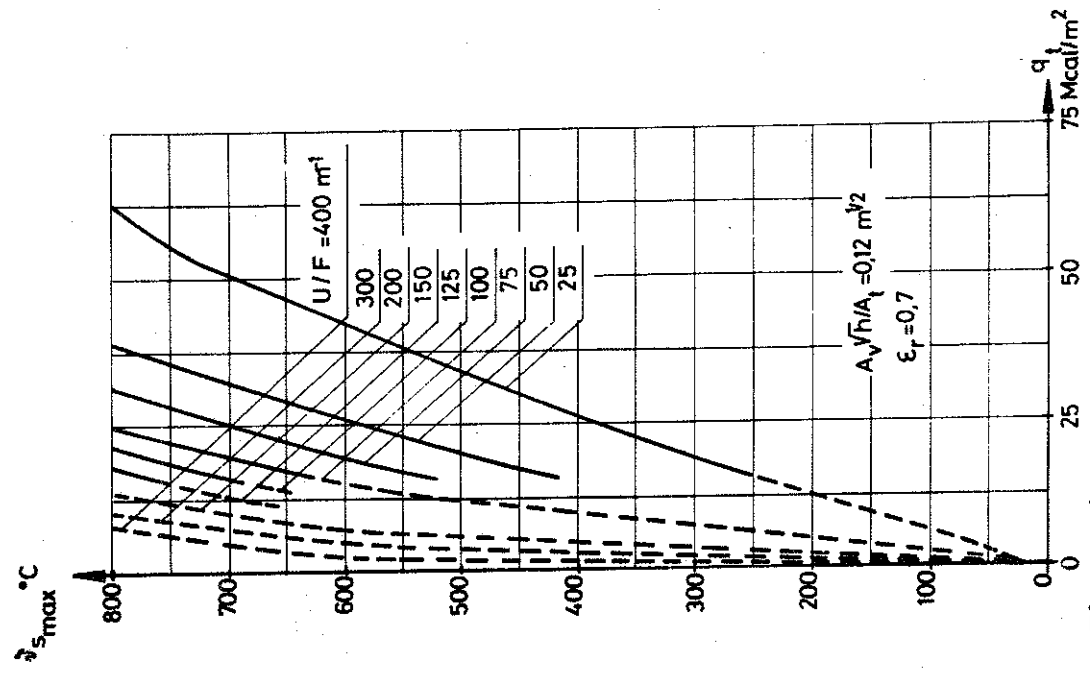


Fig. II, 43

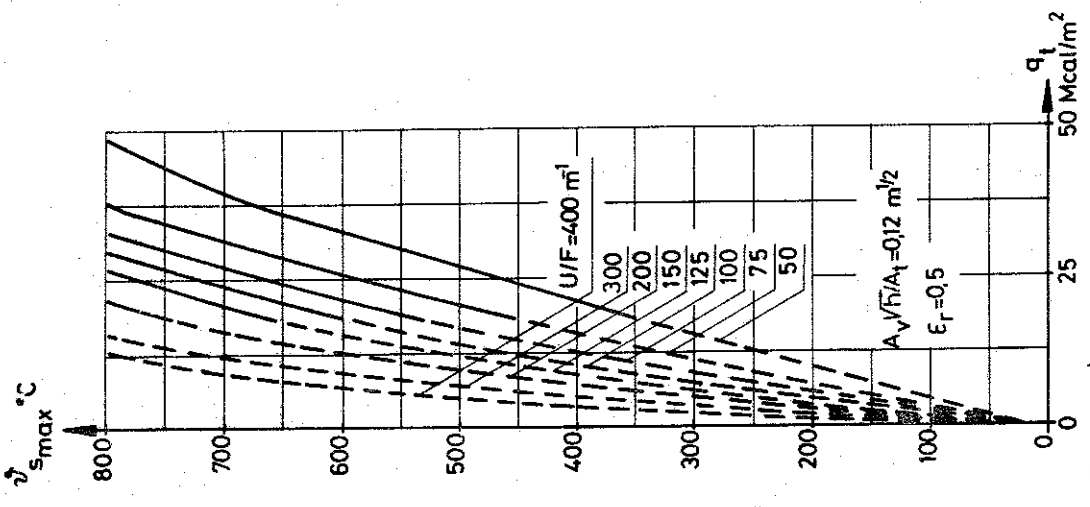


Fig. II, 42

Maximum steel temperature $\vartheta_{s,max}$ for a fire exposed, non-insulated steel structure at varying opening factor $A_v \sqrt{h}/A_t$, fire load q_t , structural parameter U/F , and resultant emissivity ϵ_r . The curves are based on characteristics of the complete process of fire development according to Fig. II, 8 - fire compartment, type A (28)

compartment, the size and shape of window and door openings and the thermal characteristics of the structures, enclosing the compartment.

(c) The determination of the corresponding temperature-time fields in the structure or the structural element, exposed to fire.

(d) The determination - on the basis of data according to (c) and data on the strength and deformation properties of the structural materials in temperature range, associated with fires - of the point of time for collapse at prescribed loading or, alternatively, of the minimum load-bearing capacity of the structure or the structural element for the process of fire development valid.

For making a differentiated structural fire engineering design according to these principles practically applicable for the structural engineer, it is necessary to supplement the procedure with design diagrams for different types of structures or structural elements. The design diagrams required must comprise informations for facilitating on one hand a calculation of the determining temperature of the fire exposed structure, on the other a translation to the corresponding static behaviour and load-bearing capacity of the structure. Examples of such diagrams for a temperature determination are shown in Fig. II,32 to II,63.

Fig. II,32, to II,43 {28} present design curves, giving directly the maximum steel temperature $\vartheta_{s_{max}}$ for a fire exposed, non-insulated steel structure at varying opening factor $A_v \sqrt{h}/A_t$, fire load q_t , and quotient U/F . Three different values of the resultant emissivities ϵ_r , viz. 0.3, 0.5, and 0.7, are covered by the curves. U is the fire exposed surface and F the volume of the steel structure per unit length. The diagrams are based on gastemperature-time curves of the fire compartment according to Fig. II,8. For fire compartments with other thermal characteristics of the surrounding structures, the same design diagrams for $\vartheta_{s_{max}}$ can be used in combination with rules for a transformation from one fire compartment to another via fictitious values of the fire load q_t and the opening factor $A_v \sqrt{h}/A_t$ according to Table II-1.

Under the same conditions of fire exposure, the design diagrams in Fig. II, 44 to II,59 {28} give the maximum steel temperature $\vartheta_{s_{max}}$ for an insulated steel structure at varying opening factor $A_v \sqrt{h}/A_t$, fire load q_t , and quotients U/F and d/λ_i . U is the inside jacket surface of the insulation per

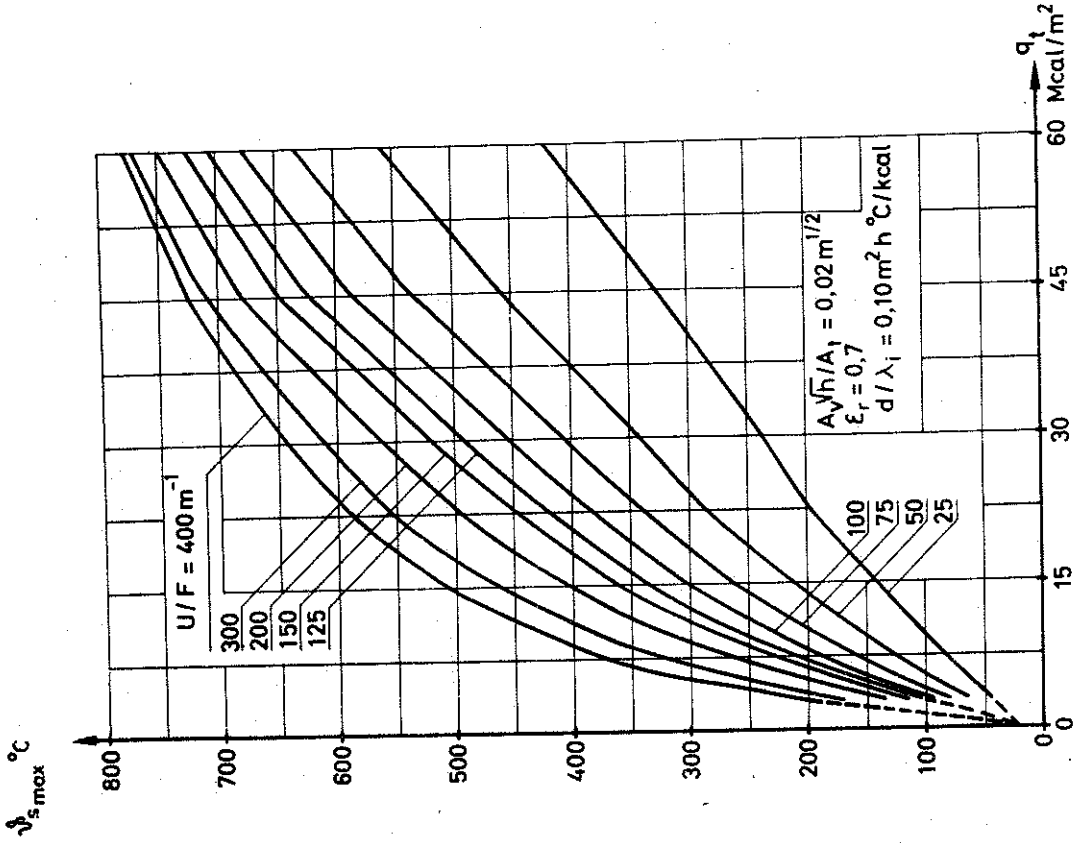


Fig. II, 45

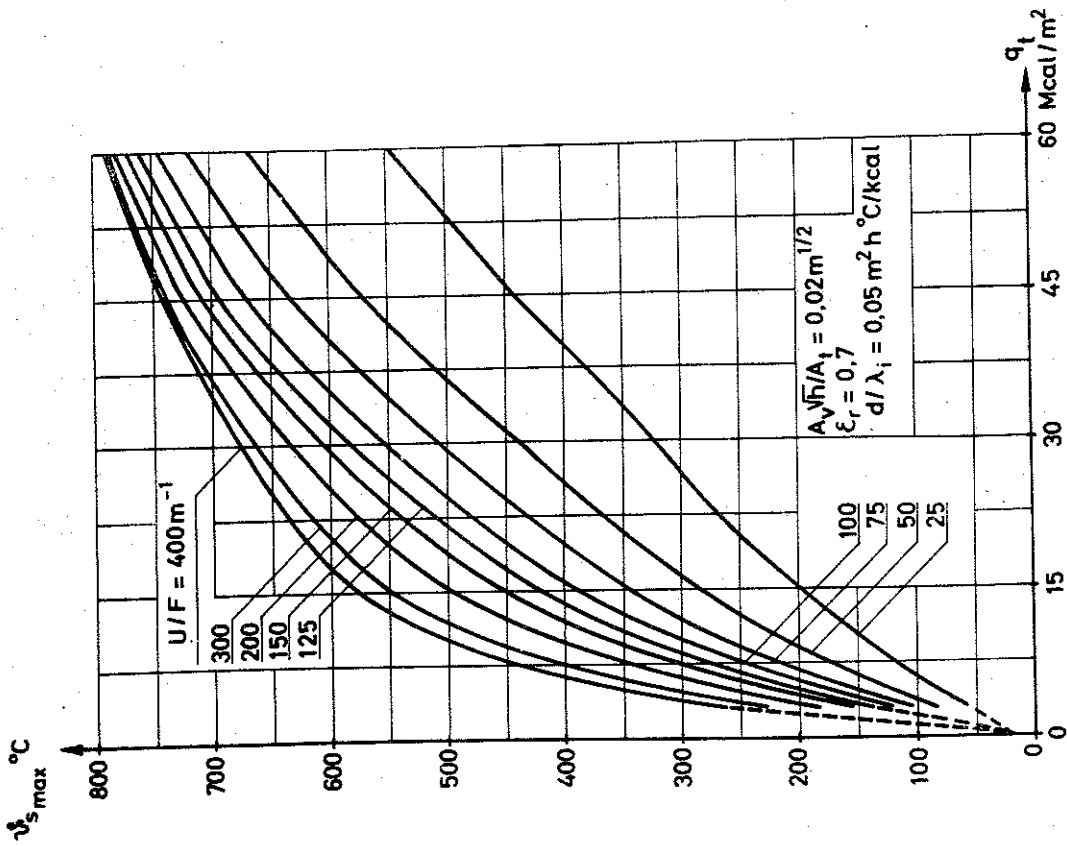


Fig. II, 44

Maximum steel temperature $\vartheta_{s,max}$ for a fire exposed, insulated steel structure at varying opening factor $A_v\sqrt{h}/A_t$, fire load q_t , and structural parameters U/F and d/λ_i . The curves are based on characteristics of the complete process of fire development according to Fig. II, 8 - fire compartment, type A (28)

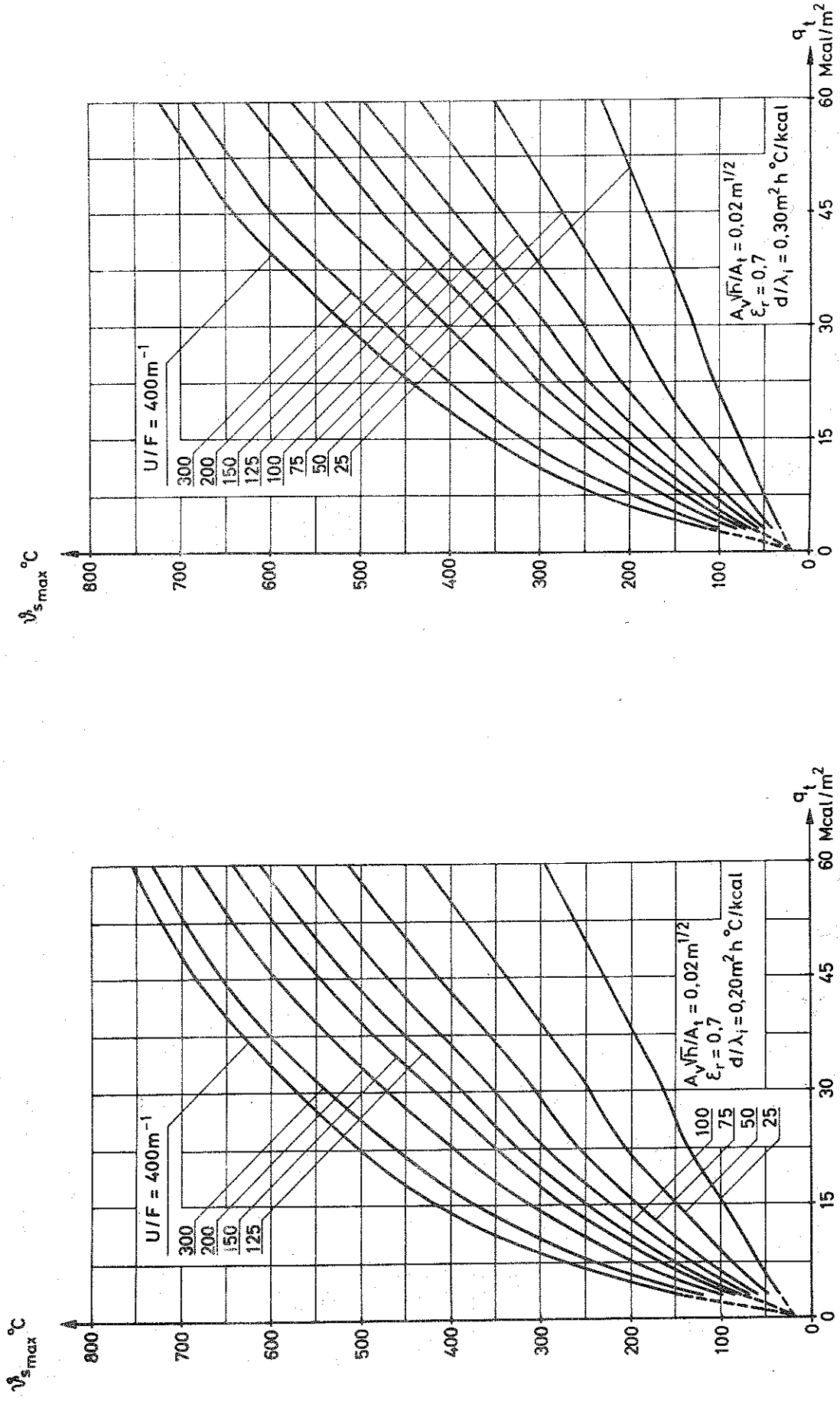


Fig. II, 47

Fig. II, 46

Maximum steel temperature $\vartheta_{s,max}$ for a fire exposed, insulated steel structure at varying opening factor $A_v/h/A_t$, fire load q_t , and structural parameters U/F and d/λ_i . The curves are based on characteristics of the complete process of fire development according to Fig. II, 8 - fire compartment, type A [28]

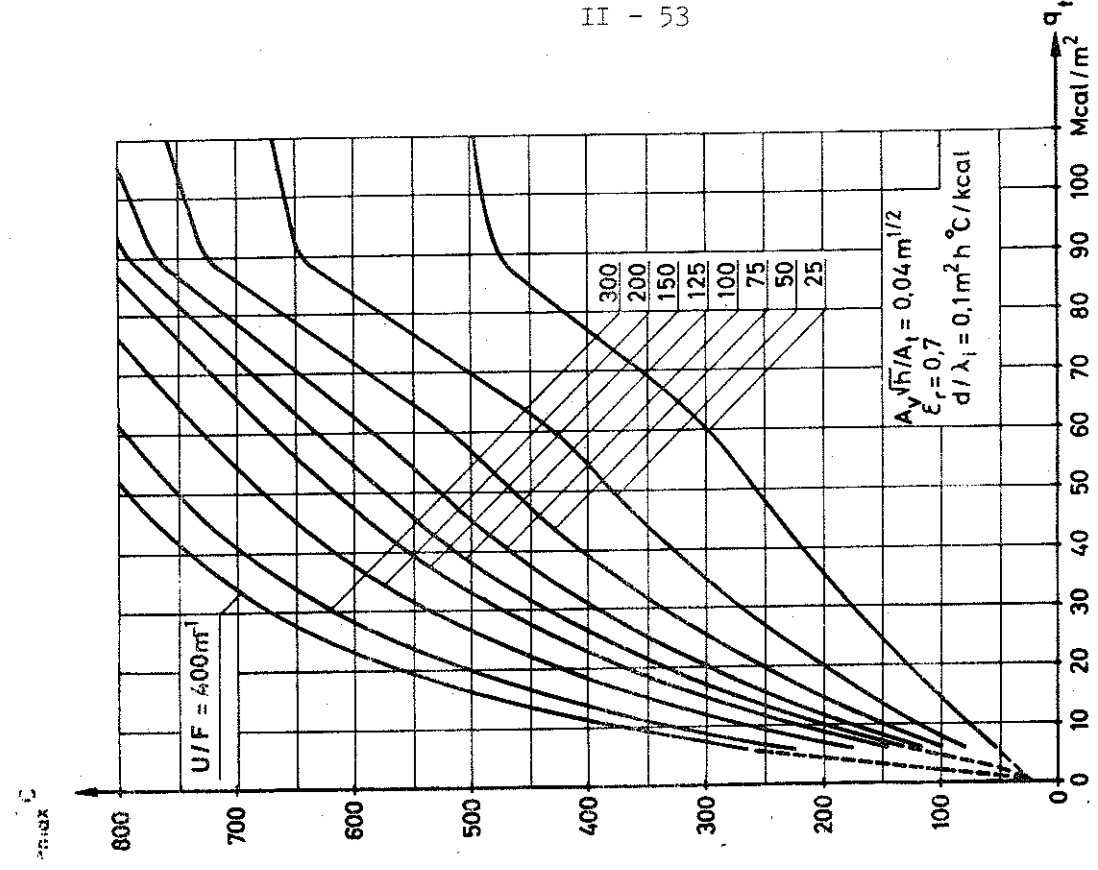


Fig. II, 49

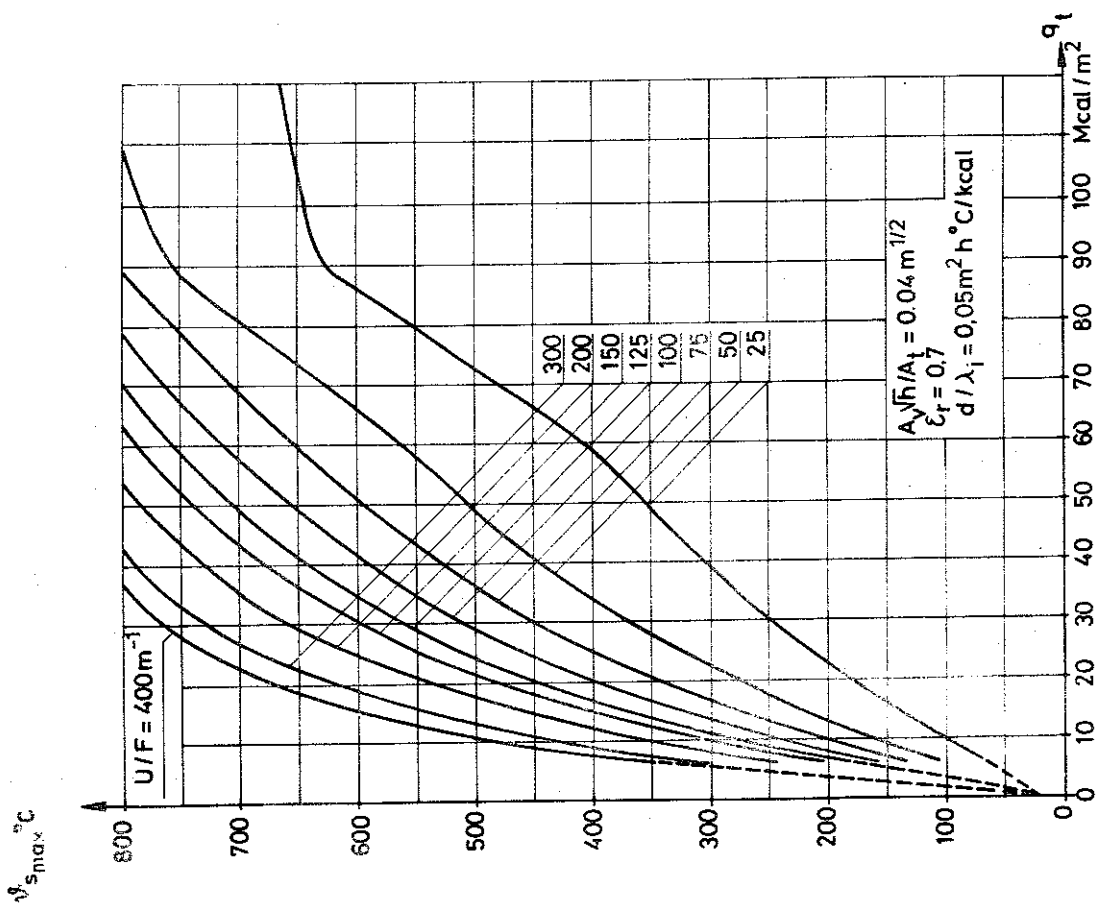


Fig. II, 48

Maximum steel temperature $\vartheta_{s,max}$ for a fire exposed, insulated steel structure at varying opening factor $A_y \sqrt{h}/A_t$, fire load q_t , and structural parameters U/F and d/λ_i . The curves are based on characteristics of the complete process of fire development according to Fig. II, 8 - fire compartment, type A {28}

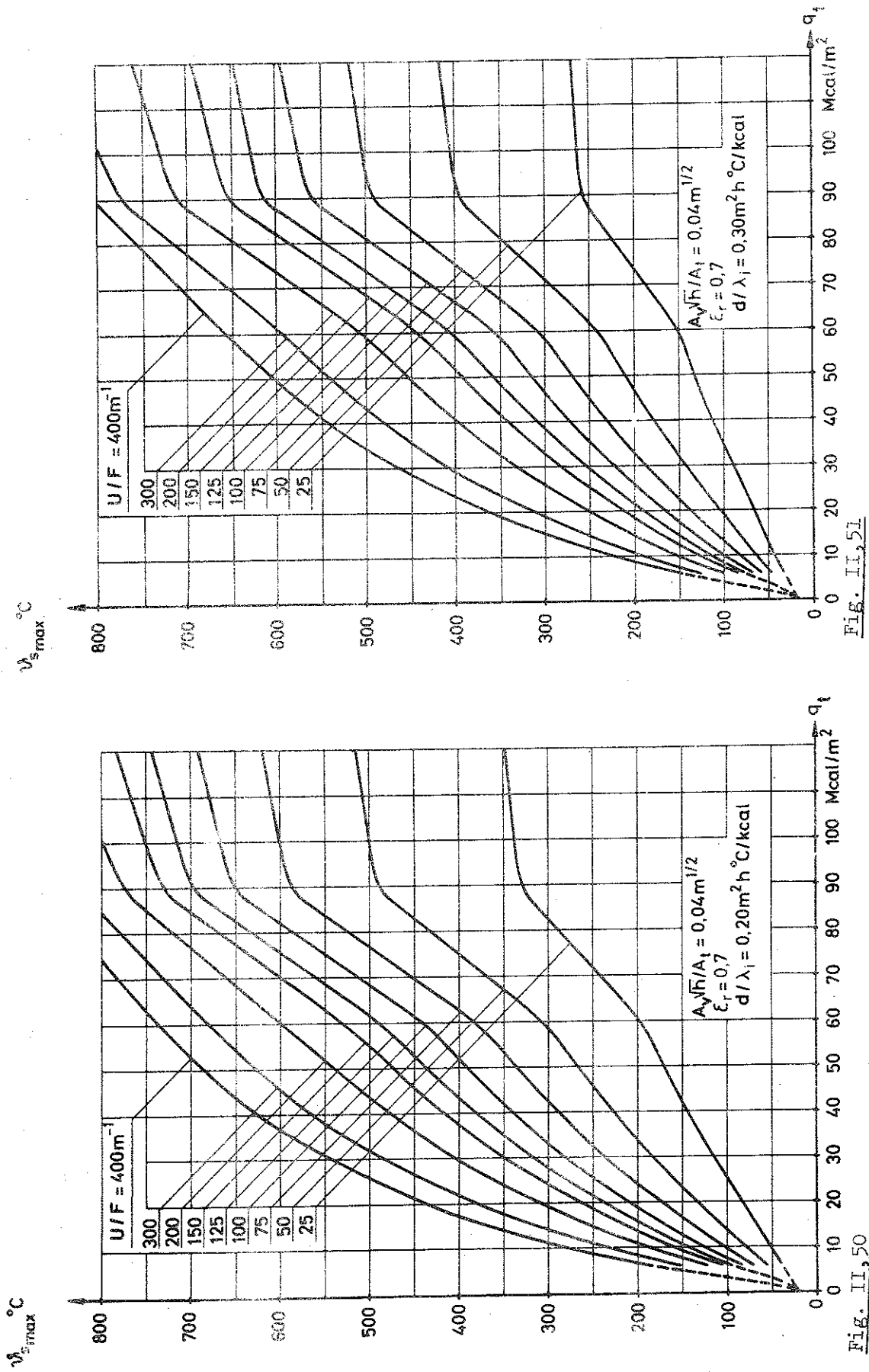


Fig. II,51

Fig. II,50

Maximum steel temperature $\vartheta_{s,max}$ for a fire exposed, insulated steel structure at varying opening factor $A_f \sqrt{h}/A_t$, fire load q_t , and structural parameters U/F and d/λ_i . The curves are based on characteristics of the complete process of fire development according to Fig. II,8 - fire compartment, type A (28)

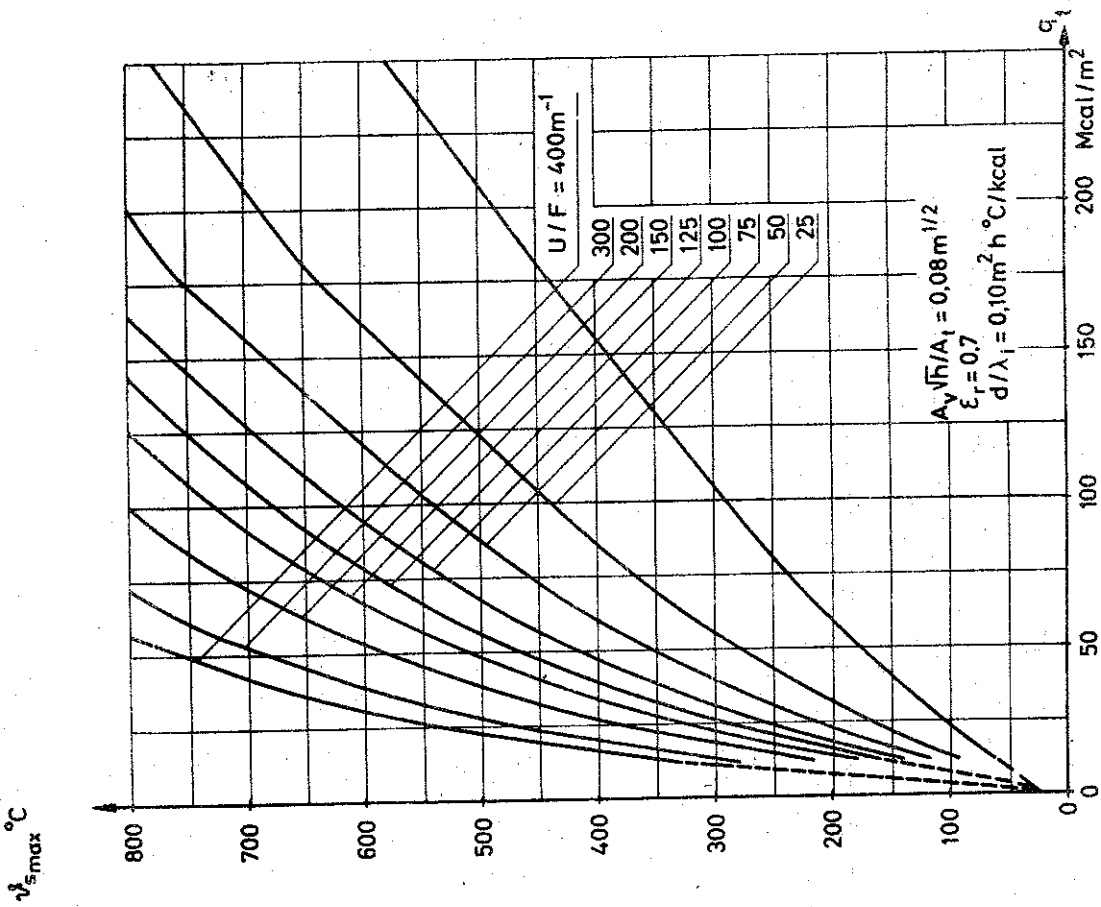


Fig. II, 52

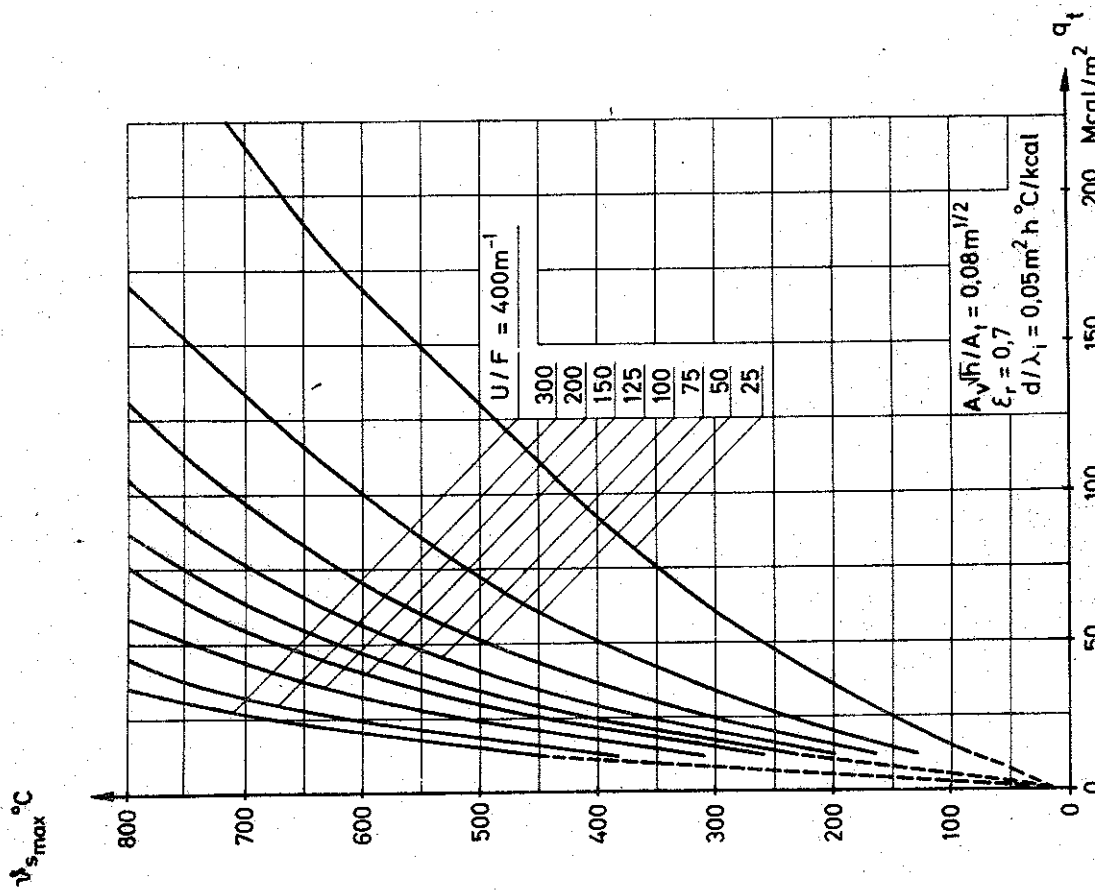


Fig. II, 53

Maximum steel temperature $\nu_{s,max}$ for a fire exposed, insulated steel structure at varying opening factor $A_V h / A_t$, fire load q_t , and structural parameters U/F and d/λ_i . The curves are based on characteristics of the complete process of fire development according to Fig. II, 8 - fire compartment, type A (28)

$\vartheta_{s,max} \text{ } ^\circ\text{C}$

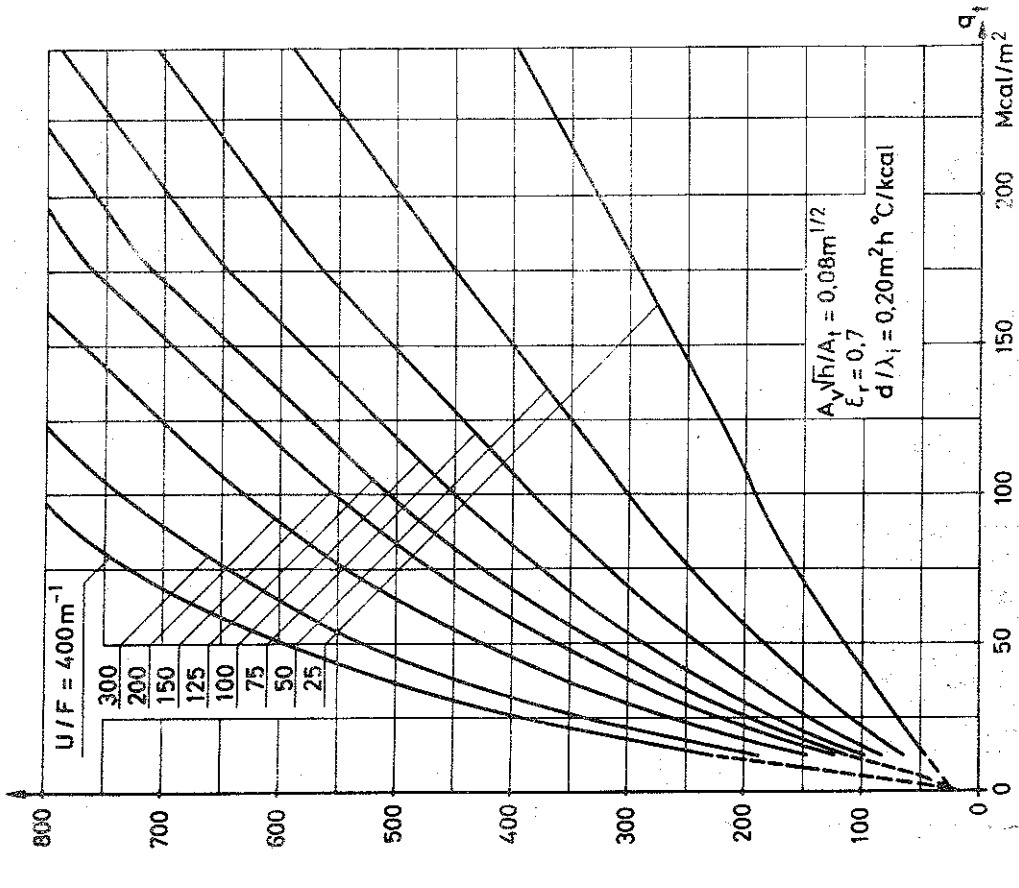


Fig. II, 54

$\vartheta_{s,max} \text{ } ^\circ\text{C}$

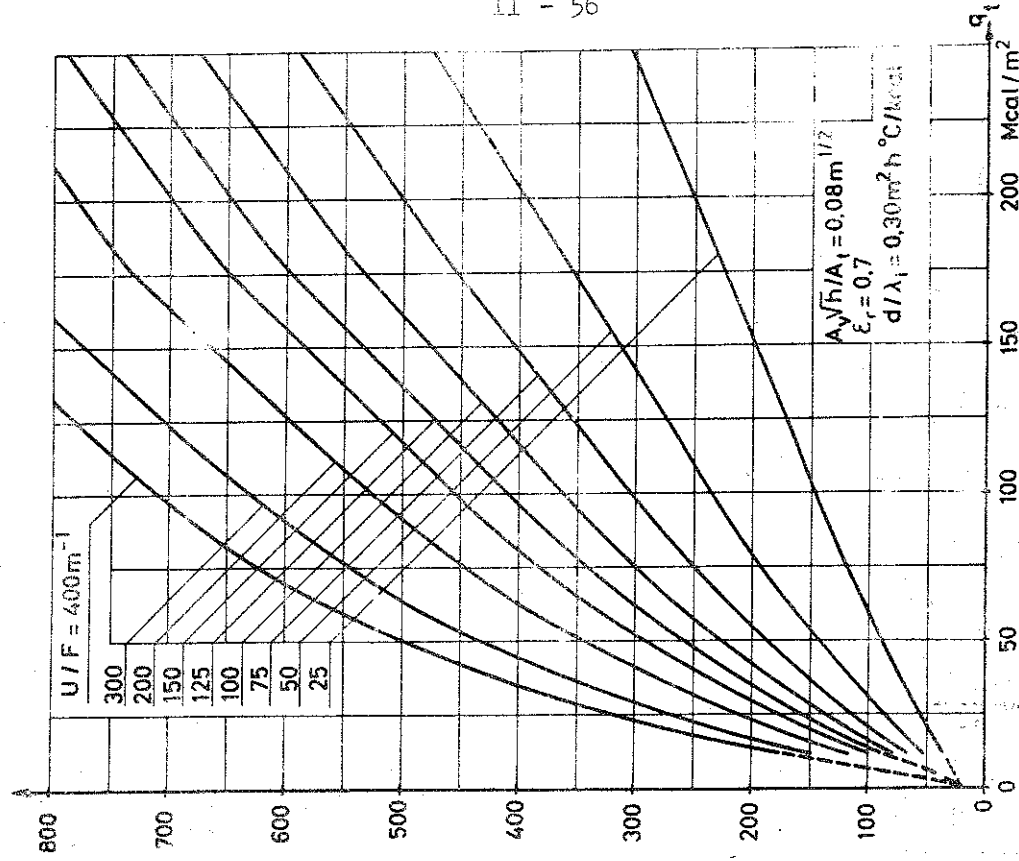


Fig. II, 55

Maximum steel temperature $\vartheta_{s,max}$ for a fire exposed, insulated steel structure at varying opening factor $A_v h/A_t$, fire load q_t , and structural parameters U/F and d/λ_t . The curves are based on characteristics of the complete process of fire development according to Fig. II, 8 - fire compartment, type A {28}

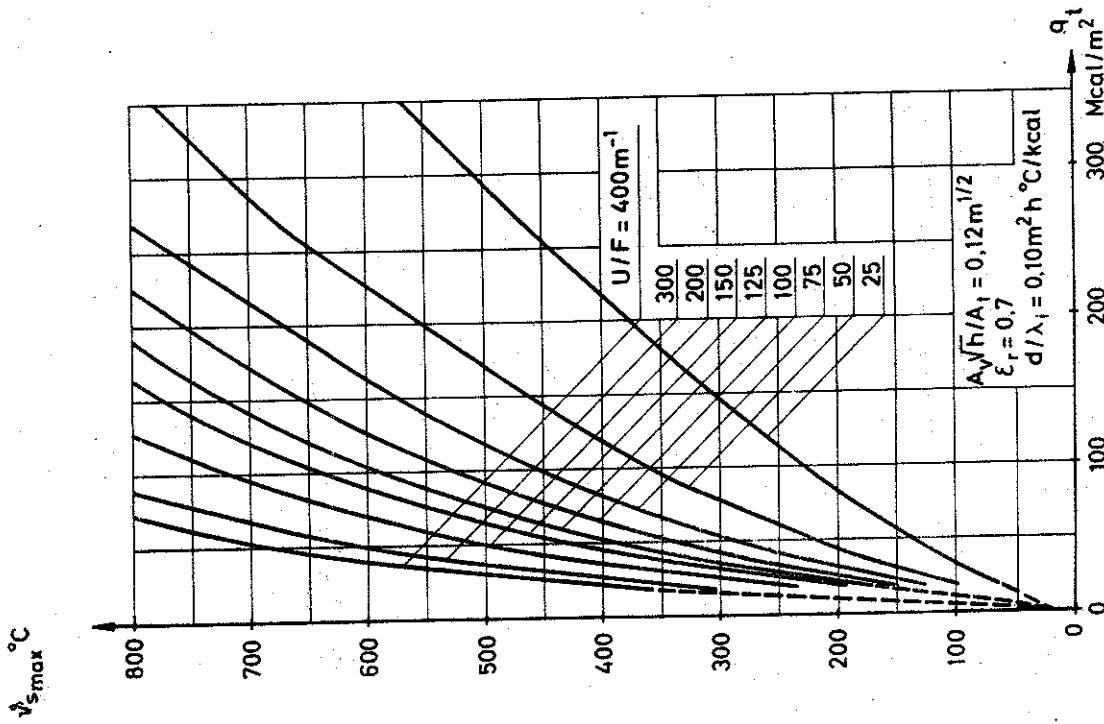


Fig. II, 57

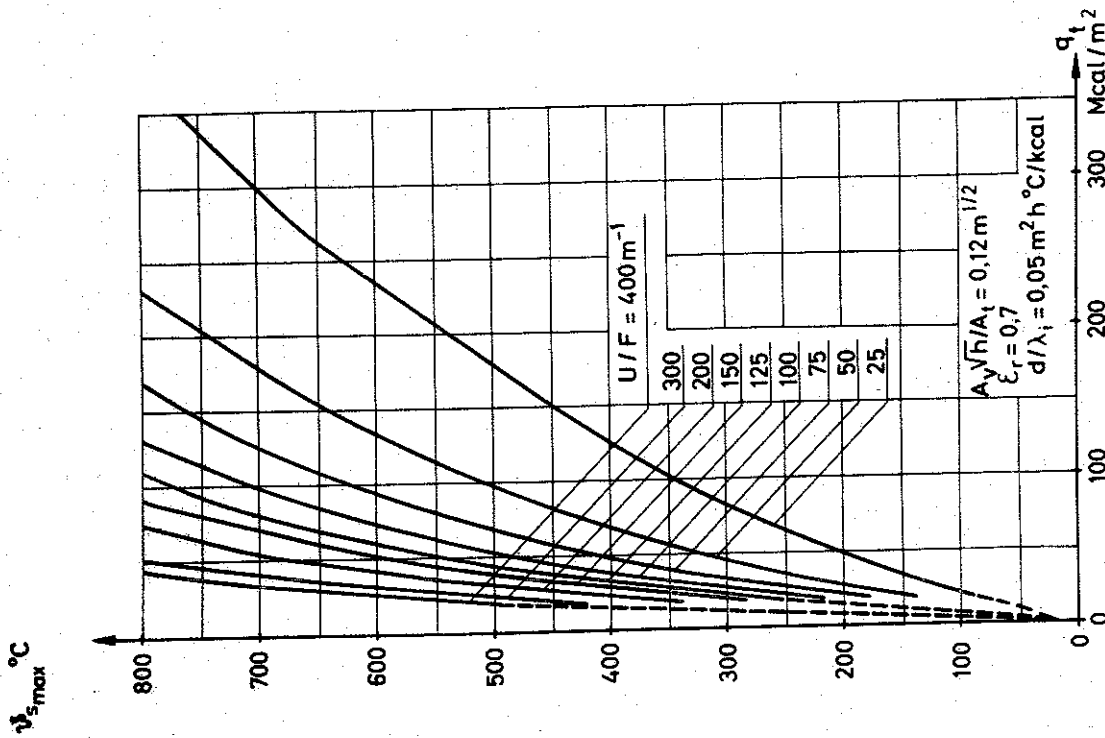


Fig. II, 56

Maximum steel temperature $\psi_{s,max}$ for a fire exposed, insulated steel structure at varying opening factor $A_v \sqrt{h}/A_i$, fire load q_t , and structural parameters U/F and d/λ_i . The curves are based on characteristics of the complete process of fire development according to Fig. II, 8 - fire compartment, type A (28)

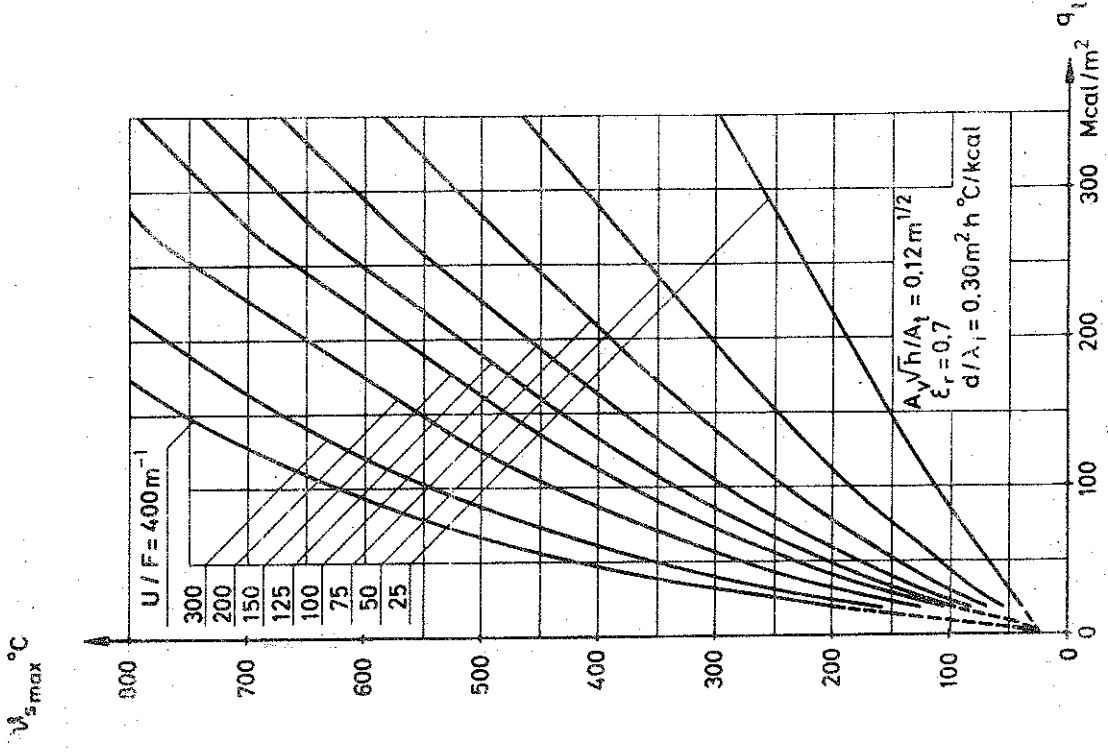


Fig. II, 59

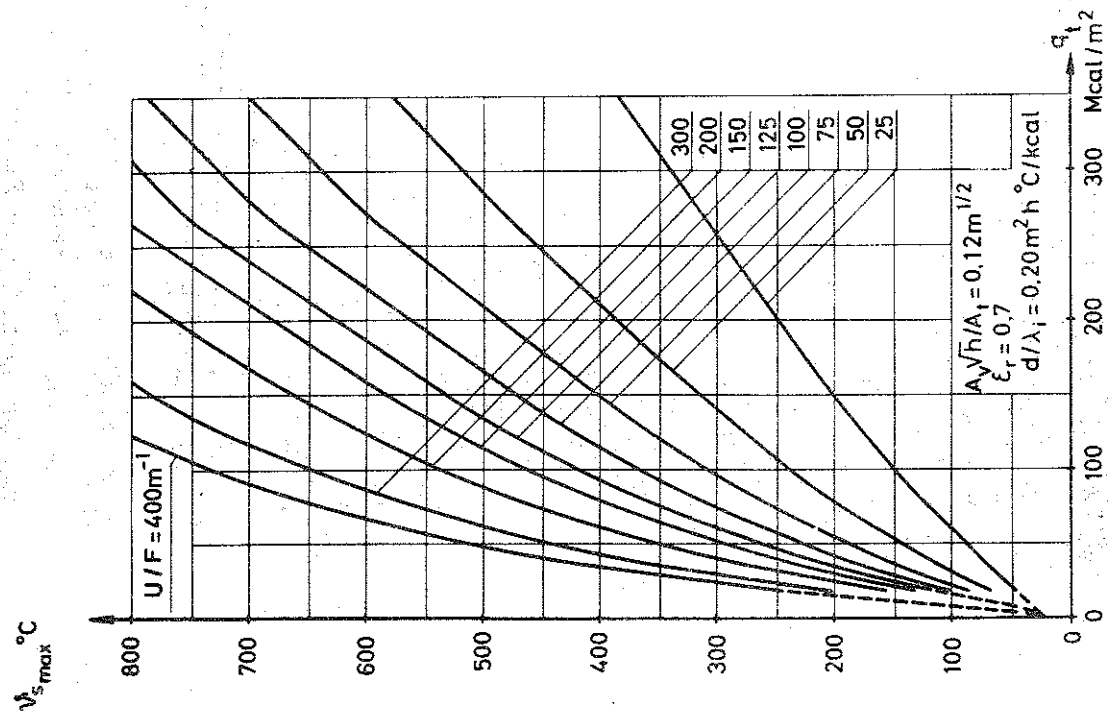


Fig. II, 58

Maximum steel temperature $t_{s,max}$ for a fire exposed, insulated steel structure at varying opening factor $A_s \sqrt{h}/A_t$, fire load q_t , and structural parameters U/F and d/λ_1 . The curves are based on characteristics of the complete process of fire development according to Fig. II, 8 - fire compartment, type A (28)

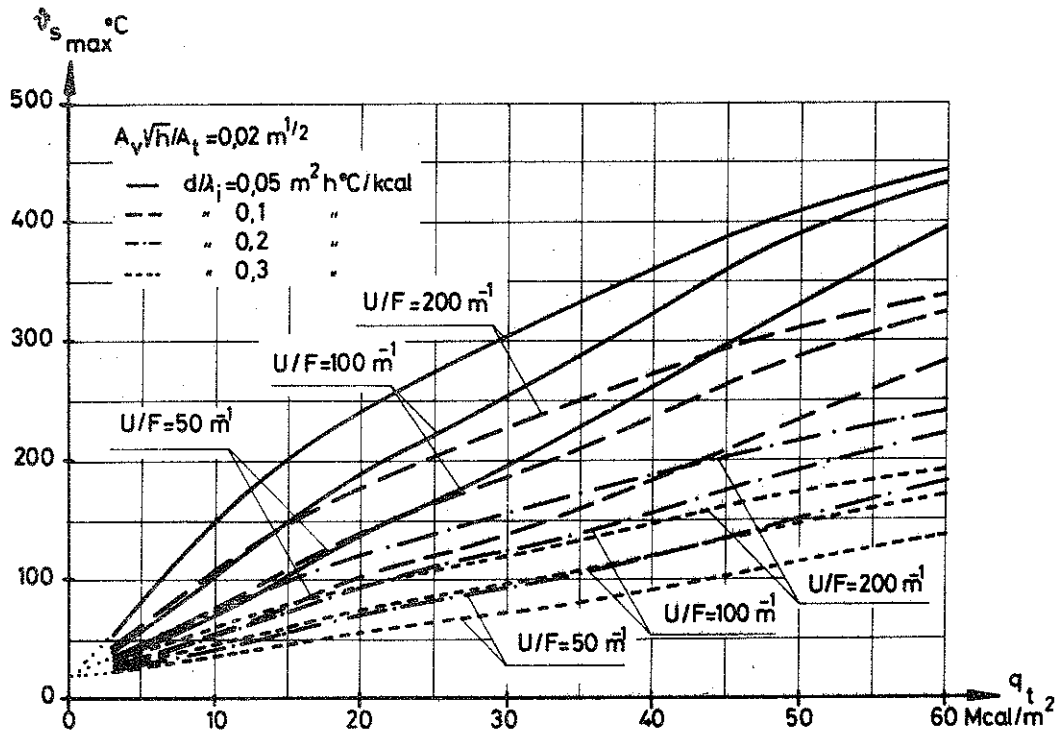


Fig. II,60

Maximum steel temperature $\vartheta_{s \max}$ for a fire exposed ceiling structure according to Fig. II,64, at varying opening factor $A_v \sqrt{h}/A_t$, fire load q_t , and structural parameters U/F and d/λ_i . The $\vartheta_{s \max}$ - values are insensitive to frequent, practical variations in the thickness of the concrete slab. The diagrams are not to be applied, if the slab is made of other materials, e.g. lightweight concrete. The curves are based on characteristics of the complete process of fire development according to Fig. II,8 - fire compartment, type A {28}

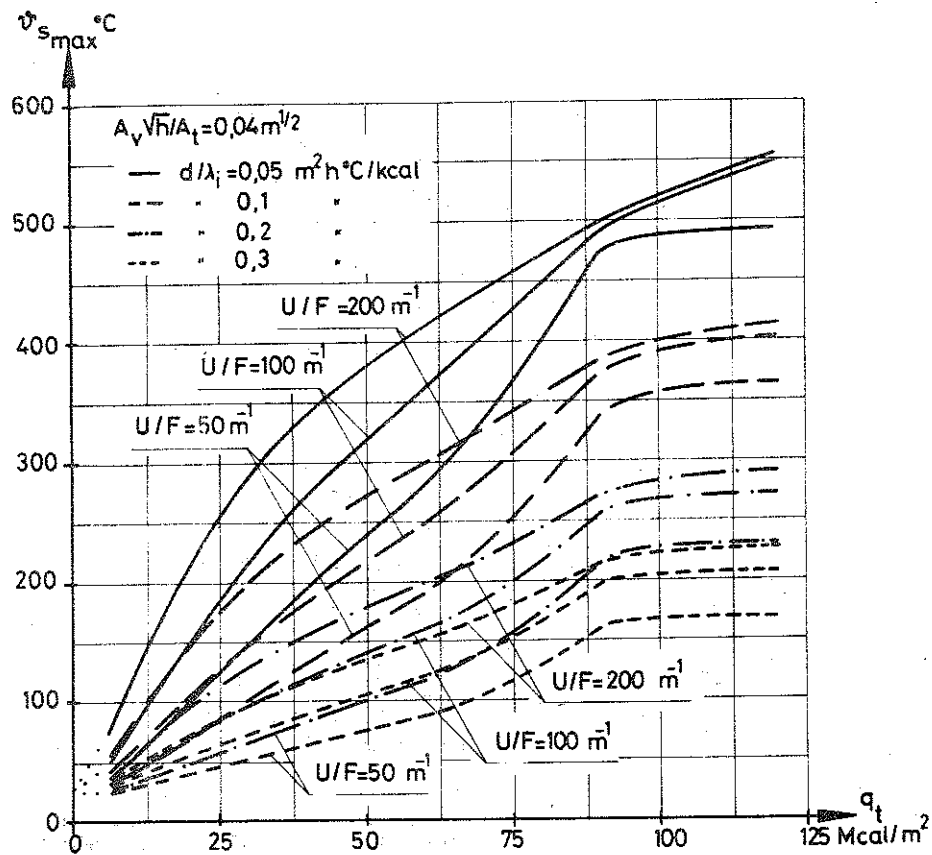


Fig. II,61

Maximum steel temperature $\vartheta_{s_{max}}$ for a fire exposed ceiling structure according to Fig. II,64, at varying opening factor $A_v\sqrt{h}/A_t$, fire load q_t , and structural parameters U/F and d/λ_i . The $\vartheta_{s_{max}}$ - values are insensitive to frequent, practical variations in the thickness of the concrete slab. The diagrams are not to be applied, if the slab is made of other materials, e.g. lightweight concrete. The curves are based on characteristics of the complete process of fire development according to Fig. II,8 - fire compartment, type A {28}

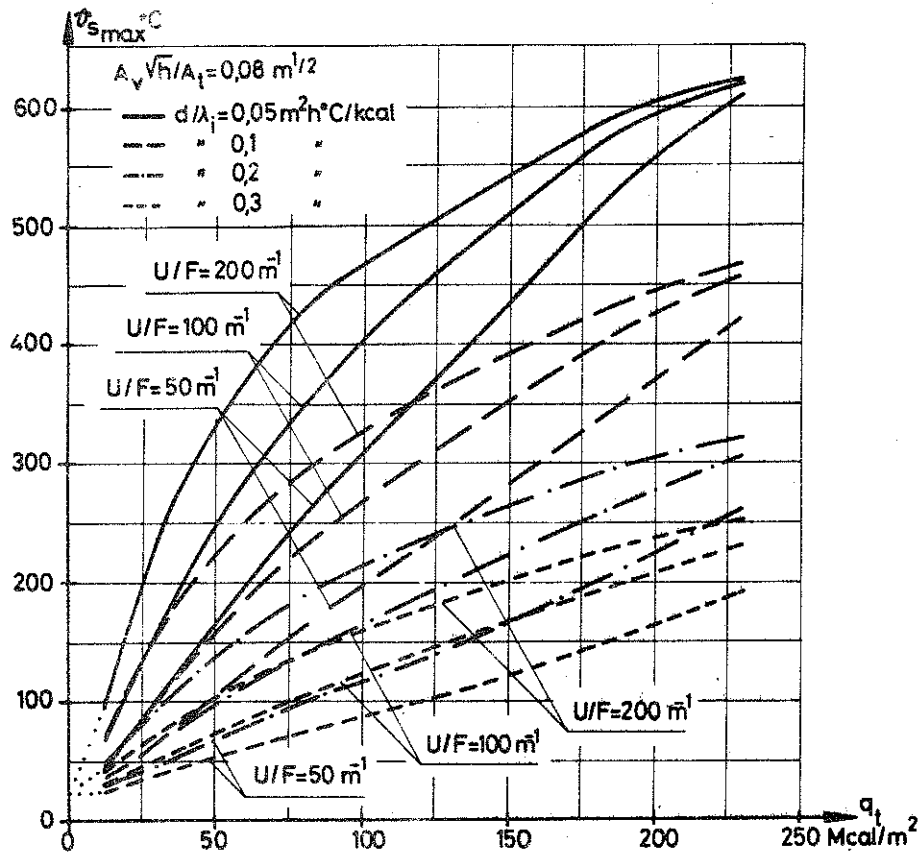


Fig. II,62

Maximum steel temperature $\vartheta_{s_{max}}$ for a fire exposed ceiling structure according to Fig. II,64, at varying opening factor $A_v \sqrt{h}/A_t$, fire load q_t , and structural parameters U/F and d/λ_i . The $\vartheta_{s_{max}}$ values are insensitive to frequent, practical variations in the thickness of the concrete slab. The diagrams are not to be applied, if the slab is made of other materials, e.g. lightweight concrete. The curves are based on characteristics of the complete process of fire development according to Fig. II,8 - fire compartment, type A {28}

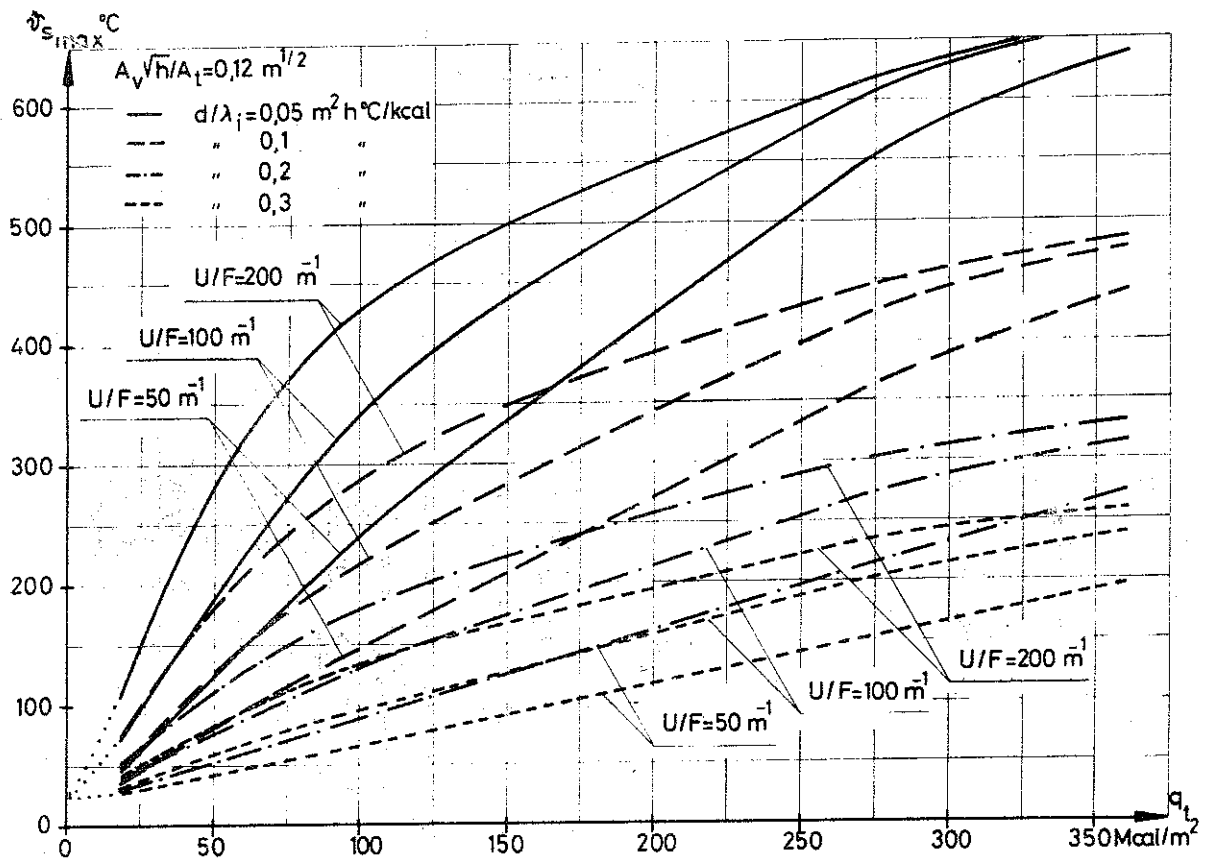


Fig. II,63

Maximum steel temperature $\theta_{s_{max}}$ for a fire exposed ceiling structure according to Fig. II,64, at varying opening factor $A_v \sqrt{h}/A_t$, fire load q_t , and structural parameters U/F and d/λ_i . The $\theta_{s_{max}}$ - values are insensitive to frequent, practical variations in the thickness of the concrete slab. The diagrams are not to be applied, if the slab is made of other materials, e.g. lightweight concrete. The curves are based on characteristics of the complete process of fire development according to Fig. II,8 - fire compartment, type A {28}

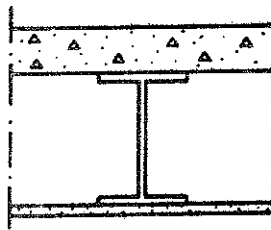
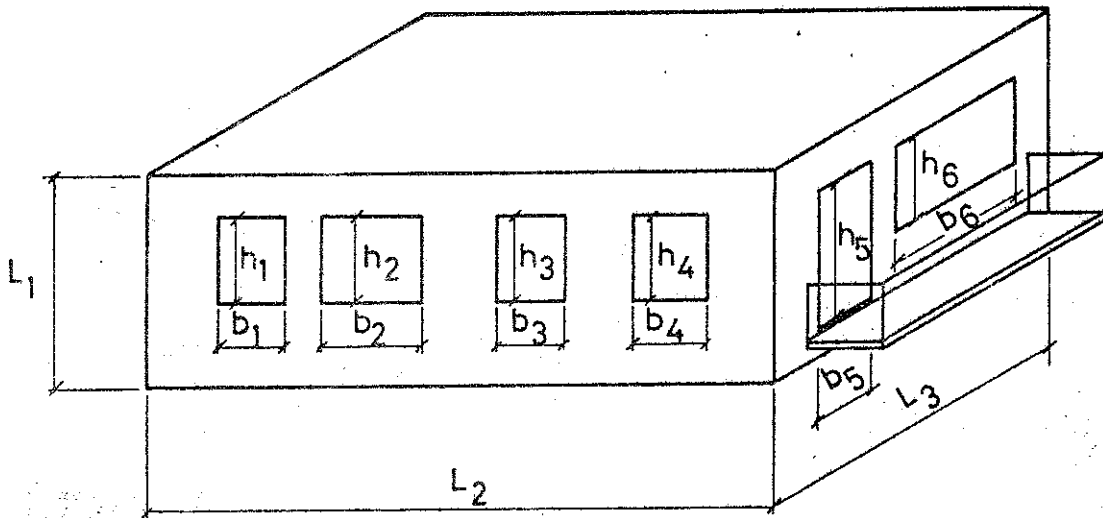


Fig. II,64 Ceiling structure, composed of a reinforced concrete slab, load-bearing steel beams, and an underlying insulation.



$$A_v = A_{v1} + A_{v2} + \dots + A_{v6} = b_1 h_1 + b_2 h_2 + \dots + b_6 h_6$$

$$h = \frac{1}{A_v} [A_{v1} h_1 + A_{v2} h_2 + \dots + A_{v6} h_6]$$

$$A_t = 2 [L_1 L_2 + L_1 L_3 + L_2 L_3]$$

Fig. II,65 Definitions of the total opening area A_v , the weighed mean value of the opening height h , the total interior area of the surrounding structures A_t , and the opening factor $A_v \sqrt{h} / A_t$ of a fire compartment.

of the compartment, calculated according to Fig. II,65, and f_k = a dimensionless multiplier, given by the alignment chart in Fig. II,66. For the notations used in this chart, then see Fig. II,67.

A determination of the equivalent opening factor $(A_v \sqrt{h}/A_t)_e$ over Eq. (II-12) and Fig. II,66 presupposes that the gas flow through the horizontal openings of the roof is not predominant. This can be examined via the quotient $A_v \sqrt{h_2}/A_v h$, which has an upper limit at which the applied gas flow model ceases to be valid. This upper limit is given by the values

$$\frac{A_v \sqrt{h_2}}{A_v h} = \begin{matrix} 1.76 \text{ at } \vartheta_t = 1000^\circ\text{C} \\ 1.37 \text{ at } \vartheta_t = 500^\circ\text{C} \end{matrix} \dots \dots \dots \text{ (II-13)}$$

At these limit values, the neutral zone coincides with the upper edge of the vertical opening. Tests have indicated the validity of the applied model up to these upper limits {30}. For larger values of the quotient $A_v \sqrt{h_2}/A_v h$ than these limit values, all combustion gases will be vented through the horizontal openings of the roof and the gas flow becomes unstable and difficult to analyse by a simple theoretical model {31}.

In{9} also a method is outlined for a determination of the equivalent opening factor for the case where the compartment is ventilated through air inlets and outlets by means of a fan installation.

7. Summary conclusions

With regard to a differentiated, practical, structural fire engineering design, the analysis and discussion presented above can be summarized by the following alternative and equivalent design procedures.

7.1 Design procedure based on the concept equivalent time of fire duration

The design procedure comprises the following main components.

- (a) The determination of the fire load q_t of the compartment, specified as the relevant heat value per unit area of the total interior surface bounding the compartment in Mcal/m².
- (b) The choice of representative type of fire compartment with respect to

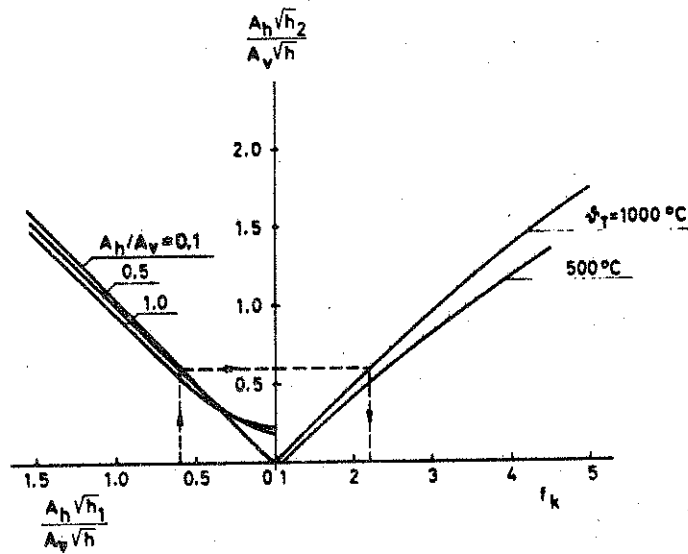


Fig. II,66 Alignment chart for a determination of the equivalent opening factor $(A_v \sqrt{h}/A_t)_e$ for a fire compartment with vertical as well as horizontal openings. For notations, see Fig. II,67 (9)

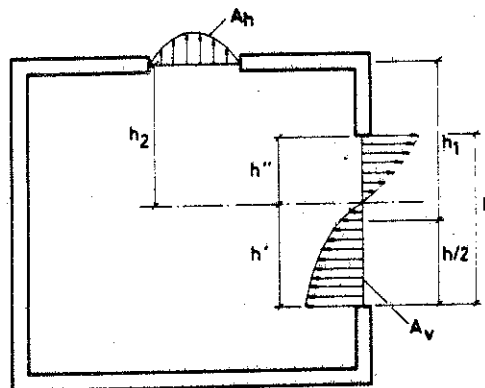


Fig. II,67 Gas flow mechanism for a fire compartment with vertical and horizontal openings.

the thermal properties of the surrounding structures. Ordinarily, this choice can be done by a direct comparison with the characteristics of the different types of fire compartments, listed on p. II-12

(c) The determination of

the total area of the window and door openings A_v in m^2 ,
 the weighed mean value of the heights of the window and door openings h in m ,
 the total interior area of the surfaces bounding the compartment A_t in m^2 ,
 and the opening factor of the compartment $A_v \sqrt{h}/A_t$ in $m^{1/2}$

These quantities are given by the formulae in Fig. II, 65, for a compartment with only vertical openings. If the compartment also comprises horizontal openings, an equivalent opening factor $(A_v \sqrt{h}/A_t)_e$ can be calculated over Eq. (II-12) and the alignment chart in Fig. II, 66. Such a calculation then is justified, if the conditions specified by Eq. (II-13) are fulfilled.

(d) The transformation, with respect to gastemperature-time characteristics of the process of fire development, of the real type of fire compartment, determined in step (b), to the basic fire compartment, type A. In obtaining this, the fire load q_t according to step (a) and the opening factor $A_v \sqrt{h}/A_t$ or the equivalent opening factor $(A_v \sqrt{h}/A_t)_e$ according to step (c) are multiplied by a transformation coefficient K_f , given in Table II-1. The procedure leads to a fictitious fire load q_f and a fictitious opening factor $(A_v \sqrt{h}/A_t)_f$ which enable that the subsequent design can be based upon the differentiated gastemperature-time curves for the basic fire compartment, type A.

(e) The proof that the fire exposed steel structure or structural element is able to fulfill the stipulated functional requirements during the fire action. For a load-bearing structure that means a proof that the load-bearing capacity does not decrease below the design load - or some other prescribed load - multiplied by a required factor of safety, during either the heating period or the subsequent cooling period of the real process of fire development.

The design step (e) contains two subcomponents. One component comprises the determination of the critical steel temperature ϑ_{crit} of the actual steel or structural element, which depends on the degree of stress utilization, the type of cross section, the characteristics of support and restraint

conditions, the type of failure, and the strength and deformation properties of the material at elevated temperatures. The determination of the critical steel temperature is outside the scope of this chapter and therefore on this point reference is made only to chapter IV and to the literature, e.g. [20], [27], [29], [32], in this connection.

The other subcomponent of the design step (e) consists of a proof that the maximum steel temperature of the fire exposed structure or structural element ϑ_{smax} does not exceed the critical steel temperature ϑ_{scrit} during the fire process. Over the concept equivalent time of fire duration T_e , this can be done either experimentally or theoretically.

An accurate, differentiated determination of T_e can be carried out quickly from Fig.II,10 to II,21 for un-insulated steel structures and from Fig.II,22 to II,25 for insulated steel structures. Entrance quantities for the diagrams in the figures are the fire load q_f and the opening factor $(A_v \sqrt{h}/A_t)_f$ according to step (d) and the structural parameters U/F (Fig.II,10 to II,21) and $U\lambda_1/Fd$ (Fig.II,22 to II,25), respectively. U is the fire exposed surface per unit length for un-insulated steel structures, and the inside jacket surface of the insulation per unit length for insulated structures, F the volume of the steel structure per unit length, λ_1 the thermal conductivity of the insulating material, and d the thickness of the insulation. For un-insulated steel structures (Fig.II,10 to II,21) the influence of variations in the resulting emissivity ϵ_r is added.

After having found the equivalent time of fire duration T_e , the maximum steel temperature ϑ_{smax} can be determined experimentally in a standard fire resistance test by heating a test specimen of the actual structure or structural element according to the standard time-temperature curve, Eq. (II-10), during the time $T = T_e$. Alternatively, the determination of the maximum steel temperature ϑ_{smax} can be carried out by theoretical calculations. With an accuracy which will be sufficient in most practical applications ϑ_{smax} can then be taken directly from Fig.II,32 to II,43 for fire exposed un-insulated steel structures and from Fig.II,44 to II,59 or from the dash-line curves in Fig.II,22 to II,25 for fire exposed insulated steel structures.

For a more rough estimation of the equivalent time of fire duration T_e , the curves in Fig.II,28 or II,31 or Eq. (II-11) can be used for insulated steel

structures and the curves in Fig. II,29 for un-insulated steel structures. Generally, these curves and the formula according to Eq. (II-11) are based on the assumption of a critical steel temperature $\vartheta_{s_{crit}} = 500^{\circ}\text{C}$. The values of T_e , determined in this more rough way, depend only on the fire load and the fire compartment properties but not on the design of the structure. T_e values of this character belong primarily to a preliminary design stage.

7.2. Design procedure, directly based on differentiated gastemperature-time curves

Such a design procedure, summarily described in chapter II.5, coincides with the design procedure according to chapter II.7.1, as concerns the design components (a) - (d). This part of the design procedure leads to a fictitious fire load q_p and a fictitious opening factor of the fire compartment $\left[\frac{A_{v/h}}{A_t}\right]_f$. These quantities determine from Fig. II,8 that gastemperature-time curve of the process of fire development, upon which the further design is to be based.

The design step (e) then comprises a determination of the corresponding time curve of the steel temperature ϑ_s of the fire exposed structure or structural element, particularly the maximum value of the steel temperature $\vartheta_{s_{max}}$ during the complete fire process. For most practical applications, this determination can be done very quickly by the existence of systematized design diagrams. Examples of such diagrams, giving directly the maximum steel temperature $\vartheta_{s_{max}}$, are shown in Fig. II,32 to II,43 for un-insulated steel structures, in Fig. II,44 to II,59 for insulated steel structures, and in Fig. II,60 to II,63 for a ceiling structure, composed of a reinforced concrete slab, load-bearing steel beams, and an underlying insulation. Additional diagrams can be found in the literature, cf. e.g. [28].

The differentiated design procedures presented above are to be seen as an attempt to build up a logical system for a structural fire engineering design based on functional requirements. Fundamentally, such a system is in agreement with the present development of building codes and regulations. It is well suited to stimulate the architects and the structural engineers to solve the fire engineering problems in a more scientific manner by a design procedure which is equivalent to the conventional design procedure applied with respect to, for instance, static loading. The structural fire engineering

design system presented is not homogeneous with respect to the present basis of knowledge for the different design steps which can be put forward as a criticism of the system. However, such a remark is not essential. Instead, this fact ought to be used as an important guide on how to systematize a future research work for making possible a successive improvement of the system.

8. Applications

Example 1

A fire compartment has geometrical characteristics according to Fig. II,68. The interior height $L_1 = 2.5$ m, the interior width $L_2 = 6$ m, and the interior length $L_3 = 15$ m. The compartment has one door opening (D) and five window openings (1) to (5) with positions and dimensions h and b , specified in the figure. The roof of the compartment comprises six horizontal openings with the total area $A_h = 6.6$ m².

The compartment has boundary structures with the following percentage of boundary surface area: 18% lightweight concrete of density $\rho = 500$ kg/m³ and 82% concrete.

The fire load $q_t = 15$ Mcal/m² of the total surrounding surface.

Within the compartment, there are uninsulated steel columns with a structural design corresponding to $U/F = 75$ m⁻¹.

Determine

- (1) the fictitious opening factor $(A_v \sqrt{h}/A_t)_f$ and fire load q_f , and
- (2) the equivalent time of fire duration T_e and the corresponding value of the maximum steel temperature $\vartheta_{s_{max}}$ at fire.

The problem is solved in conformity with the design procedure - step (a) to (e) - summarised in chapter II.7.1.

Step (a)

The fire load $q_t = 15$ Mcal/m².

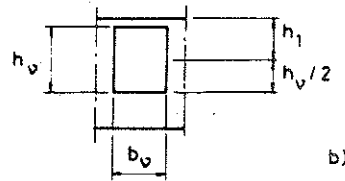
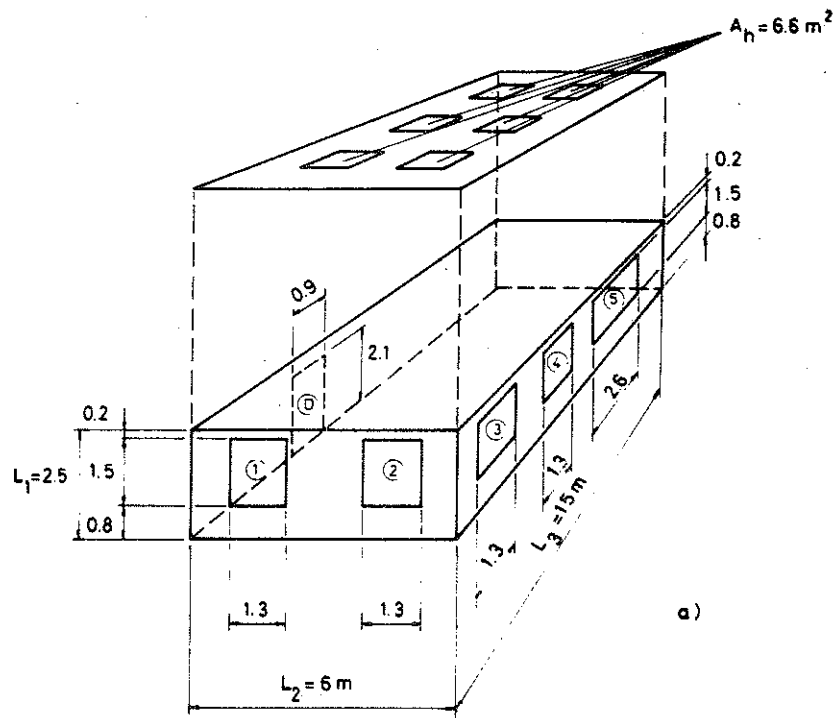


Fig. II,68

Geometrical characteristics of fire compartment, used in Example 1.

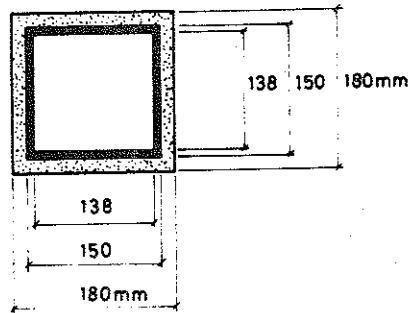


Fig. II,69

Cross section of a fire exposed, insulated steel column, Example 2.

Step (b)

The actual fire compartment has a boundary structure surface of 18% lightweight concrete and 82% concrete.

With respect to the thermal properties of the surrounding structures, the actual compartment lies between the fire compartment, type B, characterized by a boundary structure surface of, cf. p. II-12, 0% lightweight concrete and 100% concrete and the fire compartment, type D, with a boundary structure surface of 50% lightweight concrete and 50% concrete.

The fundamental characteristics of the actual compartment - the fictitious fire load q_f and opening factor $(A_v/h/A_t)_f$ - can be calculated from the corresponding characteristics of the fire compartment types B and D by linear interpolation. For the coefficient K_f according to Table II,1, this gives the value

$$K_f = (K_f)_B + \frac{18}{50} \left[(K_f)_D - (K_f)_B \right] = 0.64 (K_f)_B + 0.36 (K_f)_D \dots \dots (a)$$

where $(K_f)_B$ and $(K_f)_D$ are the values of K_f for the compartment type B and D, respectively.

Step (c)

This step contains as a first subcomponent a determination of the opening factor $(A_v/h/A_t)_v$ of the vertical openings of the fire compartment. This determination - based on the formulae in Fig. II,65 - is presented in Table II,3 with notations according to Fig. II,68b. The table gives for the total, vertical opening area

$$A_v = \sum A_{vv} = b_v h_v = 13.59 \text{ m}^2 \dots \dots \dots (b)$$

and for the weighed mean value of the heights of the vertical openings

$$h = \frac{1}{A_v} \sum A_{vv} h_v = \frac{21.519}{13.59} = 1.583 \text{ m} \dots \dots \dots (c)$$

The total interior area of the surfaces bounding the compartment is

$$A_t = 2(L_1L_2 + L_1L_3 + L_2L_3) = 2(2.5 \times 6 + 2.5 \times 15 + 6 \times 15) = 285 \text{ m}^2 \quad (d)$$

Table II 3

Opening	b_v	h_v	$A_{vv} = b_v h_v$	$A_{vv} h_v$	h_{1v}	$A_{vv} h_{1v}$
①	1.3	1.5	1.95	2.925	0.95	1.853
②	1.3	1.5	1.95	2.925	0.95	1.853
③	1.3	1.5	1.95	2.925	0.95	1.853
④	1.3	1.5	1.95	2.925	0.95	1.853
⑤	2.6	1.5	3.90	5.850	0.95	3.705
⑥	0.9	2.1	1.89	3.969	1.45	2.741
$\Sigma A_v = 13.59$				21.519		$\Sigma 13.858$

The calculated values of A_v , h and A_t then give for the opening factor of the vertical openings

$$\left(\frac{A_v \sqrt{h}}{A_t}\right)_v = \frac{13.59 \sqrt{1.583}}{285} = 0.0600 \text{ m}^{1/2} \quad \dots \quad \dots \quad \dots \quad \dots \quad (e)$$

The second subcomponent of step (c) comprises a determination of the influence of horizontal openings on the opening factor. This influence can be taken into account by Eq. (II-12), giving the equivalent opening factor $(A_v \sqrt{h}/A_t)_e$. The calculation is based on the alignment chart in Fig. II,66 with notations according to Fig. II,67. Additional quantities to be determined are the total horizontal opening area

$$A_h = 6.6 \text{ m}^2 \quad \dots \quad \dots \quad \dots \quad \dots \quad \dots \quad \dots \quad \dots \quad (f)$$

and the vertical distance h_1 from the horizontal opening level to the centre

level of the vertical openings. At varying centre levels h , is then to be calculated as a mean value, weighed with respect to each individual opening area by the formula

$$h_c = \frac{1}{A_v} \sum A_{v_i} h_i = \frac{13.858}{13.59} = 1.020 \text{ m} \dots \dots \dots (g)$$

cf. Fig.II,68b and Table II-3.

With

$$\frac{A_n \sqrt{h_c}}{A_v \sqrt{h}} = \frac{6.6 \sqrt{1.020}}{13.59 \sqrt{1.583}} = 0.390 \dots \dots \dots (h)$$

and

$$\frac{A_n}{A_v} = \frac{6.6}{13.59} = 0.486 \dots \dots \dots (i)$$

As entrance-quantities, Fig.II,66 gives - with the gastemperature

$\vartheta_{T1} = 1000^\circ\text{C}$ as an estimation on the safe side

$$f_k = 1.760 \dots \dots \dots (j)$$

$$\frac{A_n \sqrt{h_c}}{A_v \sqrt{h}} = 0.39 < \text{upper limit value according to Eq. (II-13).}$$

This means that the calculation is justified and that the derived f_k value can be applied for a determination using Eq. (II-12) of the equivalent opening factor $(A_v \sqrt{h}/A_t)_e$ for the actual fire compartment with the actual surrounding structures, i.e.

$$\left(\frac{A_v \sqrt{h}}{A_t}\right)_e = f_k \left(\frac{A_v \sqrt{h}}{A_t}\right)_v = 1.760 \times 0.0600 = 0.106 \text{ m}^{1/2} \dots \dots \dots (k)$$

Step (d)

Via fictitious values of the fire load q_p and the opening factor $(A_v \sqrt{h}/A_t)_f$,

Consequently, the real fire exposure of the steel columns is equivalent to a heating in a standard fire resistance test during the time $T_e = 0.28 = 17$ min. In such a test as well as under real fire conditions, the maximum steel temperature will then be $\vartheta_{s_{max}} = 540^\circ\text{C}$.

Example 2

A fire exposed steel column with a cross section according to Fig. II,69 is protected with an insulation, 15 mm in thickness. The column is placed in a fire compartment, type A, with an opening factor $A_v\sqrt{h}/A_t = 0.02 \text{ m}^{1/2}$. The fire load $q_t = 35 \text{ Mcal/m}^2$ of the total surrounding surface of the compartment.

Determine the equivalent time of fire duration T_e and the corresponding value of the maximum steel temperature $\vartheta_{s_{max}}$ at fire. The thermal conductivity of the insulation $\lambda_i = 0.10 \text{ Kcal/m h}^\circ\text{C}$, chosen as a mean value within a temperature range from 0 to about 500°C .

The steel volume per unit length

$$F = (15^2 - 13.8^2) \times 10^{-4} = 34.6 \times 10^{-4} \text{ m}^3/\text{m} \dots \dots \dots (a)$$

the inside jacket surface of the insulation per unit length

$$U = 4 \times 15.0 \times 10^{-2} = 60.0 \times 10^{-2} \text{ m}^2/\text{m} \dots \dots \dots (b)$$

and the thickness of the insulation

$$d = 1.5 \times 10^{-2} \text{ m} \dots \dots \dots (c)$$

These values give for the structural parameter

$$\frac{U\lambda_i}{Fd} = \frac{60.0 \times 10^{-2} \times 0.10}{34.6 \times 10^{-4} \times 1.5 \times 10^{-2}} = 1155 \text{ Kcal/m}^3\text{h}^\circ\text{C} \dots \dots \dots (d)$$

With this structural parameter and the fire load $q_t = 35 \text{ Mcal/m}^2$ as entrance quantities, Fig. II,22 gives the equivalent time of fire duration

$$T_e = 0.97 \text{ h} \dots \dots \dots (e)$$

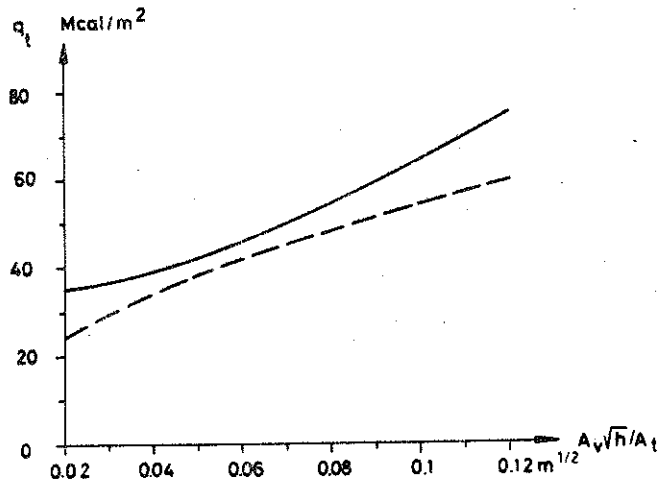


Fig. II,70

Relationship between the opening factor $A_v\sqrt{h}/A_t$ and the fire load q_t for an insulated steel column with the structural parameter $U\lambda_1/Fd = 2000 \text{ kcal/m}^3\text{h}^\circ\text{C}$, fire exposed within a fire compartment, type A, to a maximum steel temperature $\theta_{s_{max}} = 600^\circ\text{C}$. The full-line curve corresponds to an accurate calculation, based on Fig. II,22 to II,25. The dotted-line curve corresponds to an approximate determination, based on Eq. (II-11).

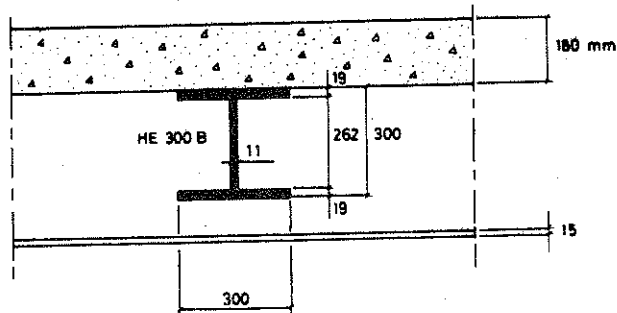


Fig. II,71

Fire exposed ceiling structure, composed of a reinforced concrete slab, load-bearing steel beams, and an underlying insulation, Example 4.

$$48 = 0.28 \frac{B}{\sqrt{A_v A_t} \sqrt{h}} = 0.28 \frac{q_t A_t}{\sqrt{A_v A_t} \sqrt{h}}$$

$$q_t = 171 \sqrt{\frac{A_v \sqrt{h}}{A_t}}$$

corresponding to the dash-line curve in Fig. II,70.

Example 4

A ceiling structure, composed of a reinforced concrete slab, load-bearing steel beams, and an underlying insulation according to Fig. II,71, is fire exposed from below. The insulation is made of a material with a thermal conductivity $\lambda_i = 0.12 \text{ kcal/m h}^\circ\text{C}$ as a representative mean value within the temperature range from 0 to about 500°C . The structure is placed within a fire compartment with a fire load $q_t = 100 \text{ Mcal/m}^2$ of the total surrounding surface.

Determine

- (1) the maximum steel temperature $\vartheta_{s_{\max}}$, corresponding to the opening factor values $A_v \sqrt{h}/A_t = 0.04, 0.08$ and $0.12 \text{ m}^{1/2}$, if the fire compartment is of type A, and
- (2) the maximum steel temperature $\vartheta_{s_{\max}}$, if the fire compartment is of type C with an opening factor $A_v \sqrt{h}/A_t = 0.04 \text{ m}^{1/2}$

The problem can be solved over the diagrams in Fig. II,60 to II,63.

(1) Fire compartment, type A

The entrance quantities of Fig. II,60 to II,63 are:

exposed steel surface per unit length

$$U = (30.0 + 2 \times 28.9 + 2 \times 30.0) \times 10^{-2} = 1.478 \text{ m}^2/\text{m} \quad \dots \quad \dots \quad \dots \quad (a)$$

steel volume per unit length

$$F = 1.491 \times 10^{-2} \text{ m}^3/\text{m} \text{ (from catalogue)} \quad \dots \quad \dots \quad \dots \quad \dots \quad (b)$$

steel beam quotient $\frac{U}{F} = \frac{1.478}{1.491 \times 10^{-2}} = 99 \text{ m}^{-1} \dots \dots \dots (c)$

and insulation quotient $\frac{d}{\lambda_i} = \frac{1.5 \times 10^{-2}}{0.12} = 0.125 \text{ m h}^\circ\text{C/kcal} \dots \dots (d)$

With these values of U/F and d/λ_i , Fig.II,61 to II,63 give for the fire load $q_t = 100 \text{ Mcal/m}^2$

$A_v \sqrt{h}/A_t = 0.04 \text{ m}^{1/2}:$	$\vartheta_{s_{\max}} = 360^\circ\text{C}$
$A_v \sqrt{h}/A_t = 0.08 \text{ m}^{1/2}:$	$\vartheta_{s_{\max}} = 245^\circ\text{C}$
$A_v \sqrt{h}/A_t = 0.12 \text{ m}^{1/2}:$	$\vartheta_{s_{\max}} = 195^\circ\text{C} \dots \dots (e)$

The low steel temperature values, calculated for a comparatively high fire load $q_t = 100 \text{ Mcal/m}^2$ demonstrate the high degree of fire resistance of this type of structure. The $\vartheta_{s_{\max}}$ values also clearly demonstrate the great influence of variations of the opening factor $A_v \sqrt{h}/A_t$.

(2) Fire compartment, type C

The gastemperature-time characteristics of this type of fire compartment can be transformed to the corresponding gastemperature-time characteristics of a fire compartment, type A, via fictitious fire load q_f and opening factor $(A_v \sqrt{h}/A_t)_f$. Table II-1 then gives for the transformation coefficient K_f in this case - $A_v \sqrt{h}/A_t = 0.04 \text{ m}^{1/2}$

$K_f = 3.0$

which means that $q_f = K_f q_t = 3.0 \times 100 = 300 \text{ Mcal/m}^2 \dots \dots (f)$

$(A_v \sqrt{h}/A_t)_f = K_f A_v \sqrt{h}/A_t = 3.0 \times 0.04 = 0.12 \text{ m}^{1/2} \dots \dots (g)$

With these values and with $U/F = 99 \text{ m}^{-1}$ and $d/\lambda_i = 0.125 \text{ m}^2\text{h}^\circ\text{C/kcal}$, it follows from Fig.II,63 that

$\vartheta_{s_{\max}} = 400^\circ\text{C} \dots \dots (h)$

Consequently, the influence on the maximum steel temperature of variation in the thermal properties of the surrounding structures is comparatively small in this case.

Table II-1. Coefficient K_f for transforming real fire load q_t and real opening factor $A_v\sqrt{h}/A_t$ of a fire compartment to fictitious fire load q_f and opening factor $(A_v\sqrt{h}/A_t)_f$, corresponding to a fire compartment, type A.

$$q_f = K_f q_t \qquad (A_v\sqrt{h}/A_t)_f = K_f A_v\sqrt{h}/A_t$$

Type of fire compartment	Opening factor $A_v\sqrt{h}/A_t \text{ m}^{1/2}$					
	0.02	0.04	0.06	0.08	0.10	0.12
Type A	1	1	1	1	1	1
Type B	0.85	0.85	0.85	0.85	0.85	0.85
Type C	3.0	3.0	3.0	3.0	3.0	2.5
Type D	1.35	1.35	1.35	1.50	1.55	1.65
Type E	1.65	1.50	1.35	1.50	1.75	2.00
Type F*	1.00 to 0.50	1.00 to 0.50	0.80 to 0.50	0.70 to 0.50	0.70 to 0.50	0.70 to 0.50
Type G	1.50	1.45	1.35	1.25	1.15	1.05

* The highest value of K_f applies to a fire load $q_t > 120 \text{ Mcal/m}^2$, the lowest value to a fire load $q_t < 15 \text{ Mcal/m}^2$. For intermediate fire loads, linear interpolation gives sufficient accuracy.

For the definition of the different types of fire compartment, cf. P. II-9, 10 and 12.

If the calculated value of $(A_v\sqrt{h}/A_t)_f$ is greater than $0.12 \text{ m}^{1/2}$, the diagrams in Fig. II,10 to II,25 and II,32 to II,63 are insufficient for a determination of the equivalent time of fire duration T_e and the maximum steel temperature $\theta_{s_{max}}$, respectively. In such a case, the diagrams belonging to $(A_v\sqrt{h}/A_t)_f = 0.12 \text{ m}^{1/2}$ can be used as an approximation on the safe side. The corresponding value of

$$K_f = \frac{0.12}{A_v\sqrt{h}/A_t} \text{ - then must be applied in determining } q_f \text{ too.}$$

Table II-2. In ISO Recommendation R 834 specified relationship between the temperature rise within the test furnace $\vartheta_T - \vartheta_o$ and the time T, Eq: (II-10).

Time T in minutes	Elevation of furnace temperature $\vartheta_T - \vartheta_o$	
	DegC	DegF
5	556	1001
10	659	1186
15	718	1292
30	821	1478
60	925	1665
90	986	1775
120	1029	1852
180	1090	1962
240	1133	2039
360	1193	2147

References

- {1} THOMAS, P.H. - HESELDEN, A.J.M. - LAW, M., Fully-Developed Compartment Fires - two kinds of behaviour. Fire Research Technical Paper No. 18, Ministry of Technology and Fire Offices' Committee, Joint Fire Research Organisation, Her Majestys Stationary Office, London, 1967.
- {2} THOMAS, P.H. - HESELDEN, A.J.M., Fully-Developed Fires in Single Compartments. A Co-Operative Research Programme of the Conseil International du Batiment (C.I.B. Report No. 20). Fire Research Note No. 923, Fire Research Station, Borehamwood, Herts, 1972.
- {3} HESELDEN, A.J.M. - THOMAS, P.H. - LAW, M., Burning Rate of Ventilation Controlled Fires in Compartments. Fire Technology, Vol. 6, No. 2, May 1970.
- {4} KAWAGOE, K. - SEKINE, T., Estimation of Fire Temperature-Time Curve in Rooms. Building Research Institute, Occasional Report No. 11, Tokyo, 1963 - KAWAGOE, K., Estimation of Fire Temperature-Time Curve in Rooms. Building Research Institute, Research Paper No. 29, Tokyo, 1967.
- {5} HARMATHY, T.Z., A New Look at Compartment Fires. Part I, Fire Technology, Vol. 8, No. 3, August 1972. - Part II, Fire Technology, Vol. 8, No. 4, November 1972.
- {6} MAGNUSSON, S.E. - THELANDERSSON, S., Comments on Rate of Gas Flow and Rate of Burning for Fires in Enclosures. Bulletin No. 19, Division of Structural Mechanics and Concrete Construction, Lund Institute of Technology, Lund, 1971.
- {7} SJÖLIN, V., Brand i bostadsrum antända genom värmestrålning från kärnvapen (Fires in Residential Spaces Ignited by Heat Radiation from Nuclear Weapons). Stockholm 1969.
- {8} ÖDEEN, K., Theoretical Study of Fire Characteristics in Enclosed Spaces. Division of Building Construction, Royal Institute of Technology, Bulletin No. 10, Stockholm, 1963.

- {9} MAGNUSSON, S.E. - THELANDERSSON, S., Temperature-Time Curves for the Complete Process of Fire Development. A Theoretical Study of Wood Fuel Fires in Enclosed Spaces. Acta Polytechnica Scandinavica, Civil Engineering and Building Construction Series, No.65, Stockholm, 1970.
- {10} ÖDEEN, K., Experimentellt och teoretiskt studium av brandförlopp i byggnader (Experimental and Theoretical Study of the Process of Fire Development in Buildings). Report No. 23:1968 from the National Swedish Institute for Building Research.
- {11} SMITH, E.E., Heat Release Rate of Building Materials. ASTM Special Technical Publication 502, 1972, p.119.
- {12} PARKER, W.J. - LONG, M.E., Development of a Heat Release Rate Calorimeter at NBS. ASTM Special Technical Publication 502, 1972, p.135.
- {13} BUTCHER, E.G. - BEDFORD, G.K. - FARDELL, P.J., Further Experiments on Temperatures Reached by Steel in Building Fires. Behaviour of Structural Steel in Fire. Symposium No.2, Proceedings of a symposium held at the Fire Research Station, Borehamwood Herts., on 24 Jan. 1967, Her Majesty's Stationary Office, 1968, Paper 1. - HESELDEN, A.J.M., *ibid*, Paper 2. - LAW, M., *ibid*, Paper 3.
- {14} EHM, H. - ARNAULT, P., Versuchsbericht über Untersuchungen mit natürlichen Bränden im kleinen Versuchsbrandhaus. Document CEACM 3.1 - 69/29 - D,F, Oktober 1969.
- {15} MAGNUSSON, S.E., Probabilistic Analysis of Fire Safety. ASCE - IABSE International Conference on Planning and Design of Tall Buildings, Lehigh University, Bethlehem, Pennsylvania, August 21 - 26, 1972. Conference Preprints: Volume DS, p.424.
- {16} ISO/TC 92, Revised Draft Proposal for ISO/R 834 - Fire Resistance Tests of Elements of Building Construction. ISO/TC 92/WG 11 (Secretariat - 2) 2, February 1972.

- {17} ISO/TC 92, Commentary on ISO/R 834 - Fire Resistance Tests of Elements of Building Construction. ISO/TC 92/WG 11 (Sweden - 2) 5, April 1972.
- {18} KNUBLAUCH, E., Über Ausführung und Aussagefähigkeit des Normbrandversuches nach DIN 4102, Blatt 2 im Hinblick auf die Nachbildung natürlicher Schadensfeuer. BAM-Berichte Nr. 16, Berlin, August 1972.
- {19} EHM, H., Tendenzen im baulichen Brandschutz. Bauen heisst experimentieren, Stahlbau-Verlags GmbH, Köln, 1970.
- {20} PETERSSON, O., The Possibilities of Predicting the Fire Behavior of Structures on the Basis of Data from Standard Fire Resistance Tests. A Critical Analysis with Respect to Varying Characteristics of the Fire Load and the Fire Compartment. Provocative Paper, Centre Scientifique et Technique du Batiment, Colloque sur les Principes de la Sécurité au Feu des Structures à Paris les 2 - 3 et 4 Juin 1971. Bulletin No. 20, Division of Structural Mechanics and Concrete Construction, Lund Institute of Technology, Lund, 1971.
- {21} THOR, J., Strålningspåverkan på oisolerade eller undertaksisolerade stålkonstruktioner vid brand (Radiation Effects of Fire on Steel Structures either without Insulation or Insulated by Ceiling). Bulletin No. 29, Division of Structural Mechanics and Concrete Construction, Lund Institute of Technology, Lund, 1972.
- {22} BUTCHER, E.G. - LAW, M., Comparison Between Furnace Tests and Experimental Fires. Behaviour of Structural Steel in Fire, Symposium No.2, Proceedings of a symposium held at the Fire Research Station, Borehamwood, Herts., on 24 Jan. 1967, Her Majesty's Stationary Office, 1968, p.46.
- {23} LAW, M., A Relationship Between Fire Grading and Building Design and Contents. Joint Fire Research Organisation, Fire Research Note 877, Borehamwood, Herts. 1971.

- {24} LAW, M. - ARNAULT, P., Fire Loads, Natural Fires and Standard Fires. ASCE-IABSE International Conference on Planning and Design of Tall Buildings, Lehigh University, Bethlehem, Pennsylvania, August 21 - 26, 1972. Conference Preprints: Reports Vol. 1b - 8, p.13.
- {25} PETERSSON, O., General Programme for Scandinavian Long-Term Fire Engineering Research. Proceedings No. 129, National Swedish Institute for Materials Testing, Stockholm, 1964.
- {26} PETERSSON, O., Structural Fire Engineering Research Today and Tomorrow. Acta Polytechnica Scandinavica, Civil Engineering and Building Construction Series, No.33, Stockholm 1965.
- {27} PETERSSON, O., Principer för en kvalificerad brandteknisk dimensionering av stålöbärverk (Principles of a Qualified Fire Engineering Design of Load-Bearing Steel Structures). Lectures and Discussions at Stölbyggnadsdagen (Day of Steel Structures) 1968, Stockholm, 1969.
- {28} MAGNUSSON, S.E. - PETERSSON, O., Brandteknisk dimensionering av stölkonstruktioner (Fire Engineering Design of Steel Structures). Handbook, issued by Norrbottens Järverk AB, Luleå, 1972.
- {29} PETERSSON, O., Some Characteristics of Modern Swedish Structural Fire Engineering Design (written discussion). ASTM Special Technical Publication 502, 1972, p.152.
- {30} THOMAS, P.H. - HINKLEY, P.L. - THEOBALD, C.R. - SIMMS, D.L., Investigations into the Flow of Hot Gases in Roof Venting. Fire Research Technical Paper No.7, Fire Research Station, London, 1963.
- {31} BROWN, W.G. - WILSON, A.G. - SOLVASON, K.R., Heat and Moisture Flow Through Openings by Convection. Research Paper No. 200, National Research Council of Canada, Division of Building Research, Ottawa 1963.
- {32} THOR, J., Beräkning av brandöpäverökade statistiskt bestämöda och statistiskt obestämöda stölbalkars deformation och kritiska belastning (Calculation of Deformation and Critical Load of Statically Determinate and Indeterminate Steel Beams Exposed to Fire). Report No. 22:9 Swedish Institute of Steel Construction, Stockholm, 1972.